JPRS-JST-87-028
6 OCTOBER 1987

FOREIGN BROADCAST INFORMATION SERVICE

JPRS Report

Science & Technology

Japan

JPRS-JST-87-028

6 OCTOBER 1987

SCIENCE & TECHNOLOGY

JAPAN

CONTENTS

/12223

GAS SEPARATION USING SOLID ELECTROLYTES DESCRIBED

Tokyo KINO ZAIRYO in Japanese Mar 87 pp 5-12

[Article by Prof Hiroyasu Iwahara, Tottori University Engineering Department; first paragraph is editorial introduction]

[Text] Solid electrolyte gas separation processes still remain in the laboratory test phase. Unlike high molecular membrane and porous diaphragm processes previously used, they are capable of separating a 100 percent pure gas at an advantageous time. Because of this, the processes appear very promising. This paper will deal with the principle and features and briefly describe what gas is capable of being separated by various solid electrolytes.

1. Introduction

Ionic conductor solids are generically called solid electrolytes. Usually, only a single type of ion is movable therein, i.e., only one kind of material is permeable to the solid electrolytes. Based on this principle, they are capable of separating only a single type of gas from gas mixtures.

Unlike high molecular membrane and porous diaphragm processes that have recently been developed, solid electrolyte processes are capable of separating a 100 percent pure gas at a time to the greatest advantage. However, they still remain in the laboratory test phase. The most advantageous use may cause striking progress, provided good ones are discovered.

This paper will deal with the principle and features of solid electrolyte gas separation processes and briefly describe what gas is capable of being separated by various solid electrolytes.

2. Principle of Gas Separation

Various processes can be used with solid electrolytes. Their principle will be discussed below in connection with oxygen.

2.1 DC Power Supply Process

As shown in Figure 1, either of the porous electron conductor pieces on both sides of stabilized zirconia, or other oxygen ion conductor diaphragm, is exposed to air at temperatures of more than several hundred degrees and

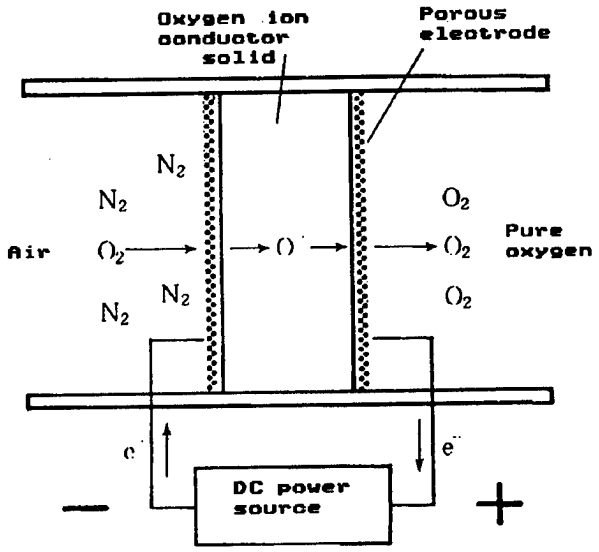

Figure 1. Oxygen Separation by DC Power Supply Process

supplied with DC power with its air side used as the negative electrode. Then, the oxygen molecules in the air are dissociated, and obtained oxygen ions move in the electrolyte and discharge electrons at the positive electrode to become oxygen molecules. That is, oxygen permeates through the diaphragm in the following electrochemical process:

$$\text{Negative electrode: } 1/2O_2(\text{air}) + 2e^- \rightarrow O^{=} \qquad (1)$$

(Negative electrolyte)

$$\text{Positive electrode: } O^{=} \rightarrow 1/2O_2 + 2e^- \qquad (2)$$

Only oxygen ions can move in a solid electrolyte, and nitrogen, argon, carbon dioxide, etc., cannot move toward the positive electron side. Therefore, only pure oxygen gas is selectively separable.

2.2 Concentration Cell Shortcircuit Process

The same system as shown in Figure 1 is used for this process. When either of the diaphragms is exposed to air and the other is subjected to pressure reduction without any power supply from the outside, a concentration cell with a positive air electrode is formed to generate an electromotive force given by equation:

$$E = \frac{RT}{4F} \ln \frac{P_1}{P_2} \qquad (3)$$

wherein P_1 and P_2 are the partial pressures of the oxygen in the air and the pressure reducing chamber, R is the air constant, F is the Faraday constant, and T is the absolute temperature.

When both electrodes of the concentration cell are shorted, an electromotive force is generated due to the difference of the partial pressures in both gas chambers.

Reaction progresses as follows:

$$\text{Positive electrode of air chamber: } 1/2O_2(\text{air}) + 2e^- \rightarrow O^{=} \quad (4)$$

$$\text{Negative electrode of air chamber: } O^{=} \rightarrow 1/2O_2 + 2e^- \quad (5)$$

Further, oxygen transfers from the high partial oxygen pressure side to the low side. As shown in Figure 2, ions other than oxygen do not move in the solid electrode so only oxygen gas is separable.

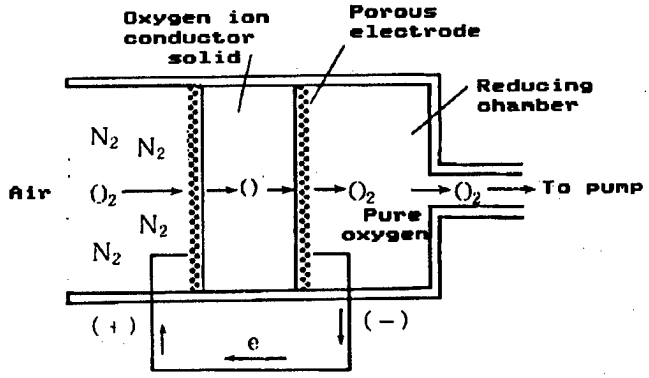

Figure 2. Oxygen Separation by Concentration Cell Shortcircuit Process

2.3 Mixture Conductor Process

Electrons flow and only oxygen electrochemically permeates through the membrane when a solid electrolyte itself is made electron conductive despite causing current flow with the outside circuit shorted by the concentration cell shortcircuit process. The solid materials in which both ions and electrons can move are called mixture conductor materials. The good ones can be used for gas separation.

When either of the two chambers separated by an oxygen ion-electron mixture conductor membrane is exposed to oxygen and the other is subjected to suction as shown in Figure 3, an oxygen concentration cell is formed but shorted through the conduction of the electrons therein. In this case also, what are represented by equations (4) and (5) progress and only oxygen permeates the membrane.

The process requires no lead wire for the outside circuit. It advantageously permits simplification of separators since selective permeation of oxygen is made possible by simply giving a pressure differential between both sides of the barrier.

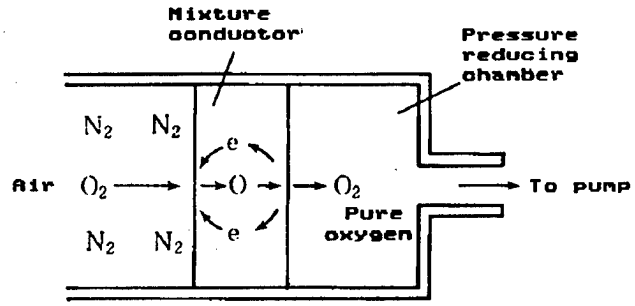

Figure 3. Oxygen Separation by Oxygen Ion-Electron Mixture Conductor

2.4 Vapor-Phase Electrolytic Process

So-called vapor phase electrolyte gas separation is also possible. Therein a pure gas is separated form mixture gases and a specific kind of atom is electrochemically drawn out of the compound gases by a solid electrolyte. The process is applied to water-vapor electrolysis, with an oxygen ion conductor material for example, for obtaining hydrogen by separating oxygen from water vapor (gaseous water molecules). The efficient hydrogen production process for future hydrogen energy systems appears promising. The principle of water vapor electrolysis is shown in Figure 4.

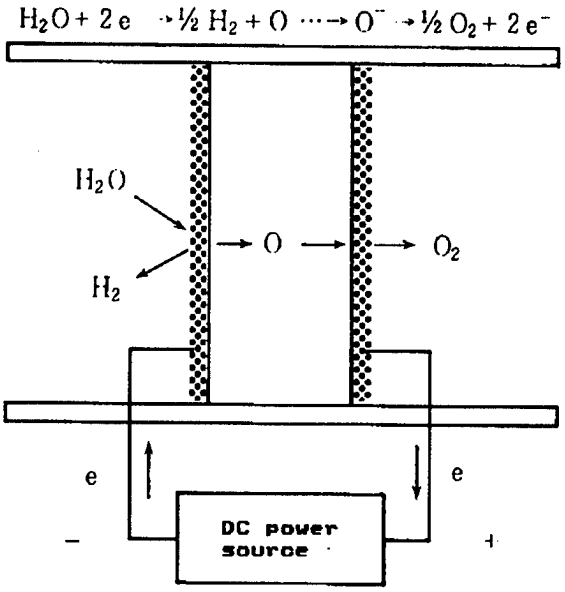

Figure 4. Water Vapor Electrolysis by Oxygen Ion Conductor

3. Features of Solid Electrolyte Gas Separation Processes

Table 1 collectively shows the features and the separation rate equation of the above mentioned processes. The major feature of all of them is that a 100 percent pure gas is obtainable in one-step separation.

Table 1. Features of Solid Electrolytic Process Gas Separation

Process	Separation rate v (cm^3(STP)/sec·cm^2)	Features
Power supply	$v = 0.116 \frac{i}{n}$	(1) Neither boosting nor reducing pump needed (2) Gas separation rate is controllable with oxygen (3) Gas extraction pressure is controllable with applied voltage
Concentration cell shortcircuit	$v = \frac{1.15 \times 10^{-5}}{n^2} \frac{T\sigma_{O^=}}{d} \log \frac{P_1}{P_2}$	(1) Only specific kind of gas is selectively permeable when pressure differential is given (2) Gas permeation rate is proportional with logarithm of the partial oxygen pressures between both chambers
Mixed conductor	$v = \frac{1.15 \times 10^{-5}}{n^2} \frac{T\sigma_i \sigma_e}{(\sigma_i + \sigma_e)d} \log \frac{P_1}{P_2}$ When $\sigma_i \ll \sigma_e$ $v = \frac{1.15 \times 10^{-5}}{n^2} \frac{T\sigma_i}{d} \log \frac{P_1}{P_2}$	(1) Only specific kind of gas is selectively permeable when pressure differential is given (2) Gas permeation rate is proportional with logarithm of the partial oxygen pressures between both chambers (3) Separator can be simplified since no lead wire is needed for electrodes and outside circuits
Electrolytic	$v = 0.116 \frac{i}{n}$	(1) Only specific kind of atoms can be extracted from compound gases (2) Extraction rate is controllable with oxygen

i: current density (A/cm^2),
σ_1: ion conductivity (Scm^{-1})
σ_e: electron conductivity (Scm^{-1})
n: ion value
d: thickness (cm) of barrier
P_1,P_2: partial gas pressures
T: temperature (K)

Power supply and electrolytic processes are convenient since separation itself neither requires pressure boosting nor reducing pump and is easy to control with current and voltage. As shown in Table 1, their gas separation rate per unit time depends on only current (i) under Faraday's law and easy to control with current and they permit the reversal of permeating direction through that of current direction.

The gas permeation rate of the concentration cell and the mixture conductor processes is proportional with logarithm of the ratio between the partial pressures in both gas chambers. In this respect, they substantially differ from the existing membrane separation processes whose permeation rate is proportional with the difference of partial pressures. On the extraction of oxygen gas from one atmospheric pressure air for example, solid electrolyte process permits an increase of the pressure reduction ratio so the permeation rate may be raised accordingly while the high-molecular process shows limited reduced pressure (one atmospheric pressure) differential.

Ideally useful in separating a mixture gas by applying a solid electrolyte is only the energy corresponding to the free enthalpy of mixtures. It increases in proportion to absolute temperature. Permeation rate of the ions in a solid electrolyte occurs to cause increase of separation efficiency with the rise of temperature. Being a high temperature type, many solid electrolytes used for gas separation are capable of separating the gases generated at high temperatures without lowering them.

4. Solid Electrolytes for Gas Separation

The solid electrolytes for gas separation are required to have the following properties.

1) Conductor ions become gaseous molecules on discharge.

2) Sufficiently high ion conductivity at working temperature.

3) Sufficiently low electron conductivity (power supply and electrolytic processes) or sufficiently high electron conductivity (mixture conductor process).

4) Compact and no gas leak.

5) Chemically stable.

6) Easy production, etc.

Particularly the first item is indispensable and, for efficient separation, items two to four also.

Cited among the solid electrolytes that become gaseous molecules on ion discharge are hydrogen, chlorine, and fluorine ion conductors besides the previously mentioned oxygen. Representative electrolytes are shown in Table 2 and the relationship between their conductivity and temperature in Figure 5. Showing low conductivities at room temperature, they largely require high temperatures for gas separation.

Briefly described below are examples of the solid electrolytes and their application to gas separation. The application to gas separation still largely remains in the early developmental stage.

Table 2. Solid Electrolytes That Can Be Used for Gas Separation

Gas to be separated	Ion condition	Solid electrolyte	Working temperature, etc.
Oxygen	Oxygen	$(ZrO_2)_{0.9}(Y_2O_3)_{0.1}$ $(ZrO_2)_{0.85}(CaO)_{0.15}$ $(CeO_2)_{0.8}(Y_2O_3)_{0.2}$ $(Bi_2O_3)_{0.75}(Y_2O_3)_{0.25}$	} Stabilized zirconia and ceria } more than 500°C Bismuth oxides 400 ~ 800°C Unstable in reducing atmosphere
Hydrogen	Proton	$H_3Mo_{12}PO_{40} \cdot 29H_2O$ $HUO_2PO_4 \cdot 4H_2O$ $Sb_2O_5 \cdot 4H_2O$ $SrCe_{0.95}Yb_{0.05}O_{3-\alpha}$ $H_3O^+ - \beta$ alumina	Room temperature } Readily deteriorates, losing crystal water, when heated Less than 100°C 200°C " 400 ~ 1000°C Difficult to mold in the presence of hydrogen or water vapor 100 ~ 200°C
Fluorine	Fluorine	PbF_2 (+ 2% KF) $PbSnF_4$	} 100 ~ 250°C Susceptible to hydrolysis at high temperature
Chlorine	Chlorine	$PbCl_2$ (+ 1% KCl) $SnCl_2$	} 100 ~ 300°C Susceptible to hydrolysis at high temperature, hygroscopic
Sodium vapor	Sodium	Na - β alumina $Na_2O \cdot 11Al_2O_3$	200 ~ 400°C

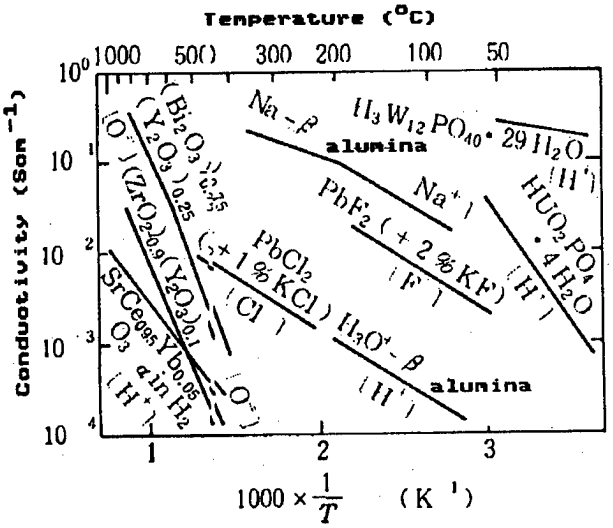

Figure 5. Conductivity of main Solid Electrolytes
(Items in ( ) are kinds of conductor ions)

4.1 Oxygen Ion Conductors

Bismuth oxides, ceria, and zirconia are known oxide ion conductors. Stabilized zirconia solid electrolytes show higher practicability than the former two because they are stable in pressure reduced atmosphere and have high ceramic strengths despite slightly lower oxygen ion conductivities.

Stabilized zirconia varies. Generally used are those with components $(ZrO_2)_{0.9}$ $(Y_2O_3)_{0.1}$ and $(ZrO_2)_{0.85}$ $(CaO)_{0.15}$. They generally require high temperatures above 600°C for an increase in conductivity.

Various kinds of oxygen separators (or selective permeaters) have been devised for applying the above-mentioned solid electrolytes. Shown in Figure 6 is the construction of a gas oxygen concentration controller (oxygen pump). A stabilized zirconia tube with electrodes serves as the pump capable of feeding only oxygen to the gas in the system from outside air and drawing it out on the principle stated in 2.1. Partial pressures of oxygen in the system are detectable by applying equation (3) with the electromotive force of an oxygen concentration cell to a part of stabilized zirconia and, when the current (or applied voltage) supplied to the oxygen pump is controlled with its voltage signal fed back, can be kept constant. A commercially available oxygen pump (Photo 1 [omitted]) is used for study of the atmospheric gas control on heat-treatment of semiconductors and inorganic materials and for control of partial oxygen pressures in the experiments on the culture of microbes and of corrosion and oxidation of metals.

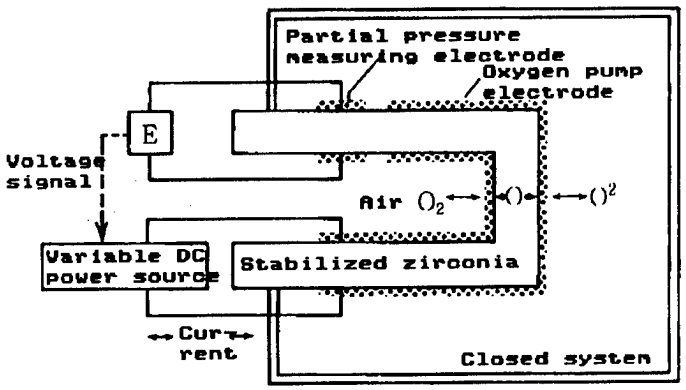

Figure 6. Principle of Oxygen Pumps

Use of zirconia is studied for decomposition of nitrogen oxides[2] and carbon dioxide gas.[3] A U.S. patent has been granted for an oxygen concentration extractor for concentration cell shortcircuit process.[4] Study is underway to develop the above-mentioned hydrogen production system for water vapor electrolysis. Being developed in West Germany is a system with a stabilized zirconia tube module as shown in Figure 7 for producing great amounts of inexpensive oxygen.[5]

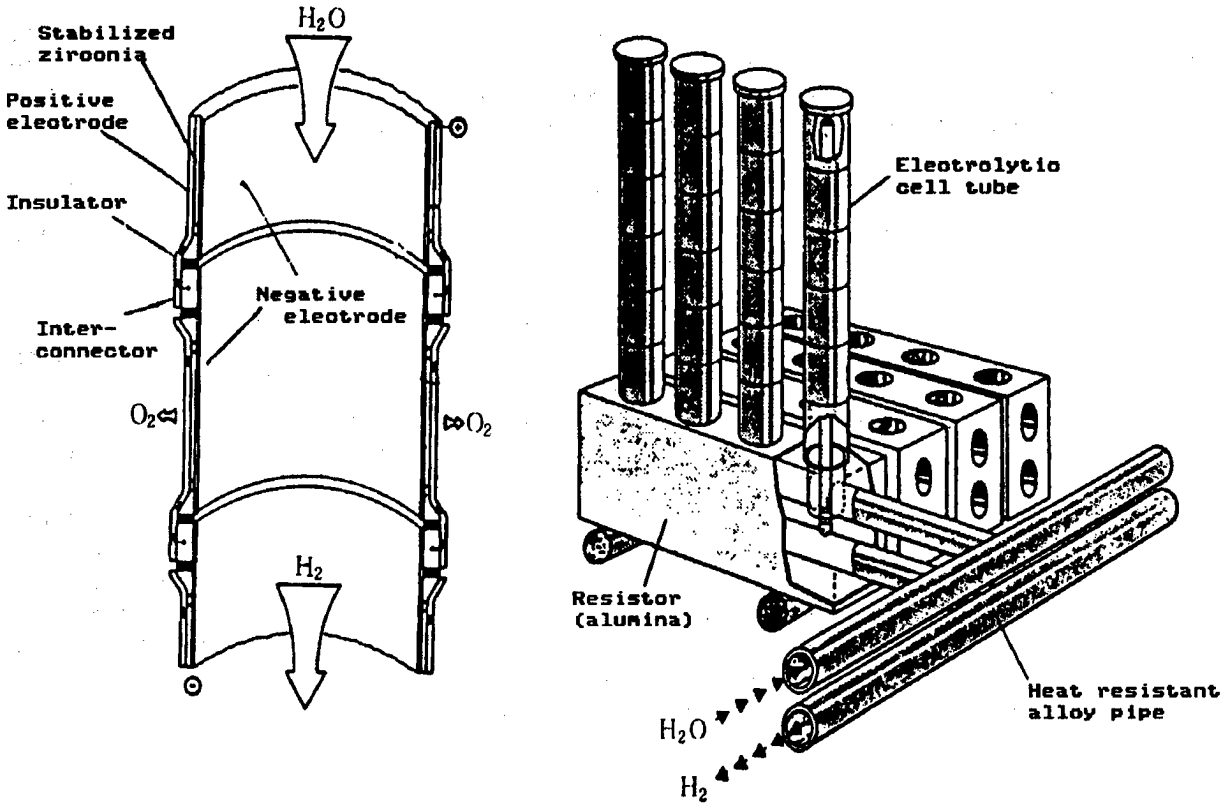

Figure 7. HOT ELLY Project Water Vapor Electrolyzer (Quoted from W. Doenitz, et al., INT.J. HYDROGEN ENERGY)

A system has not been put in practical use as yet for large-scale extraction of oxygen from air. This is because stabilized zirconia does not have sufficiently high conductivity (high resistance) so a large current supply is not possible. In this connection, the problem is how to decrease the membrane in thickness for decreasing resistance.

4.2 Hydrogen Ion Conductors

Water containing heteropolyacid $H_3M_{12}PO_{40}\cdot 29H_2O$(M = Mo or W) crystal is known to be a solid showing high hydrogen ion conductivities at normal temperatures. Relative humidities more than 70 percent are necessary for their constant use. Water containing uranylphosphoric acid $HUO_2PO_4\cdot 4G_2O$ and antimonic acid $Sb_{05}\cdot 4H_2O$ are considerably stable even in dry atmosphere despite two-digit lower conductivities. They are therefore used to attempt hydrogen separation at normal temperatures in the power supply process.[6]

Hydronium and ammonium substituted β-alumina would not be suitable for hydrogen separation because it is compact, thin, and substantially difficult to produce a ceramic membrane despite hydrogen ion conductivities.

Hydrogen is separable by using high temperature hydrogen ion conductors[7] discovered by the author and others. These ceramics, whose base material is cerium strontium trioxide ($SrCe_{0.95}Yb_{0.05}O_{3-\alpha}$, etc.), show considerable hydrogen ion conductivities in the presence of hydrogen or water vapor at high temperatures of more than 400°C. They have confirmed, in a small-scale experiment, that hydrogen can be extracted from ethylene- and carbon dioxide-hydrogen mixture gases. Figure 8 shows an example of the relationship between the current and hydrogen extraction rate in separation of hydrogen from a thermally ethane decomposed gas by the power supply process.[8]

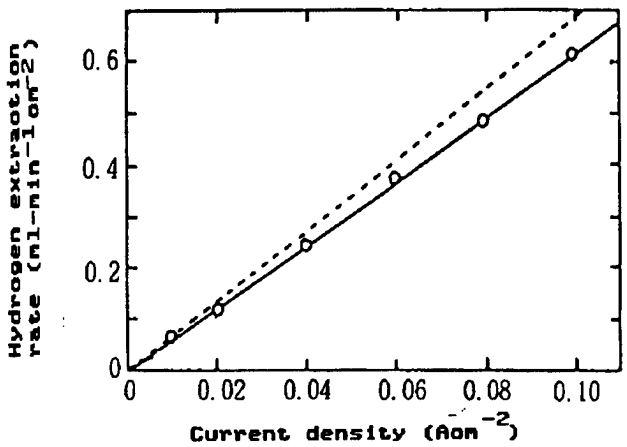

Figure 8. Hydrogen Extraction From Thermally Ethane Decomposed Gas by Power Supply Process
(800°C, solid electrolyte $SrCe_{0.95}Yb_{0.05}O_{3-\alpha}$,
broken line: theoretical values)

Besides, they have successfully obtained pure, very dry (water vapor partial pressure: 0.38 Torr) hydrogen by using a high temperature electrolytic system trial manufactured by applying a hydrogen ion conductor on the principle in Figure 9.[8] The ceramic has no sufficiently high hydrogen ion conductivity for its application to large-scale gas separation. It is desired, therefore, to decrease its membrane in thickness and search for better solid electrolytes.

4.3 Halogen Ion Conductors

Among fluorine ion conductor solids, the sinterings whose base material is calcium or lanthanum fluoride, $PbSnF_4$, etc. are known to have considerably higher conductivities than oxygen ion conductors. No attempt has been made to separate fluorine gas by applying them as yet.

Lead and antimony chloride sinterings are known chlorine ion conductors. However, they are not suitable for separation of water containing mixture gases because they have lower conductivities than fluorine conductors and are susceptible to hydrolysis.

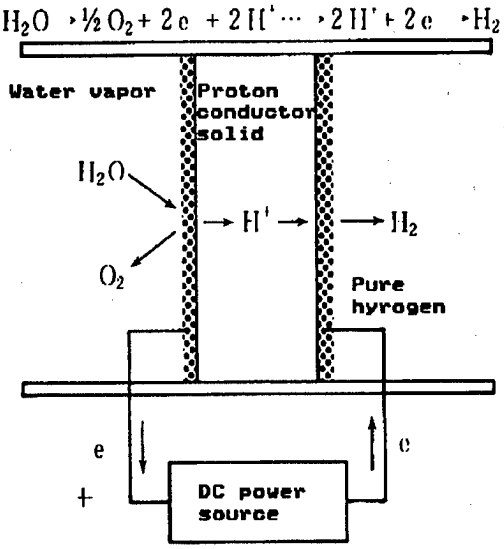

Figure 9. Water Vapor Electrolysis by Proton Conductor

4.4 Mixture Conductors

Cobalt or iron containing perovskite type oxides[9-11] and cerium containing zirconia[12] are known oxygen ion-electron mixture conductors. Their oxygen ion conductivity is 10^{-2} to $10^{-1}Scm^{-1}$ (electron conductivity: one to three digits higher than it), equal or slightly higher than that of stabilized zirconia, at 1,000°K. Manufacture of good oxygen separating membranes from ceramics is therefore anticipated, provided their membranes can be decreased in thickness.

Figure 10 shows the results of computing, by applying the equation in Table 1, the relationship obtained between the suction pressure P_2 and permeation rate when pure oxygen is extracted from the atmosphere by using a 10 μ-thin mixture conductor with an oxygen ion conductivity of $10^{-2}Scm^{-1}$ at 1,000°K attached to a porous tube.[13]

For comparison, the broken line in the drawing represents the results of computing, by applying the well-known equation:

$$\nu = \frac{f\ (P_1 - P_2)}{d} \quad (cm^3(NTP)/sec \cdot cm^2)$$

the oxygen permeation rate (ν) obtained by applying a silicon membrane (permeability coefficient (f) = $3.5 \times 10^{-8} cm^3 \cdot cm/cm^2 sec \cdot cm$ Hg) with the same thickness. The drawing indicates that the mixture conductors with the same thickness are far superior in oxygen permeability.

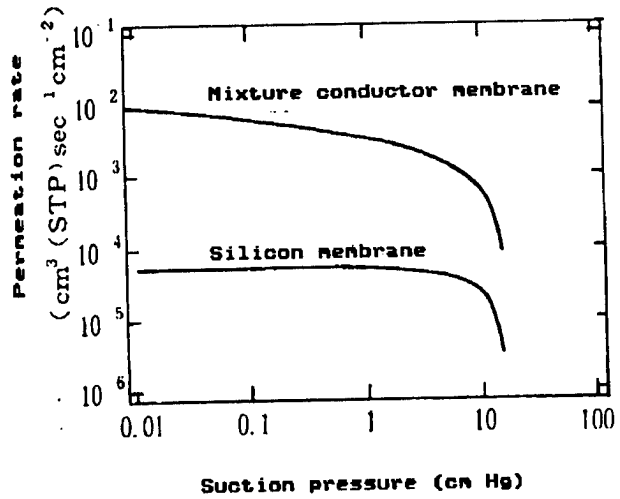

Mixture conduotor membrane (1,000K) $\sigma_0 = 10^{-2}\ \mathrm{Scm}^{-1}$, $\sigma_e = 10\ \mathrm{Scm}^{-1}$

Silicon membrane (300K) $f = 3.5 \times 10^{-8}\ \mathrm{cm}^3(\mathrm{STP})\ \mathrm{cm}^{-1}\mathrm{sec}^{-1}\mathrm{cm\ Hg}$

Figure 10. Oxygen Gas Permeation Rates in Comparison to Mixture Conductors and Silicon Membranes (10 μ-thick)

5. Problems of and Future Prospects for Solid Electrolyte Processes

Cited among the problems of solid electrolyte gas separation processes are:

1) Power supply and electrolytic processes require attachment of electrodes and lead wires to complicate structure of the systems.

2) Being ceramic, many solid electrolytes are not convenient for making thin, compact separating membranes.

3) Ion conductivity requires too high of a temperature in many cases.

4) Required thermodynamic energy for separation becomes large at high temperatures.

Particulary items two and three are the most serious. Ions do not sufficiently move therein. One solution to the problems is to establish a technology for decreasing ion permeation resistance by making a thin membrane of solid electrolytes or raising the temperature.

As to the oxygen ion conductors for oxygen separation, the technology for making thin membranes of stabilized zirconia and fitting gas electrodes has remarkably progressed in the course of development and study of solid electrolytes. They are regarded as promising among third generation fuel

batteries.[14] They require attachment of several μ-thick layers of a porous electrode material, a compact stabilized zirconia, and a porous electrode material one by one to the surface of a porous support tube. This technology can directly be applied to the manufacture of gas separators.

Provided thin flexible sheets can be manufactured from solid electrolytes, the decrease in thickness of systems will probably result in a considerable increase in separation efficiency. Lately, a halogen ion conductor of crown ether-halide complex has been discovered.[15] It is plastic. Its thin film may be used as a halogen separating membrane if it can be manufactured.

The development of good oxygen or hydrogen ion conductor solid electrolytes is anticipated. If they are successfully manufactured, particularly from mixture conductors, they will be very useful as perfectly selective permeation membranes to be substituted for high-molecular ones previously used (selectivity; not 100 percent). In this connection, further progress of study is awaited although their synthesization is not assured to be theoretically possible.

FOOTNOTES

1. H. Iwahara, CHEMICAL SYSTEMS, January 1986, p 90.

2. T.M. Guel and R.A. Huggins, J. ELECTROCHEM. SOC., Vol 126, 1979, p 1067.

3. T.E. Erstfeld, et al., PAP. AMER. INST. AERONAUT ASTRONAUT, 1979, pp 79-1375.

4. Sun Oil Company, USP. 4,131,514 (26 December 1978).

5. W. Doenitz and E. Erdle, INT. J. HYDROGEN ENERGY, Vol 10, 1985, p 291.

6. N. Miura, Y. Ozawa, N. Yamazoe, and T. Seiyama, CHEM. LETT., 1980, p 1275.

7. H. Iwahara, T. Esaka, H. Uchida, and N. Maeda, SOLID STATE IONICS, Vol 3/4, 1981, p 359.

8. H. Iwahara, et al., Ibid., Vol 18, 1986, p 1003.

9. Teijin, Laid-Open Patent Gazette No 92103/1981.

10. Y. Teraoka, et al., The 13th Solid Ionics Discussion, Tokyo, October 1986, Lecture Summaries p 87.

11. T. Esaka, et al., The 50th Electrochemical Society Meeting Lecture Summaries, 1985, p 211.

12. B. Cale's and J.F. Baumard, J. ELECTROCHEM. SOC., Vol 131, 1984, p 2407.

13. H. Iwahara, ENERGIES AND RESOURCES, Vol 6 No 3, 1985, p 192.

14. T. Takahashi, "Fuel Batteries," KYORITSU SHUPPAN, 1984, p 113.

15. D.S. Newman, et al., SOLID STATE IONICS, Vol 3, 1981, p 389.

20115/9365
CSO: 4306/7559

NEW APPLICATION OF TRANSITION METAL CARBIDES DETAILED

Tokyo KINO ZAIRYO in Japanese Mar 87 pp 13-20

[Article by Yoshio Ishizawa, collective researcher, Inorganic Material Research Institute; first paragraph is editorial introduction]

[Text] Many IV_a to VI_a-family metal carbides are compounds with high melting points of more than 3,000°C. Recently, growth of their monocrystals has become possible with the elucidation of their basic properties. This paper will detail the processes for manufacturing a surface treated TiC <110> field emitter recently developed as an example of the new application of metal carbides as well as with its electron emission characteristic.

1. Introduction

As shown in Table 1, IV_a to VI_a-family metal carbides such as titanium carbide (TiC)[1] are compounds with high melting points at more than about 3,000°C and highly hard, good electric heat conductors with small work functions of less than 4 eV. IV_a- and V_a-family metal carbides have NaCl type structures except vanadium carbide and tungsten structures of the VI_a-family metal carbides are of the simple cubic lattice type (WC type structure). The former features wide bertholide composition ranges since holes constantly exist at carbon atoms. TiC_x, for example, constantly has NaCl structures at the wide composition range of x = 0.5 to 0.96. These days, basic study is underway as to the monocrystals of metal carbides.[2,3]

So far, metal carbides have mainly been used for cutting and other tools. Additionally, study has been carried out for their application to the production of nuclear fission reactor first walls,[4] catalysts,[5] superconductors,[6] electrodes,[7] solar energy selective membranes,[8] etc. Recently, research is underway on their use for producing monocrystal substrates[9] and intensifier ion emitters.[10,11] Introduced herein will be the latest results of studying a field type electron emitter as a new application example of TiC.

2. Application of Metal Carbide to Electron Emitters

2.1 Field Emission

Figure 1 shows the principle of field emission. Surface potential energy is given as sum -eFx of the image-force term and the $-e^2/4x$ and electric field

Table 1. Properties of Transition Metal Carbides[1]

	IVa family			Va family			VIa family
	TiC	ZrC	HfC	VC	NbC	TaC	WC
Melting point *2 /°C	3067	3420	3928	2648	3600	3983	2776
Hardness (room temperature, kg/mm²)	2900	2700	2300	3000	2400	1600	2300
Electric resistance (room temperature, μΩ-cm)	130	40	34	46	32	18	17
Work function (eV)	3.8*3	3.5*3	3.4	3.8	3.8	3.8	3.7
Bertholide composition range (carbon/metal)	0.55~0.96	0.60~0.99	0.6~0.98	0.72~0.89	0.72~0.98	0.75~0.99	1.0

*1 Carbides with composition similiar to nonbertholide ones
*2 Highest value of compositions
*3 Work fuontion at (100)-plane of monocrystals, others--work function of polycrystals

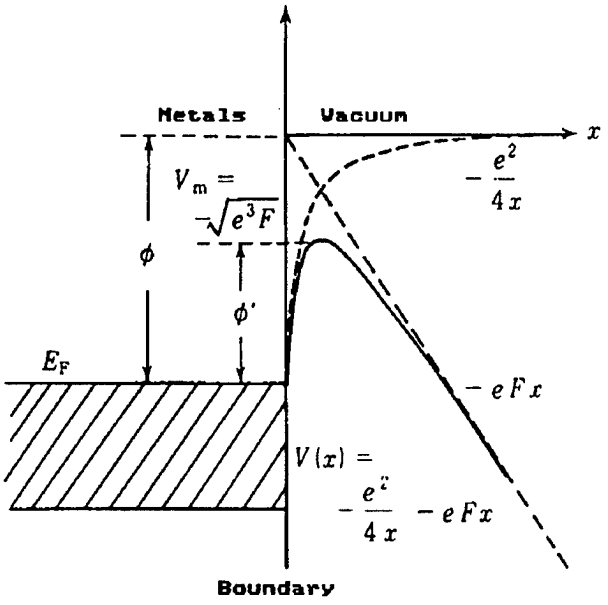

Figure 1. Principle of Field Emission

F term. Therein, the x-axis is orthogonal with the surface. When the cathode chip temperature is sufficiently high, the electrons, with larger energies than potential barrier V_m, are emitted outside. This is called electron emission. On the other hand, when it is about room temperature, very few electrons can run over the barrier. In this case, the quantum mechanical tunnel effect, produced when potential is decreased in width by intensifying applied electric field, is used for taking out electrons. This is called field emission.[12]. For giving rise to it, it is necessary to apply an intense electric field of 10^7 to 10^8 to the chip surface.

Field emission electron sources feature two-digit high brightness, about one-fifth large emission energy widths, and three-digit small size as compared with other cathodes. In recent years, demand has grown for the new electron sources with such features. Monocrystal tungsten has been put to practical use among field emitters. It is hoped, however, that field emitters with higher stabilities will become available. The author and others have found that very stable field emitters can be manufactured by treating the surface of TiC monocrystal chips with <110>-oriented axis.[3,13] Discussed below are the technologies for growing TiC monocrystals and treating the chip surface as well as the emission characteristic of the surface treated TiC<110> field emitters.

2.2 TiC Monocrystal Growing Technology

When a field emitter is manufactured, TiC is required to produce a large-sized monocrystal with a composition having the fewest carbon atom holes ($x = C/Ti = 0.96$). it is grown by the high frequency heating floating zone process in a high-pressure gas atmosphere. However, the ordinary floating zone process is not capable of producing a homogeneous composition monocrystal. That of TiC is grown in the zone leveling-floating zone process.[14,15] Figure 2 shows the principle of this growth. It is essential for the principle to keep composition of melting belts at a fixed value while moving. Namely, an X_1-composition monocrystal is grown by keeping it at X_3 as illustrated in Figure 2. The composition of supplied sintering rods is changed from X_1 to X_2 for adjustment. Figure 3 [omitted] shows photos of the vertical and horizontal sections of the $TiC_{0.96}$ monocrystal grown in the process. It measures about 10 mm in outside diameter and several centimeters in length.

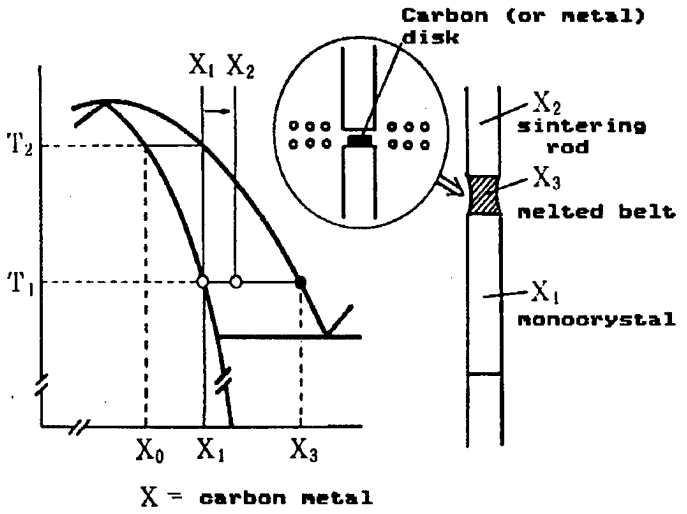

Figure 2. Principle of Zone Leveling-Floating Zone Process

2.3 TiC<110>-Chip Surface Treating Technology

The chips with <110>-oriented axis are significant for application. Other axis orientation chips, e.g., TiC<100>- and <110>-oriented chips do not emit electrons in axis direction.[16] For manufacturing their field emitter, they are cut in 0.2 x 0.2 x 3 mm^3 rectangular solid specimens and fluorinenitric acid electrolytic polishing process is applied. This is shown in Figure 4 [omitted]. The metal wire welded to the metal sheets surrounding it, as shown in Figure 4(b) [omitted], is made from tantalum. Tantalum wire joule heating is carried out for it. It has a curvature radius of about 0.1 μm.

TiC<110>-chips are evaluated by using a field emission characteristic evaluating system.[17] Figure 5(a) shows patterns of the electron emission. They are obtained through flush heating at 1,500 to 1,600°C. These values correspond to clean surface making temperatures. The patterns are elucidatory under the electron emission from the angular local parts with high field intensities at its tip.[15] This is because upon heating it acquires a facet structure surrounded by developed (100)- and (111)-planes. Figure 5(b) shows a model of its tip shape.

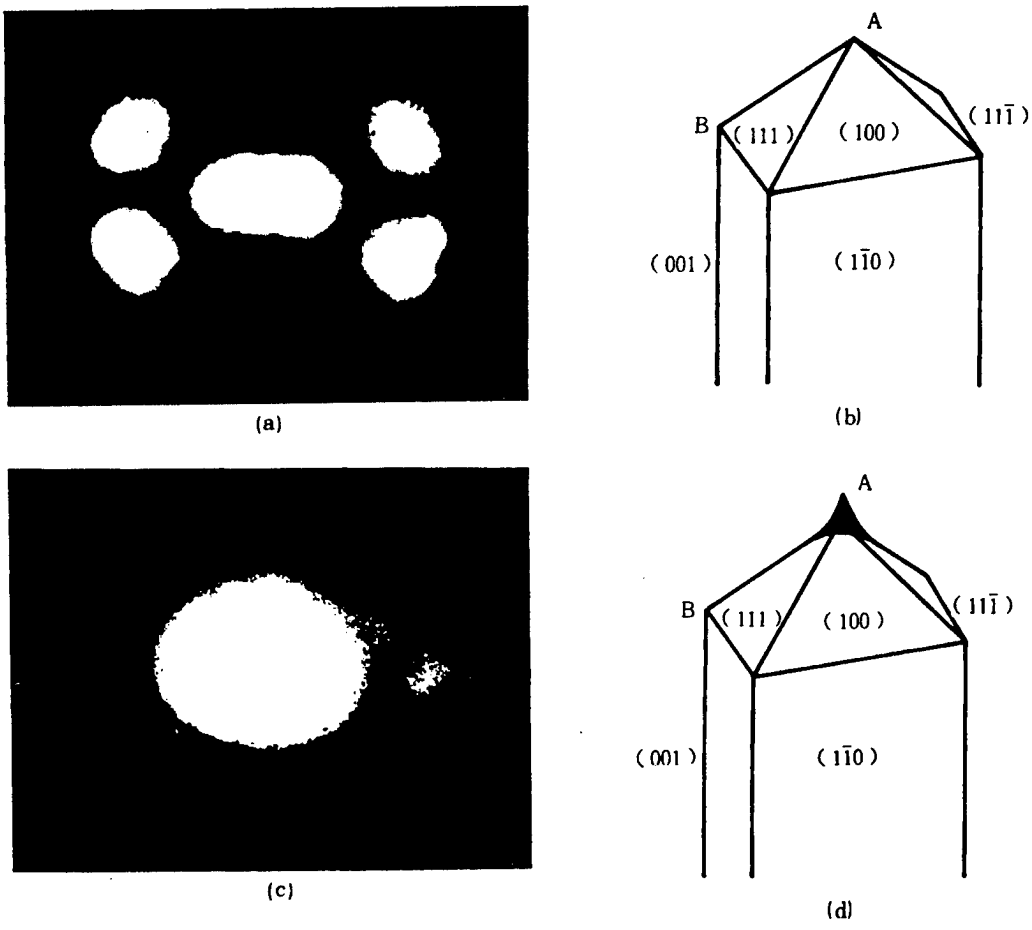

Figure 5. Patterns of Electron Emission From TiC<110> Chips and Their Tip Shape
(a), (b): Clean surface TiC<110> chips
(c), (d): O_2(8L, 1,100°C) surface treated TiC<110> chips

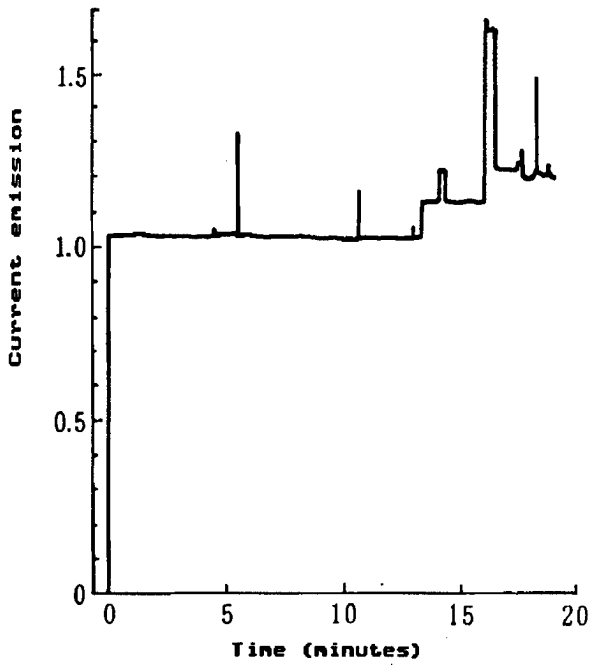

Figure 6. Electron Emission Characteristics of Clean Surface TiC<110> Chips Flush heating temperature 1,600°C, P = 3.2 x 10^{-8} Pa

Figure 6 shows electron emission characteristics of the clean surface TiC<110>-chip. Emitted current shows step- and spike-shaped noises. Generation of such noises and the very stable characteristic between them are peculiar to TiC field emitters. The current emitted from TiC is not practical because its stable component shows a small value although amelioration of its instability occurs with increase of vacuum degree. Reproducible, practical field emitters are obtained by heating the chip surface as described below.

The following is the procedure of treating the surface of the TiC<110>-chip.[18] First the chip is heated to 1,500 to 1,600°C and an electron emission pattern, as shown in Figure 5(a), is confirmed. Next, it is heated to about 1,100°C at the 1.33 x 10^{-4}Pa vacuum degree obtained by introducing a surface treating gas. If heating time is (x)-seconds, gas exposure amount is xL (1L(langmuir) = 1.33 x 10^{-4}Pa·sec). Next, ultrahigh vacuum is attained through evacuation and electron emission is continued at 10 μA for 30 minutes. Oxygen, ethylene, and hydrogen sulfide have been found among the surface treating gases. If the 20L, 1,100°C heating surface treatment with oxygen gas is denoted by O_2(20L, 1,100°C), the two-step surface treatment with oxygen and ethylene gases, e.g., C_2H_4(100L, 1,100°C) + O_2(20L, 1,100°C), and three-step surface treatment with three kinds of gases are possible.

The following three can be cited among the surface treatment effects of the TiC<110>-chip.

(1) Change of electron emission pattern
(2) Increase of current emission
(3) Stabilization of current emission

Whether surface treatment is completed can be judged in terms of the change of electron emission pattern and increase of current emission.

Figure 5(c) shows a pattern of the electron emission from the clean chip surface treated with oxygen gas, O_2(8L, 1,100°C), indicating that its central part has become very bright. It neither depends on the types of surface treating gas nor the treating procedures. There is, however, the minimum exposure value that causes pattern change. Those of oxygen, ethylene, and hydrogen sulfide are 3L, 500L, and 3L, respectively. The surface treated chip emission pattern can be interpreted to come from sharpening of its tip.[18]

When the chip surface is treated, change of emission pattern causes an increase of current emission. Figure 7 shows the relationship between the applied voltage and exposure in the course of its surface treatment with oxygen gas at a constant current. In the figure, curve (a) represents the change of voltage applied immediately after gas exposure (1,100°C heating of the chip in oxygen). In this phase, the emission pattern has not changed as yet. Increase of exposure causes that of applied voltage in accordance with that of oxygen adsorption work function. Curve (b) indicates change of the voltage applied after 30 minutes 10 μA electron emission. It decreases at the exposure values more than 7L. At this time, the electron emission pattern changes, as shown in Figure 5(c).

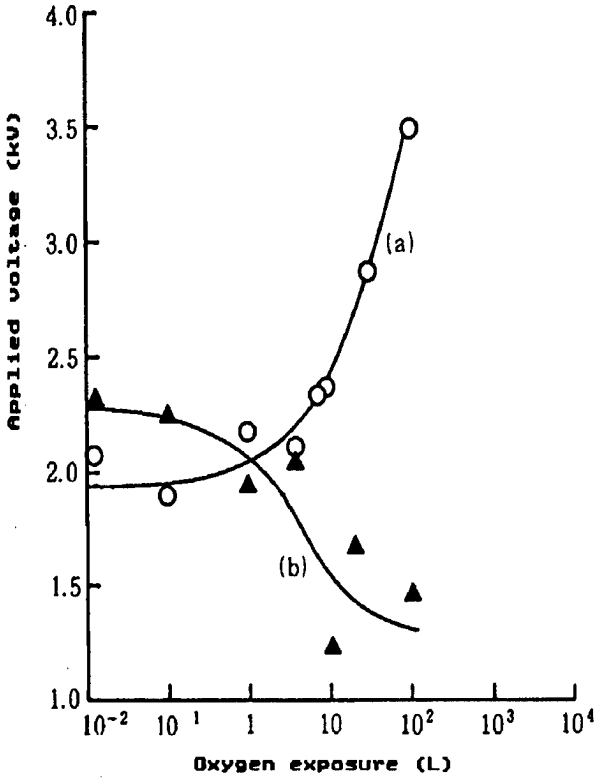

Figure 7. Relationship Between Applied Voltage and Oxygen Gas Exposure of TiC<110> Chips at Constant Current (5 nA)

2.4 Characteristics of Surface-Treated TiC<110> Field Emitter

The step- and spike-shaped noises of the current emission from the clean surface of the TiC<110>-chip strikingly decrease through its surface treatment. How to stabilize current emission is discussed below.

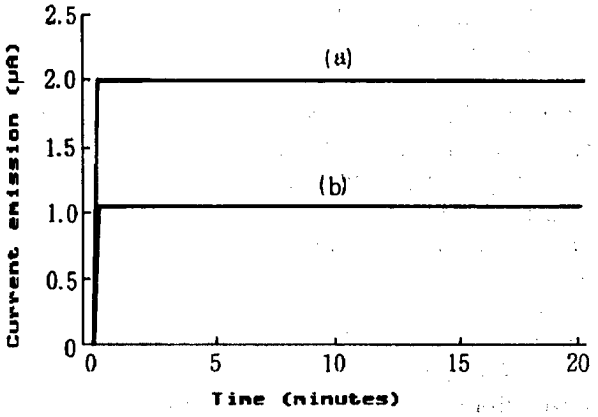

1,100 °C

(a) $\overset{\text{Surface}}{\underset{\text{treatment}}{}}$: C_2H_4 ($10^4 L$, 1,100°C), $P = 4.7 \times 10^{-9}$ Pa

(b) $\overset{\text{Surface}}{\underset{\text{treatment}}{}}$: O_2 (20 L, 1,100°C), $P = 6.7 \times 10^{-9}$ Pa

Figure 8. Hourly Variation of Current Emission From Surface Treated TiC<110> Chips
Flush heating temperature: 1,100°C

Figure 8 shows hourly variation of the current emission from the chips subjected to oxygen treatment O_2(20L, 1,100°C) and ethylene treatment (10^4L, 1,100°C). In a highly stable condition, current variation width (short time noise) amounts to less than 0.2 percent and current damping factor (drift) is small, less than 0.1 percent/hour. The current emission from hydrogen sulfide treated chips is similarly superior in stability. The small drift is included among such superior features of the surface treated chips as not observed with tungsten monocrystal chips. The maximum total current (called stable current) free from more than 1 percent noise for 20 minutes immediately after voltage application amounts to several μA in the surface treatment with a single gas.

The current emission from two-step oxygen and ethylene gas surface treated chips are strikingly superior in stability. Namely, they are capable of constantly obtaining about 10 μA ($P = 2.0 \times 10^{-9}$Pa) current as shown in Figure 9. In multistep surface treatment, current emission is superior in stability when ethylene gas is used first. C_2H_4(500L, 1,100°C) + O_2(20L, 1,100°C) surface treated chips secure about 10 μA constant current even at a vacuum degree of 1.2×10^{-8} (Figure 11).

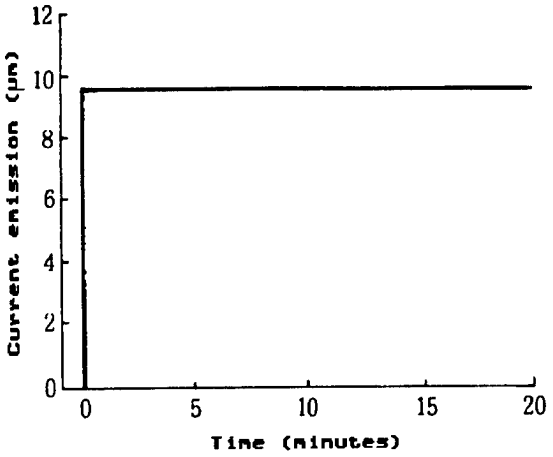

Figure 9. Hourly Variation of Current Emission From Surface Treated TiC<110> Chips
Flush heating temperature: 1,100°C
Surface treatment C_2H_4(100L, 1,100°C) +O_2(20L, 1,100°C),
P = 2.0 x 10^{-9}Pa

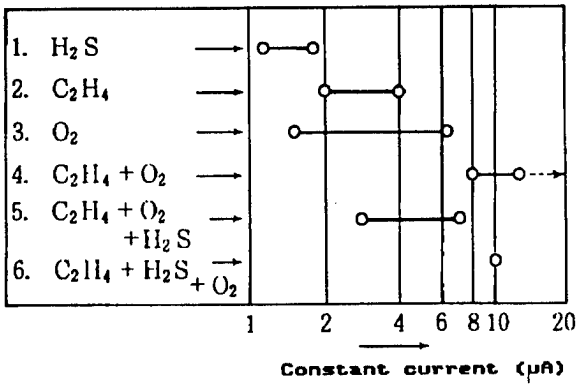

Figure 10. Relationship Between Surface Treatment and Constant Current of TiC<110> Chips
Constant current: maximum total current that does not vary by more than 1 percent during a 20 minute period, P = 3.0 x 10^{-9}Pa

Figure 10 shows current stabilities compared at the same vacuum degree among surface treatment effects of TiC<110> chips. The drawing indicates that hydrogen sulfide (single) gas surface treated chips, for example, are not capable of obtaining any constant currents more than 1 to 2 μA. It is learned from this that multistep surface treatment is superior to single gas surface treatment in providing constant current. C_2H_4 + O_2 two-step surface treatment is better in this respect, i.e., expected to supply more than about 30 μA constant current, provided it is optimum. Increase of vacuum degree causes improvement in stability of the current emission of surface treated TiC<110> chips. Figure 11 shows pressure dependence of the constant current of four kinds of surface treated chips. It shows negative 45°C gradient. This means

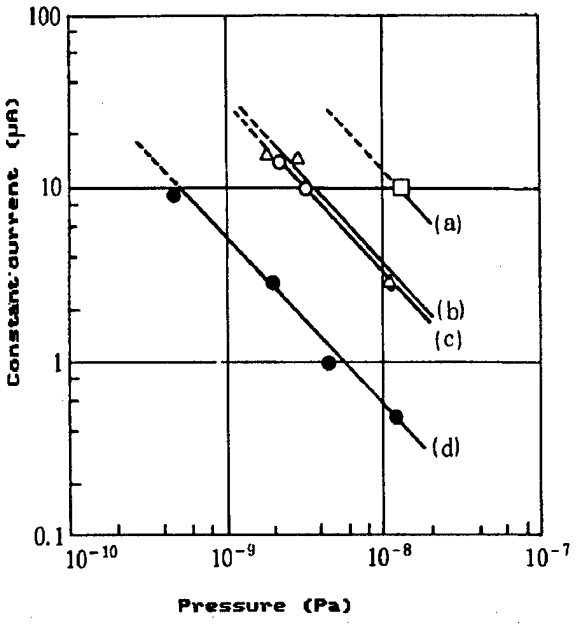

(a) C_2H_4 (500 L, 1,100°C) +O_2 (20 L, 1,100°C),
(b) C_2H_4 (100 L, 1,100°C) +O_2 (20 L, 1,100°C),
(c) C_2H_4 (300 L, 1,050°C) + H_2S (20 L, 1,050°C) +O_2 (20 L, 1,050°C),
(d) H_2S (10 L, 1,100°C).

Figure 11. Pressure Dependence of Constant Current of Surface Treated TiC<110> Chips

that current variation is proportional with product of pressure and current values. This experimental result indicates that ionization of residual gas by emitted current is concerned in generating noise.

Variation of surface treated chip current becomes large when larger current than constant value is emitted or chip environment is at high pressures. The step- and spike-shaped noises generated at this time are considered mainly attributable to the surface atom migration induced by the ions coming into the electron emission range.[18] Namely, it is considered that incident ions (mainly hydrogen) move surface atoms to the semiconstant current site through their excitation and that, after finite time Δt, the same atoms return to the first constant current site. Spike- or step-shaped noises are generated when the time is short or very long, respectively. The surface condition in which surface atom migration does not readily occur, even when ions enter the electron emission range, is imaginable in consideration of the stability of current emission depending on chip surface treating processes at one vacuum degree. It is essential for the field emitters with a very constant electron emission characteristic to form such "stable surface." The multistep surface treated TiC<110> field emitter is considered to nearly satisfy this requirement.

3. Future Prospects

It has become clear that the multistep surface treated TiC <110> field emitter shows such a very constant current characteristic that it can be called noiseless and driftless. On the other hand, it has also become evident that appropriate selection of anode materials and optimum design of anode structures are significant for them to be mounted on field emission type electron sources and that extremely high evacuation of the emitter space is desirable.[3,17] That is, for developing stable field emission type electron sources, it is indispensable to integrate cathode, anode, and vacuum materials and technologies.

Atom order level study of what a change the surface treatment of TiC<110> chips causes to their surface structure and composition is significant for further stabilization of current emission. For this purpose, it would be important to introduce atom probe and other surface study methods. Among anode materials, graphite has experimentally been pointed out to be superior and a new type structure has been proposed for it.[3] Ultrahigh evacuation technology is essential and elementary for high performances of field emission type electron sources. Electron emission has become possible at an ultrahigh degree of 10^{-10}Pa at present. This is considered to exert great influences on other sectors.

Table 2. Performance and Comparison of Various Types of Intensified Electron Sources

	LaB_6 thermionic emission type	W thermionic emission type	W field emission type	TiC field emission type (surface treated)
Brightness (A/cm^2·str)	5×10^6	5×10^5	$10^8 \sim 10^9$	$10^8 \sim 10^9$
Current stability				
Noise (percent)	0.2	0.2	5	0.2
Drift (percent/hour)	1	1	Large	0.1
Energy width (eV)	$1 \sim 2$	$2 \sim 3$	0.2	0.2
Diameter of electron sources (μm)	$10 \sim 15$	25	0.1	~ 0.05
Cathode temperature (°C)	1,550	2,550	Room value	Room value
Vaouum degree (Pa)	$10^{-4} \sim 10^{-5}$	10^{-3}	$10^{-7} \sim 10^{-8}$	$10^{-9} \sim 10^{-10}$
Life (hr)	1,000	50	1,000	(1,000)

Table 2 compares characteristics of various kinds of intensified electron sources. Metal carbides are being studied among thermionic emission materials.[19] Cited are LaB_6 and tungsten that are included among those already put to practical use. Monocrystal tungsten has become practically applicable to field emission type electron sources. As shown, high stability of the surface treated TiC<110> field emitter is evident.

The surface treated TiC<110> field emitter features high brightness, small electron emission energy, and small electron source size as well as high stability. It is therefore expected to contribute to high performances of various kinds of physical and chemical units including low acceleration scanning type, analyzing, and other electron microscopes. Additionally, it

will be mounted on the electron beam drawing systems that will ensure nanometric lithography in the near future. Its new application will be studied to new function electron microscopes, etc., by utilizing interference of electron beam.

FOOTNOTES

1. L.E. Toth, "Transition Metal Carbides and Nitrides," Academic Press, New York, 1971.

2. Inorganic Material Research Istitute Research Papers, No 40, 1984.

3. Ibid., No 48, 1986.

4. Mori, APPLIED PHYSICS, Vol 53, 1984, p 212.

5. I. Kojima and E. Miyazaki, J. CATALYSIS, Vol 89, 1984, p 168.

6. M.R. Beasley and T.H. Geballe, PHYS. TODAY, October 1984, p 60.

7. P.N. Ross, Jr. and P. Stonehart, J. CATALYSIS, Vol 48, 1977, p 42.

8. S. Yoshida and T. Gonda, APPLIED PHYSICS, Vol 50, 1981, p 385.

9. J.D. Parsons, R.F. Bunshah, and O.M. Stafsudd, SOLID STATE TECHNOLGOY, November 1985, p 133.

10. T. Kato and S. Sato, 47th Applied Physics Society Academic Lecture Manuscripts, 1986, p 336.

11. 47th Applied Physics Society Academic Lecture Manuscripts, 1986, p 338.

12. "Fine Ceramics Handbook," ed. by K. Hamano, Asakura Shoten, 1984, p 1021.

13. Y. Ishizawa, S. Aoki, C. Oshima, and S. Otani, Proc. XIth Int. Cong. on Electron Microscopy, 1986, p 223.

14. S. Otani, S. Honma, T. Tanaka, and Y. Ishizawa, J. CRYSTAL GROWTH, Vol 61, 1983, p 1.

15. J. PHYSICAL SOCIETY OF JAPAN, Vol 38, 1983, p 219.

16. APPLIED PHYSICS, Vol 53, 1984, p 206.

17. VACUUM, Vol 29, 1986, p 544.

18. Ibid., p 578.

19. K. Yada, Proc. XIth Int. Cong. on Electron Microscopy, 1986, p 227.

20115/9365
CSO: 4306/7559

MATERIAL DESIGN OF HIGH-PURPOSE GLASS DISCUSSED

Tokyo KINO ZAIRYO in Japanese Mar 87 pp 44-53

[Article by Assistant Prof Itaru Yasui, Tokyo University Production Technology Research Institute]

[Text] 4. Planning Glass Materials

The purpose of glass material planning is to obtain new glass promptly. This paper will deal with its analysis and essence.

4.1 Planning--Intellectual Job

Needless to say, planning is an intellectual job. Intellectual jobs vary considerably, from analysis to planning. Planning belongs to the category of decision making. This will be discussed briefly.

Medical diagnosis, juridical decision making, and trouble diagnosis belong to the analysis category. Their main features are that when an optimum solution is known to exist within a specific range, an intellectual job starts for its choice. In medical diagnosis, for example, there are several hundreds through several thousands of human diseases. The symptoms each of them is known to manifest enables a diagnosis of the disease to be made provided a patient fully displays symptoms in examination. Namely, the subject system of medical diagnosis is closed and its intellectual job is required to select an optimum solution within it. Backward inference process is useful for this purpose. The term "backward inference process" is given to a methodology consisting of assuming diseases as a solution, and applying all of them one by one to decide whether any can elucidate symptoms because it reverses the inherent inference process of deciding a disease in view of symptoms. Subject solutions, i.e., diseases, are assumed to form a closed system. This assumption is permissible because the existence of unknown diseases is, of course, not neglected and symptoms can be diagnosed to show an unknown disease to complete the intellectual job in a way even when not being elucidated by any known diseases.

On the other hand, included among the latter's examples are planning machinery, patterns, materials, and so forth. Their common points are existence of specification requirements and decision of a "construction" for their satisfaction. As to aircraft, for example, there are an infinite number

of solutions for rough specifications of short distance flight type 100-seat passenger planes, provided their structures are classified in full particulars. Namely, the system formed thereby is not closed. Therefore, they are not permitted to adopt backward inference process that is useful for diagnostic type expertise systems. Forward inference process is useful for the system where knowledge has progressed sufficiently for its description without anything missing. It is not applicable, however, to many planning problems because of a limited degree of knowledge. The idea of models is, therefore, adopted to solve such problems. For example, data of passenger planes put to practical use are accumulated. Those of the plane closest to the plan are drawn out and adopted as models when specification requirements have become known. An improvement is made by using it as basic material. For instancey, if data of a 150-seat passenger plane can be examined when a 100-seat one is planned, the former is adopted as the first model and its size reduction is attempted. The drawing of a new structure with reduced overall and wing lengths, for example, is adopted as the next model. In order to examine its appropriateness, it is studied aerodynamically and its strength is analyzed by applying finite element method. If any weakness is found, it is corrected and study is carried out again. The intellectual job is tentatively completed, provided the improvement successfully satisfies the specification requirements. On the contrary, the first model selected out of data bases for the first time is decided to be inappropriate and another passenger plane is drawn out. Even after a solution is obtained by such methodology, there still remains a question on whether it is most appropriate and whether any other more appropriate solution is available. This is, however, essential for planning type decision making problems.

What is described above suggests that planning type decision making problems require more creative intellectual jobs, i.e., are graded higher than analytic ones.

4.2 Definition of Material Planning

The term "material planning" has various meanings for various materials. The first question is what image does it project. According to Yanagida, material planning is divided into three phases:

(1) Search for materials
(2) Practical use of materials
(3) Selecting optimum materials out of material banks

The history of the application of high-temperature, high-strength materials will be discussed with silicon nitride used as the example. Silicon nitride became a candidate for a high-temperature, high-strength material because it was found to maintain its strength even at high temperatures, in light of the high chemical bond strength of nitrogen and silicon, and the structure of its crystal. This was the first phase of planning. Next, at the outset of the study, it was considered that sintering of high covalent bond materials such as silicon nitride might be impossible. Nevertheless, they have been put into practical use improving initiating materials and processes and selecting additives. This was the second stage of planning. In the third phase of planning, the specifications of various firms' products were accumulated in

data banks. In connection with material planning means, the first and second phases are carried out by the brain with intuitive sense and the third has been planned to undergo computerization.

As will be described later, the idea of artificial intelligence (AI) has emerged in the last 1-2 years and it is being put to practical use. In order to forecast the future trend of IA, it is necessary to study computerization as the main subject. Therefore, material planning is defined to be "determination of the structure of a material up to given specifications and selection of a synthesization process for acquiring it."

Nevertheless, it is indispensable to classify material planning at several levels of maturity. Development of materials has a broader sense than their planning. Level classification is made as follows from the former standpoint:

(1) Random, no-principle material development
(2) Material development at empirical law level
(3) Material development at experimental equation level
(4) Material development at theoretical equation level

Conventional computers have an aptitude for numerical computation. In development, therefore, they apply to the materials up to theoretical and experimental equation levels. AI, a system provided with the knowledge sets (bases) similar to mankind's to obtain a capability of decision with inference function, is intended to broaden the scope of application even to abstract problems to which conventional computers have not been applicable. It would then even cover part of material development at the empirical law level, provided the expertise system is constructed by applying it to material development.

4.3 Glass Material Planning and Numerical Computation Methods

As discussed above, glass material planning systems can be divided into AI-oriented high-grade systems and conventional computer systems. Glass material planning and conventional type numerical computation material planning processes are defined in the following. However, the latter are not said to be old. The expertise systems to be described last are also required to be capable of numerical computation.

(1) Unique glass materials

Physical properties of materials originate from their structure. Namely, physical property constant (a) is its function as represented by the equation:

$$a = f(\text{structures})$$

There are various structures. Those of sintering, for example, include such high-order structures as compositions as well as main, sub-, and other crystal grains and their sizes, grain boundaries and line, and other lattice defects, etc.[11] They are called characters. Those of sintering with complicated structures, for example, are very difficult to numerically express. Glass, a homogeneous solid produced by a melting process, has no such high-order

structure as seen with sintering. Besides, it is considered to have an atomic arrangement similar to that of liquid, nothing unique as compared to crystal structures. Moreover, that of liquids does not considerably depend on a history of production. The characters of glass are substantially specified, depending on its composition. For example, the former is well expressed by only the latter. It shows:

$$a = f \text{ (structures)}$$

Glass material planning is carried out to specify the compositions that satisfy requirements of characteristics (physical properties).

(2) Classic method

As already stated, glass permits comparatively easy description of the relationship between compositions and physical properties. Namely, its physical properties have a linear relationship with a limited range of its compositions.

$$p = \Sigma p_i \cdot n_i$$

wherein n_i is mole fraction. In other words, partial molal quantity can be specified for each set of physical properties in some cases.

The volume per unit equation amount can be cited as examples of this specification. Its coefficients have been computed by Huggins and many other researchers.[12]

$$\nu = \Sigma f_i \cdot \nu_i$$

wherein f_i is percent by weight and ν_i is the coefficient. Huggins' coefficient for SiO_2 glass depends on the silicon/oxygen ratio. This indicates that contribution of the atoms to the volume depend on their structures.

Fulcher's equation is known to hold for variation in viscosity of glasses and its parameter linearly varies according to its composition.

$$\log \eta = A + \frac{\beta}{T - T_o}$$

This linear relationship is maintained through the medium of a kind of parameter in some cases, even when such physical properties as volume have no direct linear relationship with composition.

Such a linear relationship as stated above is established at only a limited range of composition. This is effective for bottle and board glasses with a fixed range of composition. Another methodology is necessary when composition systems are unlimited.

Provided data bases of the compositions and physical properties of glass are available, those with new compositions can be estimated by using interpolation

methods with existing data. They include spline, Lagrange's, and various other mathematical interpolation methods. Glass is generally composed of at least three kinds of elements. Some are composed of more than 10 elements. Therefore, there is no appropriate multidimensional interpolation methodology. The author's research room prepared a computation program by spline interpolation. However, it was not considered as always appropriate.[13] At present the author considers it better to compute the coefficient of equation (1) by applying multivariate analytic method.

The method is, of course, applicable only when glasses with similar compositions and physical properties are contained in the data base.

(4) Simulation

The principal method used in analyzing the composition of amorphous materials, is the diffraction method with X-ray, etc. Supplemental to this, is the structural information obtained by the spectroscopic method. It is, however, unavoidable that some problems remain unsolved even in analysis. Computer simulation of molecular dynamics, for example, is useful for studying structural propriety.

Such a computer simulation method has the potential of analyzing structures of materials as well as their various physical properties. Yonezawa mentioned in Table 2 what physical properties can be analyzed with the method.[14] In order to compute their values, motion of each ion is computed and processed on the basis of statistical dynamics.

Molecular dynamic computation requires a very long time. At present, therefore, the method still remains inapplicable to material planning. It will become useful, provided supercomputers are put into daily use in the future.

4.4 Planning Various Functions of Glass

Transparency is one of the most significant features of glass. Optical fibers have been improved to attain extreme transparency. For this improvement, materials are required to be free from 1) scattering, and 2) absorption.

The former comes from an uneven diffraction rate of solids. Being free from boundaries that are seen with sintering, glass is naturally advantageous in this respect. Multicomponent glass, however, poses a problem with variation of its composition and structure. The latter can be divided into 1) impurity absorption, and 2) intrinsic absorption. Intrinsic absorption posed an an initial impurity problem in the course of developing optical fibers, particularly from transition elements. Impurities of transition metals, however, have come down to negligible levels since optical fibers began being produced by the CVD method. The remainder content of water or presence of OH-bases are also problematic. Figure 7 shows the loss curve of the latest optical fibers. It nearly agrees with theoretically computed values.[15] Namely, the spectrum of the oscillation of the silicon-oxygen bond that forms glass structures intrinsically defines long wavelength side absorption.

Table 2. Various Physical Properties That Permit Molecular Dynamic Computation[14]

I.	Structural properties
	(1) Two-body distribution functions
	(2) Structural factors
II.	Thermodynamic properties
	(1) State equations
	(2) Thermal expansion coefficient
	(3) Enthalpy
	(4) Fixed pressure specific heat
	(5) Voluminous compression ratio
III.	Dynamic properties
	(1) Speed self-correlation function
	(2) Oscillation spectrum
IV.	Transport properties
	(1) Diffusion coefficients
	(2) Viscosity
V.	Microscopic structural information
	(1) Volume distribution of Boronoy polyhedrons
	(2) Shape parameters of Boronoy polyhedrons

Compositions of infrared ray transmitting fibers will be discussed in light of what has already been described. In infrared ray transmitting fibers transmission light increases in wavelength on the shift of oscillation absorption spectrum frequency toward the long wavelength side. It is fixed by mass and bond strength of atoms as expressed by equation:

$$\omega_f \propto (k/\mu_R)^{-1/2}$$

wherein μ_R is the converted mass and k is the bond strength.

The equation indicates that it is necessary to select the compositions of heavy atoms with small bond strengths. Fluorides (ZrF_4, HfF_4, etc.) and calcogenides (AsBs, etc.) are included among the heavy metals that satisfy this requirement and form glass. Among fibers, fluoride fibers have progressed in this direction. Figure 8 shows the theoretical absorption curve of various glass.[5] As is learned from this, fluoride fibers must attain a one digit smaller loss than quartz fibers with a theoretical limit of 0.2 dB/km. However, it is noticed that they are difficult in some respects to put into

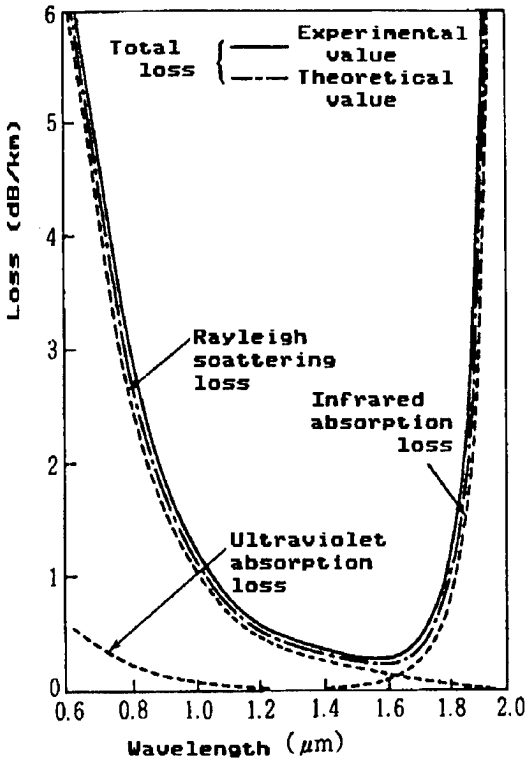

Figure 7. Loss Spectrum of Fibers Not Containing OH1[5]

Practical use. As will be stated later, selection of materials with small bond strength involves a decrease in strength of fibers and increase of thermal expansion coefficient. They are more difficult to handle than quartz fibers.

(2) Diffraction index and diffusion

A variety of glass is capable of creating new functions when the diffraction index in materials of optical fibers, rod lenses, optical waveguide courses, etc., is intentionally varied. Its control is significant for classic type optical glass. A number of studies have been carried out to solve problems in this connection.

Theoretically, provided ions cause no great interaction, diffraction index n of materials can be expressed by equation:

$$\frac{n^2 - 1}{n^2 + 2} = \frac{4\pi}{3} \Sigma N_i \alpha_i$$

wherein α is molecular polarizability of ions and N is the number of ions per unit volume. For obtaining high diffraction indexes, it is necessary to select the glass containing the atoms with high ion polarizabilities first of all. Table 3 shows the molecular polarizabilities of several kinds of ions.[16] Negative ions show higher polarizabilities than positive ones. Among the

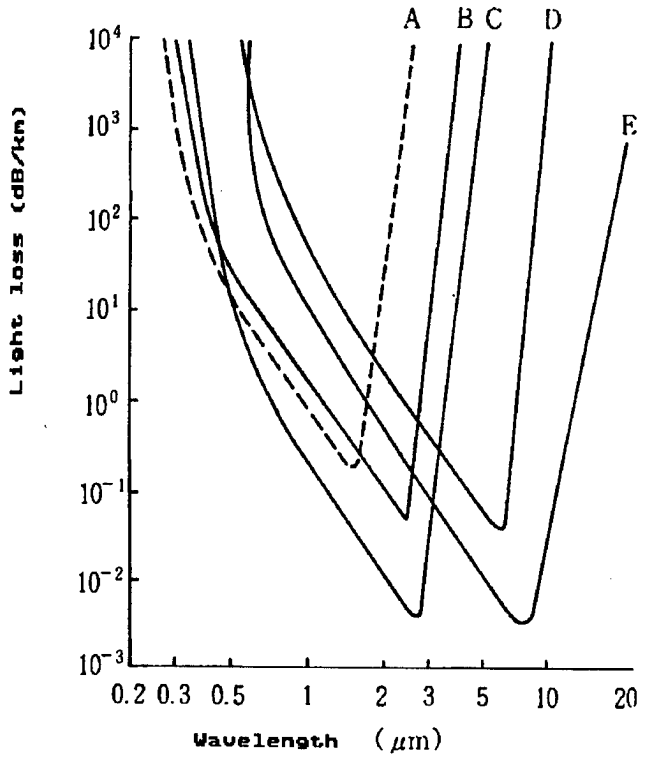

Figure 8. Theoretical Loss Spectra of Quartz Glass Optical and Representative Infrared Fibers
A: quartz glass optical fibers
B: heavy metal oxide glass optical fibers
C: fluoride glass optical fibers
D: chalcogen glass fibers
E: heavy metal halide crystal fibers

former, those with larger radii show higher polarizabilities. Cesium or thallium containing glass is, therefore, advantageous in this connection. For practical purposes, however, those containing such elements as barium and lead are produced with consideration given to their chemical durability, etc.

Diffraction index distributed lenses show a radial distribution of diffraction indexes, those of the central part of their thin circular surface being higher than those of their peripheral part. For constructing such glass, it is necessary to show a difference between element compositions of the peripheral and central parts, i.e., give a high concentration to the highly polarizable ions at the latter and lower concentrations to those at the former. Ion exchange, molecular stuffing, CVD and other methods can be used to give such a concentration distribution. Among them, the first, the most common method, is described. Ion exchange of glass is observed with the highly mobile monovalent positive ions therein. For obtaining a concentration distribution through ion exchange, it is inevitable to change the concentration distribution of monovalent positive ions. For this purpose, a glass containing the monovalent positive ions with high polarizabilities should be

Table 3. Polarizability of Various Kinds of Ions

Ion	Polarization of electrons (10^{-30} m^3, Å^3)
Li^+	0.03
Na^+	0.41
K^+	1.33
Rb^+	1.98
Cs^+	3.34
Tl^+	5.20
Mg^{+2}	0.09
Ca^{+2}	1.1
Sr^{+2}	1.6
Ba^{+2}	2.5
Zn^{+2}	0.8
Cd^{+2}	1.8
Pb^{+2}	4.9
La^{+3}	1.04
B^{+3}	0.003*
Al^{+3}	0.052*
Si^{+4}	0.016*
Ti^{+4}	0.18*
O^{2-}	6.2**

*Values estimated by author and others.
**Estimated value of cross-linking oxygen-noncross-linking oxygen shows about 1.3 times as large a value.

prepared and a desired concentration distribution should be given through its ion exchange in a melted salt continuing those with low polarizabilities. Use of the two kinds of monovalent positive ions with nearly the same radii, however, are recommendable for ease of ion exchange. Since the radius and polarization index of ions have a correlation as stated above, similar kinds of elements do not have nearly the same radii but considerably different polarizabilities. Thallium$^+$ ions have been selected to satisfy this requirement. Since thallium belongs to the IIIB-family, it is considered, in light of its original electron arrangement, to produce trivalent ions. It can, however, produce monovalent positive ions in the form of thallium nitrate ($TlNO_3$). As is learned from the table, Tl^+ ions show a considerably high polarizability. Potassium$^+$ ions (1.33Å) and lead$^+$ ions (1.47Å) are included among the alkaline ones that can serve as counterpart to the positive ions in exchange because the latter's radius amounts to about 1.4Å. For their production, Tl^+ ion containing glass is melted and molded columnar and a diffraction index distribution is given by processing it in a melted salt (nitrate) containing potassium$^+$ ions, etc.

Diffusion as another important parameter in planning optical lenses comes from the absorption at the ultraviolet range of glass. The glass, containing a large amount of lead, is colored yellow in some cases where it absorbs ultraviolet rays. This absorption depends on the condition of electrons, i.e., it can be considered to depend on elements. Therefore, such elements as lead cannot be used to reduce diffusion. Classic optical glass requires the use of lead for an increase in diffraction index. Glass containing lead causes an increase of diffusion index with that of its content. Therefore, no-lead lanthanum glass, etc., has been developed and applied for optical purposes.

A plotting has been prepared by specifying the point of each optical glass on a plane with two parameters--diffraction index (n) and Abbe number inverse with respect to diffusion--of optical glass taken on x- and y-axes. Manufacturers have prepared vector data of direction and distance of shift of characteristics of optical glass on addition of a desired compound to its basic composition for use in planning new ones.

(3) Thermal characteristics

Softening temperature and thermal expansion coefficient can be cited among the required thermal characteristics for glass. The development history of heat resistant glass is the same as that of high softening, low expansion glass aimed at quartz glass.

The philosophy of planning low expansion glass is discussed below. Thermal expansion comes from the inharmoniousness between bond energies of atoms, i.e., gradient being sharp or gentle in the direction of their bond distance being smaller or larger, respectively, than equilibrium distance. Inharmoniousness of bond has a negative relationship with its strength. While diamond, for example, that is representative among the materials with high bond strength, shows a thermal expansion coefficient of 10×10^{-7}, that of soft alkali metals is about 50 to 100 times as high. For obtaining glass with low thermal expansion coefficients, it is necessary to increase the strength of chemical bonds. Many types of glass contain SiO_2 and Na_2O. Silicon-oxygen has a bond strength of about 106 kcal/mol and sodium-oxygen about 20 kcal/mol. Increase occurs in the thermal expansion coefficient when such weak bonds are present. In this connection, the primary requirement is to select glass without any alkaline components. These, however, are considerably difficult to melt for producing glasses. When aluminum, boron or another trivalent element is added, sodium-oxygen ion bonds of solids are replaced with the bonds containing aluminum-oxygen covalent at high ratios. Such a structural change is observed in silicate ores. On the other hand, it has been elucidated in the latest analysis of glass structures that amorphous materials such as glass cause substantially the same structural change as crystals.[17] For producing borosilicate and aluminosilicate glass, their compositions have been so planned as to add such a trivalent element. This theory on glass gives a useful guideline in planning glass compositions.

There are other thermal coefficient factors other than bond strength. This becomes clear in observing thermal expansion coefficients of other crystals. Quartz crystal as monopolycrystalline type SiO_2 shows two kinds--α and β--

crystalline structures. Although both have silicon-oxygen chemical bonds, the latter shows a negative thermal expansion coefficient. This indicates that the thermal expansion coefficient is not only a property of chemical bonds but also a quantity whose change is considerable on atom arrangement, i.e. structure. A long time ago, it was thought that, depending on properties of chemical bonds, thermal expansion coefficient is susceptible to addability like volume and study was busily carried out to estimate factors from this standpoint.[18] However, the idea is not always effective since thermal expansion coefficient depends not only on composition of glass but also on its structure. Therefore, necessary for its numerical computation is a program that estimates new compositions by that of the contribution of each of the oxides of the materials with nearly glass structures. This will be studied in the future since it requires a considerably enormous data base.

It is considered that there are comparatively few structural factors in the softening point, another physical property, of glass since their deformation is theoretically considered to start at a weak chemical bond part. It requires specification of the parameters of the Fulcher equation as stated above because it reflects their viscosity. It is, therefore, practical to forecast that of a new glass by applying the multivariate analysis method to the data of comparatively similar compositions that are selected from a data base.

(4) Other characteristics

Hardness, Young's modulus, and other mechanical properties of glass characteristics can be discussed in connection with the theories on their chemical bonds and structures. Their strength is difficult to plan because, in many cases, their breakdown starts at fine surface flaws so it rather depends on their surface condition than being included among their inherent properties.

The glass to be crystallized permits its properties to be controlled by selecting the crystals to be produced. The crystallized glass containing such crystal with a high bonding strength as mica, for example, allows machining by a lathe, a drill, or the like. Low thermal expansion crystallized glasses are obtainable by crystallizing eucryptite ($Li_2O \cdot Al_2O \cdot 2SiO_2$), for example. Planning is thus possible to some extent by selecting a phase of the crystal produced from glass.

As to ion conductivity and diffusion coefficient of other characteristics of glass, specification of a species being conducted and estimation of their mobility are possible to some extent with a simulation method. At present, however, it is not practical since even supercomputers require a long time for their computation. Chemical durability of glass would be most difficult to plan among its characteristics because it is considered to be connected with various factors such as diffusion of ions, properties of chemical bonds, properties of surface, etc.

As described above, glass planning is at various levels--numerical planning level, knowledge-base-oriented level, and future study awaiting level. All levels, however, are desired to build up data and knowledge bases as the foundation of material planning.

4.5 Feasibility of New Glass Material Planning Support Expertise Systems

Buildup of various expertise systems is going to start by applying AI. The systems will, of course, be applied to material planning. Their feasibility is discussed below only in connection with glass material planning.

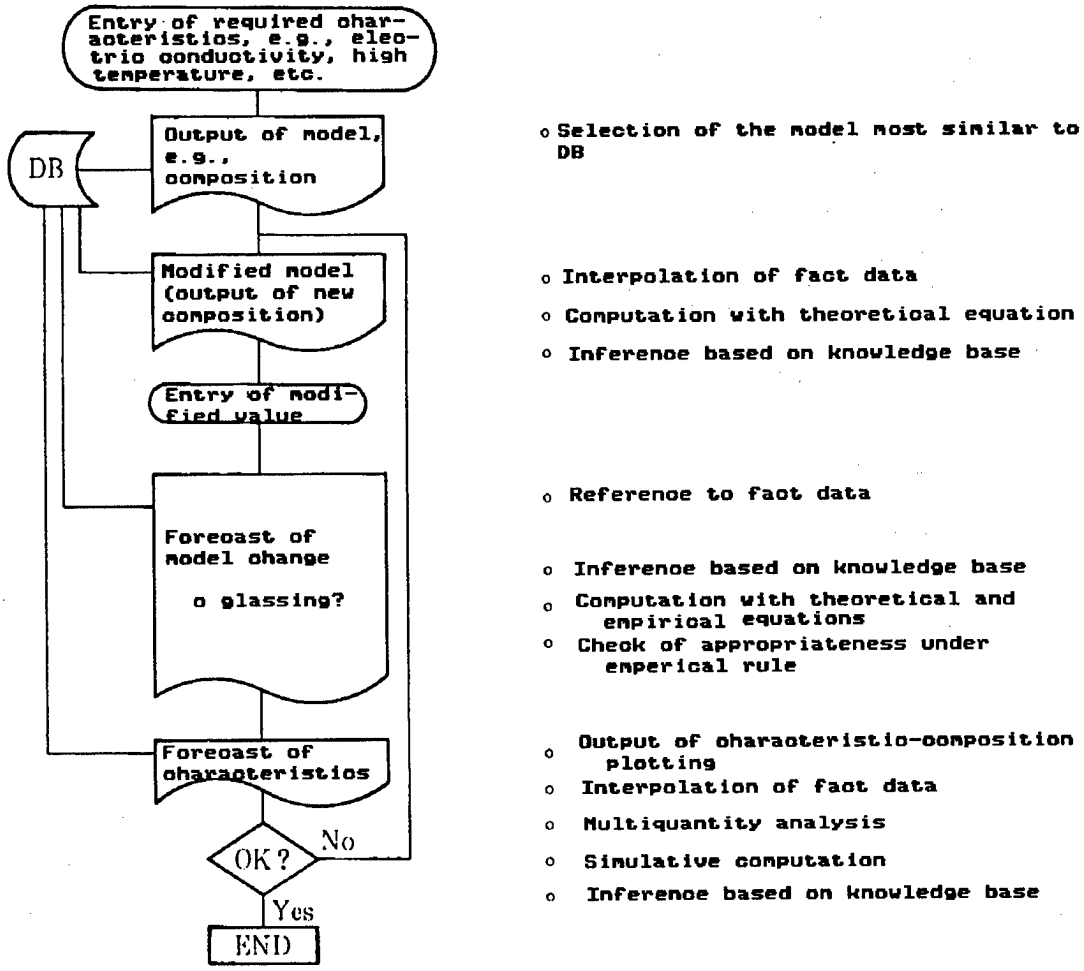

Figure 9. Example of Material Planning Procedure

Buildup of glass material planning support expertise systems involves the idea of models that is stated in section 4.1. Figure 9 is a possible flow chart. It is necessary to provide the composition-physical property and composition-glassing data base describing what physical properties the glass with certain compositions have and whether the materials with certain compositions are glassed. When the required specifications are entered in an expertise system, the glass compositions most similar are selected for the operator. The first model is thus prepared. The system computes how to change the composition to the required specifications and so notifies the operator. The operator makes a decision, based on the provided data, and gives an instruction to

change the composition. The system then computes possible physical properties of the new glass composition obtained by this change, decides whether it can be glassed, and notifies the operator of the results. The operator further changes the composition if necessary. Glass composition can be optimized in this process.

The advantages to building up expertise systems are as follows. If a data bank is enriched, a new composition similar to existing ones will efficiently be discovered. However, it might not be useful for finding out a new composition for which no search has been attempted, but it will quickly supply information to assist a researcher's intuition. The systems that contain patient information, etc. will also be useful in practical application.

Hardware units of such expertise systems are required to be capable of numerical and character display as well as graphic display that assists intuition. Besides, it is thought that dispersed type systems should be selected for this purpose because large-size computers are not considered practical in light of the latest progress of systems and their price. Their data bank would have more than several megabyte capacities. It is indispensable for researchers to improve material planning support systems in competency by occasionally adding their own unique glass data. Dispersed type systems would be ideal and practical in this respect, permitting buildup of unique data banks belonging to individual researchers and groups. Computers with capacities several times as large as the existing personal computers for MS-DOS, called engineering work stations (EWS), would be suitable for this purpose. Such EWS units are now lower priced although they were once expensive. Within 1-2 years, they would become applicable to glass material planning support expertise systems. They are forecast to have such specifications as shown in Table 4. Several have cleared them even at present. For constructing a dispersed type system, each EWS would be installed for each research group and would be interconnected by a local area network (LAN) and connected with other institutions by communication circuits.

Table 4. Specifications of Work Stations for Glass Planning

32-Bit CPU:	80386, 68020, 68030, etc.
Computation speed:	more than 4 MIPS
Floating decimal point arithmetic logic element:	80387, 68881, etc.
Memory:	more than 8 megabytes (virtual memory provided)
Graphic display:	more than 1,000 x 1,000 dots
Hard disk:	more than 1 gigabyte
CD-ROM:	1 unit
Optical disk file:	optional
Operation system:	UNIX or its variation

It has already been decided that research on a knowledge base system for material planning starts this fiscal year under the Science and Technology Agency's new 3-year project on the promotion coordinating budget. It is intended to put a C-language knowledge base system for chemical materials at large in operation with various EWS units. The knowledge bases to be built

naturally differ depending on object materials. Under the project, the knowledge bases for this purpose would be studied to some extent but the data bases to be referred to in material planning would not be built up at all. For practical use of such systems, it would become necessary to build up data bases. Anticipating this situation, the New Glass Forum is studying buildup of a data bank.

FOOTNOTES

1. I. Yasui and H. Kawazoe, "High Functional Glasses," Tokyo University Press, 1985.

2. H. Kita, et al., J. AM. CERAM. SOC., Vol 54, 1971, p 321.

3. M. Oikawa, et al., APPL. OPT., Vol 21, 1982, p 1052.

4. T. Moriyama, et al., 6th ECOC, 1980, p F11.

5. S. Takahashi, OPTICS E, Vol 34, 1982, p 70.

6. S.E. Miller, BELL SYST. TECH. J., Vol 48, 1969, p 2059.

7. K.M. Prewo, et al., J. MATER. SCI., Vol 17, 1982, p 1201.

8. K.M. Prewo, Ibid., p 3549.

9. S.D. Stooky, IND. ENG. CHEM., Vol 45, 1953, p 115.

10. H. Yanagida, CERAMICS, Vol 19, 1984, p 417.

11. I. Yasui, Ibid., p 436.

12. M.L. Huggins, J. AM. CERAM. SOC., Vol 26, 1943, p 4.

13. K. Shiraishi and I. Yasui, 24th Ceramic Industry Fundamental Discussion, 1c 01, Sendai, 1985.

14. F. Yonezawa, et al., "Topological Disorder in Condensed Matter," Springer, 1983, p 80.

15. F. Hanawa, et al., ELECTRON. LETT., Vol 16, 1980, p 699.

16. H. Kita, et al., J. AM. CERAM. SOC., Vol 54, 1971, p 321.

17. N. Aoki, et al., PHYS. CHEM. GLASSES, Vol 27, 1986, p 124.

18. K. Takahashi, J. CERAMIC INDUSTRY ASSOCIATION, Vol 63, 1955, p 142.

20115/9365
CSO: 4306/7559

PRESSURE INDUCED PHASE TRANSITIONS, SUPERCONDUCTIVITY OF PHOSPHORUS DESCRIBED

Tokyo KINO ZAIRYO in Japanese Mar 87 pp 56-63

[Article by Assistant Prof Ichimin Shirotani, Muroran Institute of Technology Engineering Department, and Haruki Kawamura, Metallic Material Engineering Research Institute (presently Himeji Institute of Technology); first paragraph is editorial introduction]

[Text] As temperature and pressure release its molecularity, phosphorus changes in the following order: white to red, rhombic black, rhombohedral black, and simple cubic. During this transition, the physical properties of phosphorus change considerably. In particular, phosphorus shows the highest superconductive transition temperature (Tc = 13°K, on set--17-18°K) among separate elements. The relationship of its structure and superconductivity is discussed in this article.

1. Introduction

Attention is drawn to black phosphorus as a new electronic material of narrow gap semiconductors. In Japan, a large-sized monocrystal of black phosphorus was grown for the first time in the world. Interesting results have been obtained in its physical properties as research progressed. These results have been published in the "Special Edition on Black Phosphorus" of MONTHLY PHYSICS.[1]

It was previously reported[2] that as temperature and pressure release its molecularity, phosphorus changes as follows: from white to red, rhombic black, rhombohedral black, and simple cubic. Meanwhile, it correspondingly changes physical properties to an insulator, a semiconductor, a semimetal, and a metal.[2] This paper will deal with the behavior of this change, particularly its pressure induced phase transition and abnormal superconductivity.

2. Synthesization of Black Phosphorus and Growth of Monocrystal

Black phosphorus was synthesized by Bridgman in 1914.[3] White phosphorus changes to amorphous or polycrystalline black phosphorus when heated at 1.2 GPa (12-k-bar, 12,000 atmospheric pressure) at low (about 120°C) or high (more than 200°C) temperatures, respectively. They can be synthesized from red phosphorus at the same pressure. However, this requires a higher temperature than that from white phosphorus. The direct conversion of red

phosphorus into black at about 8 GPa and room temperature is also possible. Table 1 shows the transition process of phosphorus. Bridgman's method is not suitable for growing monocrystal. The authors have successfully grown large-sized monocrystal black phosphorus by using a bevel driven cubic angle type high-pressure generator. For this purpose, a hole was drilled in a 21-mm or 41-mm edge pyrophyllite cube, a cylindrical graphite heater was inserted therein, and a capsule filled with red or black phosphorus was inserted. It was then melted at about 2 GPa or 1 GPa for the 21-mm or 41-mm cube, respectively, and slowly cooled. Phosphorous-arsenic alloys were also synthesized by applying the same method.

Table 1. Conversion Process of Phosphorus

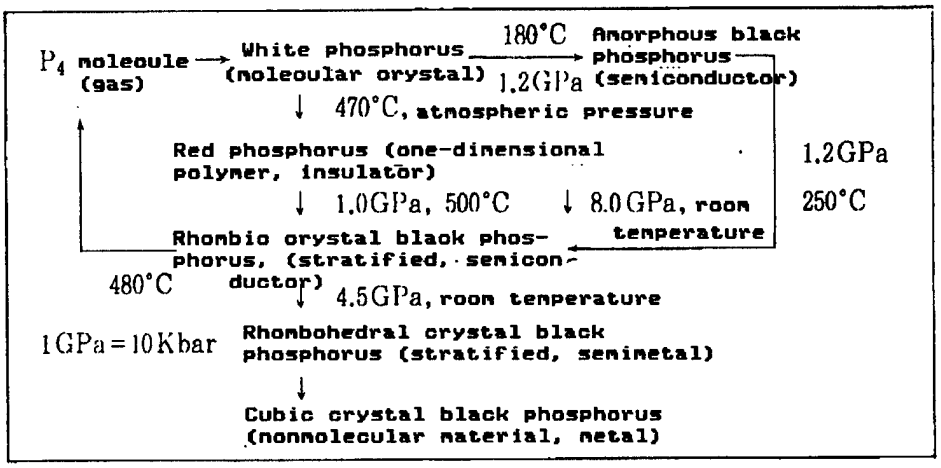

3. Pressure Induced Phase Transition

Black phosphorus, a stratified rhombic crystal at atmospheric pressure and room temperature, changes phase to the rhombohedral crystal (arsenic type structure) at about 4.6 GPa and to the simple cubic crystal at about 10 GPa. Many discussions have been held about the mechanism of this transition.[6-8] This aspect will not be described further in this article. This phase transition is considerably dependent on static water pressure. Figure 1 shows the X-ray diffraction pattern at room temperature and around static water transition pressure. It was measured by applying an energy diffusion method with the High Energy Research Institute's orbitally radiated beam. Used in the experiment were a DIA cubic anvil high-pressure generator, MAX80, and the 4:1 mixture pressure solvent of methanol and ethanol. The X-ray diffraction pattern occurred intensively between 4.44 GPa and 4.77 GPa. However, the peak of rhombic crystal remains at temperatures up to about 5.8 GPa and the rhombohedral and rhombic crystals readily coexist even at static water pressure. However, at semistatic water pressure, where the pressure solvent is solid, a different result is obtained by using the same high-pressure generator. Namely, the pressure of transition slightly rises to the high value side, its speed becomes very low, and the two phases readily coexist. This coexistence is observed at pressures of 4.8 to 8 GPa.

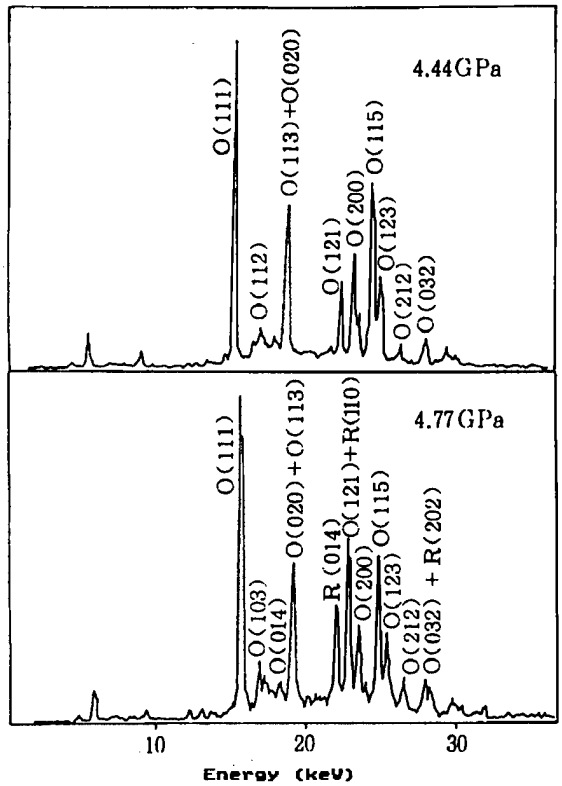

Figure 1. X-Ray Diffraction Pattern of Black Phosphorus at Room Temperature and Static Water pressure
O: rhombic crystal; R: rhombohedral crystal

Figure 2 shows an X-ray diffraction pattern of black phosphorus at liquid nitrogen temperature and high pressure. The energy diffusion method was used together with the orbitally radiated beam for its measuring also. A diamond anvil type high-pressure generator that permits variation at low temperature was used. The pressure value was fixed from the location of the NaCl diffraction peak at high pressure. At less than 77°K, the transition from rhombic crystal to rhombohedral crystal starts at about 6 GPa. It is slower than that at room temperature and both phases coexist until pressure becomes high. With the simple cubic crystal, this begins at about 10 GPa. Around this pressure, three phases--rhombic, rhombohedral, and simple cubic crystals--are considered to coexist.

This summer, the X-ray diffraction of black phosphorus was studied at temperatures less than about 11°K by using the orbitally radiated beam and a diamond anvil type high-pressure generator in combination.[9] This ultralow temperature and high pressure theory has not been examined extensively worldwide and many problems are yet to be solved. No definite conclusion, therefore, has been drawn, but several interim results have been obtained. The transition from rhombic crystal to rhombohedral crystal starts at about 10 GPa. The simple cubic crystal is dominant at more than 16 GPa. Figure 3 shows an X-ray diffraction pattern of black phosphorus at ultralow temperature

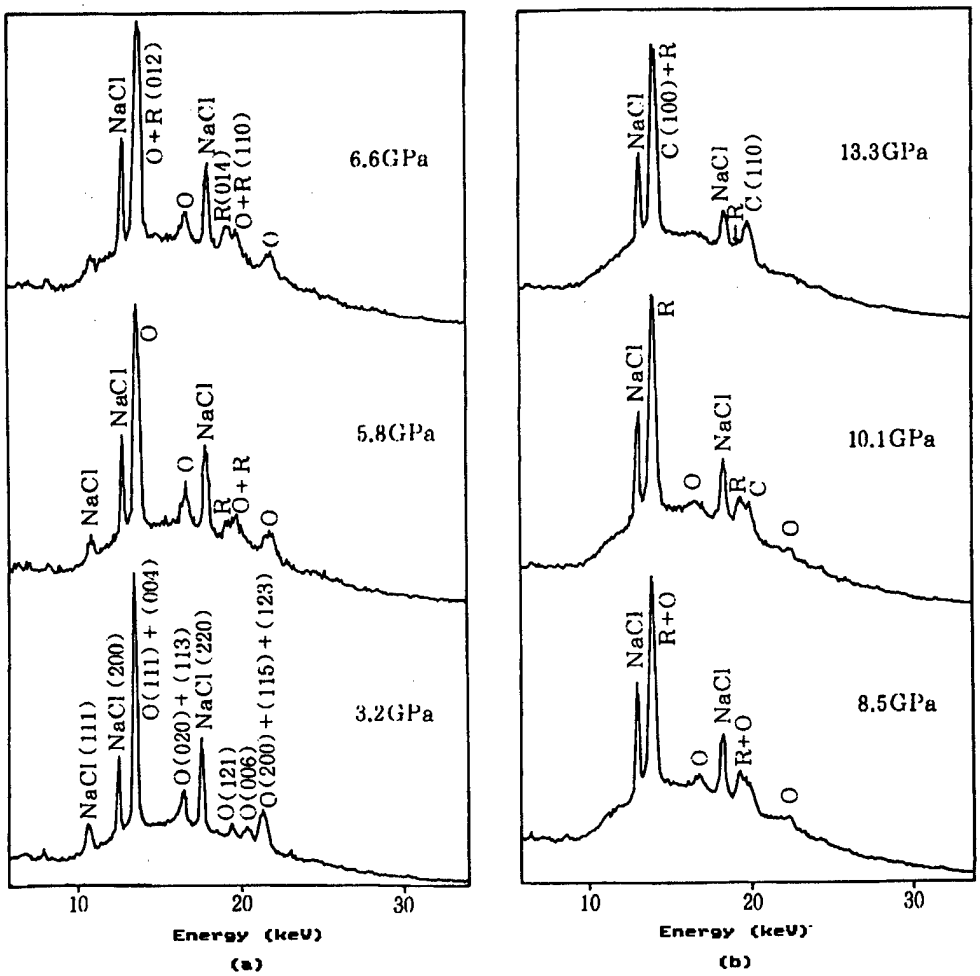

Figure 2. X-Ray Diffraction patterns of Black Phosphorus at Liquid Nitrogen Temperature and High Pressure
O: rhombic crystal; R: rhombohedral crystal; C: simple cubic crystal

and more than 25 GPa. The main peak comes from the simple cubic crystal. Besides, the peaks considered attributable to the rhombic crystal are also present.

At ultralow temperature, the same thing occurs as the change from rhombic crystal to rhombohedral and simple cubic crystals at room temperature. Rise of transition starting pressure, however, occurs with a decrease of pressure. Besides, ultralow temperature shows a wider coexistence pressure range than room temperature. The pressure applied at ultralow temperature is far from static water pressure. Nonstatic water pressure plays a significant role in the transition at low temperature.

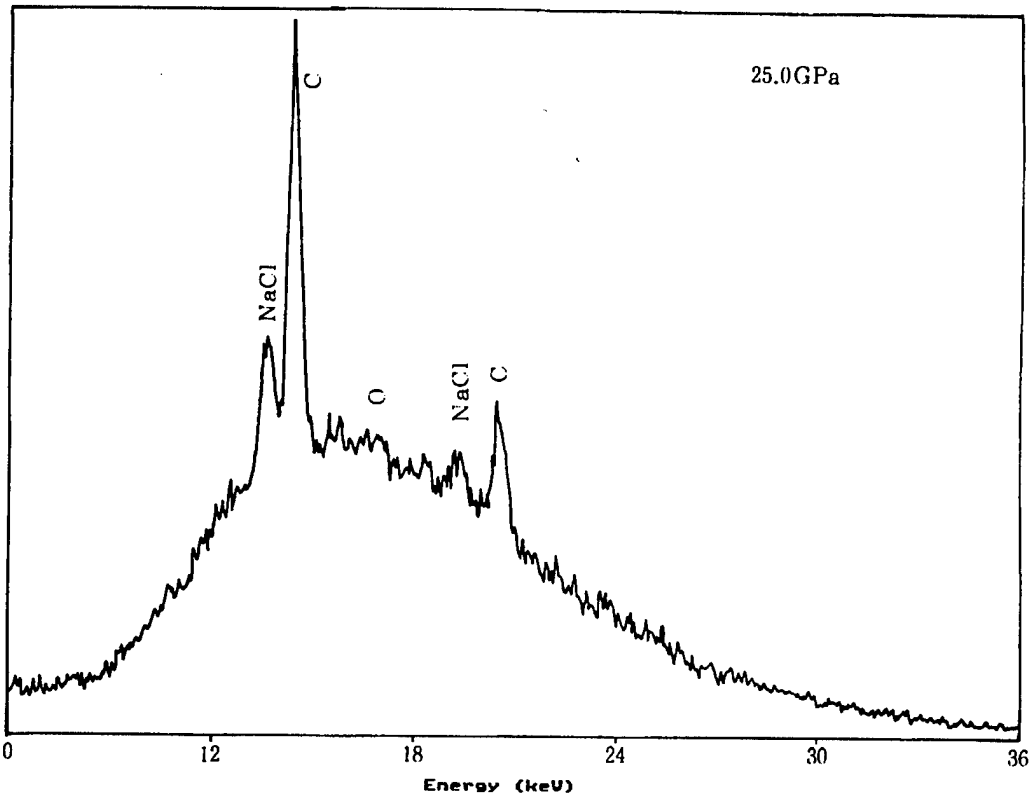

Figure 3. X-Ray Diffraction Pattern of Black Phosphorus at Ultralow Temperature and 25 GPa

4. Abnormal Superconductivity

Silicon, germanium, phosphorus (black), selenium, and tellurium are representative semiconductor elements in the periodic law table. In the 1960s, rapid progress of the study of these separate elements occurred thanks to the status of high-pressure technology with semiconductor-metal transition at high pressure attracting attention. A check of whether the semiconductor elements generated at high pressure are superconductive at ultralow temperature and high pressure was made for that of whether their high pressure phase is a metal. It was found that silicon and germanium or the simple cubic crystal of black phosphorus become superconductive at 3 to 6°K, respectively, and that selenium and tellurium become the same.[10] This has not been studied in detail because of technical difficulties at ultralow temperature and high pressure. Lately, the diamond anvil type high-pressure generators and other high-pressure technologies have advanced considerably so the superconductivity at ultralow temperature and ultrahigh pressure has been examined more thoroughly.[11] The following very interesting phenomena have been discovered: superconductive transition temperature (Tc) of black phosphorus significantly depends on the pressure application routes in the pressure-temperature correlation diagram. The relationship between its superconductivity and pressure induced transition will be discussed.

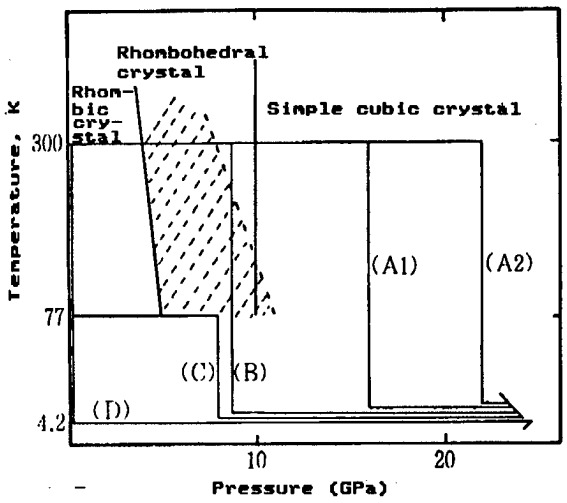

Figure 4. Schematic Condition Drawing of Black Phosphorus and Pressure Application Routes
(Broken line: coexistence range)

Figure 4 is the state of black phosphorus schematically as well as the pressure application routes for measuring its superconductivity. At route A1, the simple cubic crystal was generated by increasing pressure to 16 GPa and cooled to 4.2°K, its superconductivity was measured, and Tc was measured with pressure increase repeated at 4.2°K. Route A2 underwent the same experiment as A1 after increasing pressure to 11 GPa at room temperature. At route B, the rhombohedral crystal was generated with pressure increased to 8.7 GPa at room temperature, Tc was measured with pressure decreased to 4.2°K, and pressure was increased. At route C, the rhombic-rhombohedral coexistence phase was generated with pressure increased to 8 GPa at liquid nitrogen temperature, temperature was lowered to 4.2°K, and Tc was measured. At route D, temperature was lowered to 4.2°K at atmospheric pressure, and Tc was measured while pressure was increased.

Figure 5 shows the pressure dependence of Tc that was measured at the five routes. At routes A1 and B, Tc rises only slightly when pressure is applied at about 6°K. Route A2 was the same, in that a high Tc value was obtained although pressure was applied after producing the simple cubic crystal. Routes C and D show different Tc values at low pressure and high Tc values above 102°K at high pressure.

Wittig, et al.,[13] measured the superconductivity of black phosphorus while constantly increasing pressure at room temperature. The results of this measuring and the pressure dependence of Tc at route D are shown in Figure 6. They observed its superconductivity with temperature lowered to 4.2°K after increasing pressure at room temperature and obtained the pressure dependence of Tc with temperature raised to room value and, after increasing pressure, lowered to 4.2°K again. Tc rapidly rises with the increase of pressure, becomes maximum at about 12 GPa, lowers a little, rapidly rises again, and lowers again at about 23 GPa. As Shown in Figure 1, black phosphorus has a

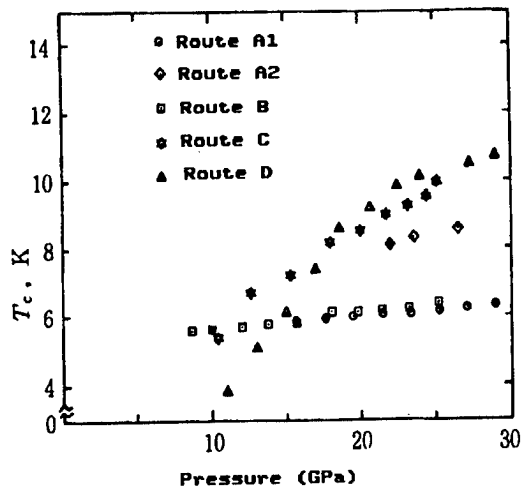

Figure 5. Pressure Dependence of Tc Measured at Five Pressure Application Routes

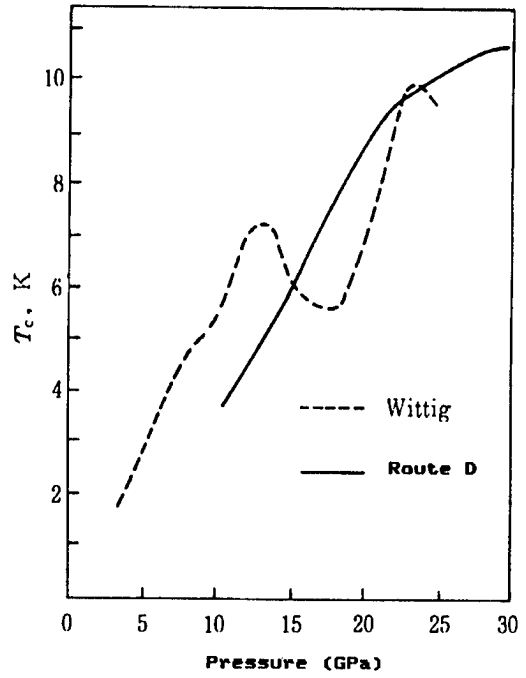

Figure 6. Pressure Dependence of Tc Measured at Wittig's Route and Route D

rhombic crystal structure at 4.4 GPa selected for their observation of its superconductivity. A small amount of its rhombohedral crystal may be mixed in, depending on the pressure solvents and methods. Its greater part is, however, accounted for by the rhombic crystal. Conversely, at about 10 GPa, where it started measuring its superconductivity at route D, the transition from rhombic crystal to rhombohedral crystal starts at ultralow temperature, the former still accounting for a great part. The Tc measured at this pressure is higher than that obtained by Wittig, et al., at 4.4 GPa. This is

attributable to a small amount of the rhombohedral crystal being mixed in. It should be noted that route C, where the rhombic and rhombohedral crystals were intentionally mixed, showed a higher Tc value than route D at low pressure. It is mostly covered by the rhombohedral crystal at room temperature and 8 to 10 GPa and at ultralow temperature and 13 to 15 GPa. There, Tc measured 5 to 6°K as is learned with Route A. However, Tc value rapidly increases when pressure comes above 20 GPa. Route D shows neither the maximum nor minimum Tc values obtained by Wittig. This is considered to be closely connected to the fact that pressure application at room temperature is more suited for coexistence than that at 4.2°K. Besides, it is interesting that his routes show the maximum Tc value at about 10°K and tend to lower Tc at higher temperatures. On the other hand, route D continues to further rise Tc, approaching about 11°K. This difference suggests that the high Tc values of its superconductivity are considerably dependent on the simple cubic crystal.

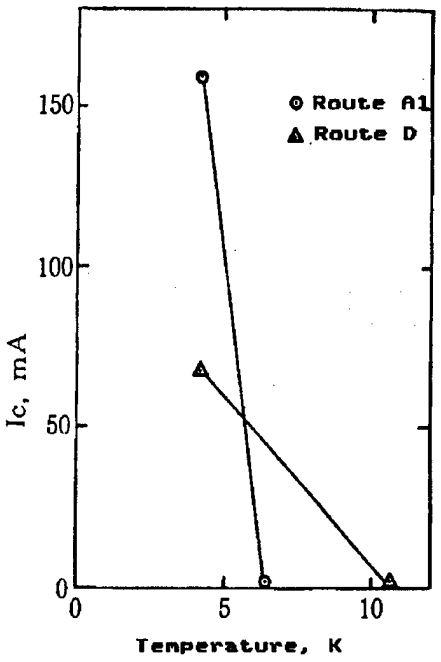

Figure 7. Temperature Dependence of Limit Current at Route A1 at 29 GPa

Figure 7 shows the temperature dependence of the limit currents at routes A1 and D at 29 GPa. Their difference is considerable, although that of the limit current density at 4.2°K is very small. This indicates that the routes are by no means in the same condition, even at as high a pressure as 29 GPa.

Figure 8 shows the behavior of the superconductive transition obtained when pressure is applied to route D by using a high purity red phosphorus as the departing material. It is considered that the same result may be obtained as route D because red phosphorus changes to black phosphorus at high pressure. Red phosphorus as the departing material, however, raises Tc to 13°K far more rapidly than black phosphorus Of on-set temperatures, as high a transition is not considered possible for a separate element, i.e., 17 to 18°K has been

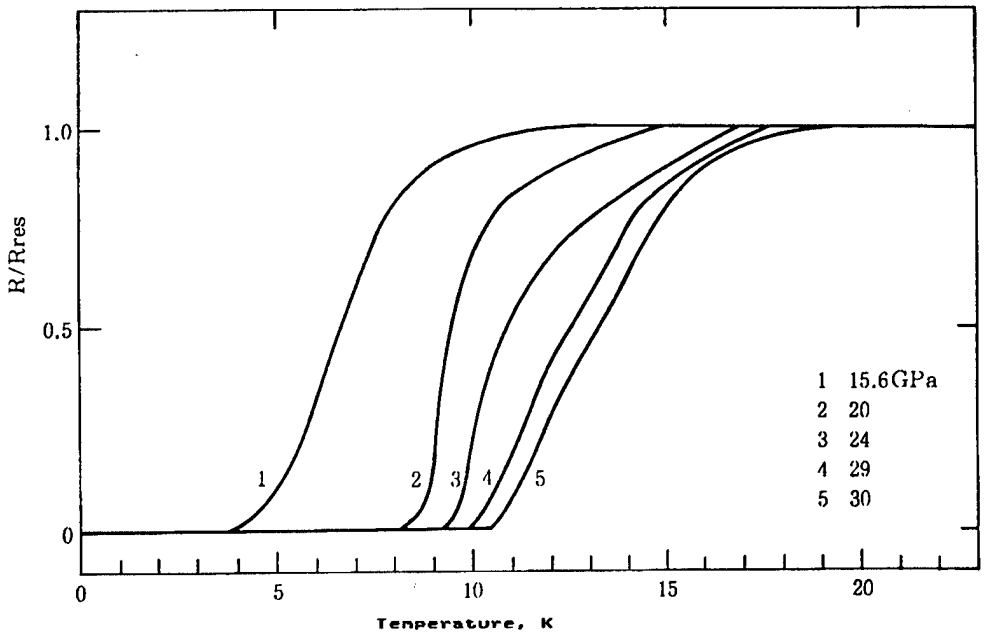

Figure 8. Superconductive Transition of High Purity Red Phosphorus as Departing Material on Pressure Application at Route D

obtained. Recently, Yokovlev, et al.,[14] USSR, published the same result by using quite a different high-pressure generator. Red phosphorus has no specific structure and is divided into crystalline and amorphous examples. It is converted directly into black phosphorus in its existing condition. As a departing material it shows a higher inhomogeneity than black phosphorus because the former requires one more phase transition than the latter. There is a great possibility of it causing high Tc superconductivity.

Figure 9 shows the dependence of the Tc of black phosphorus-arsenic alloys on pressure. It was obtained in the experiment on the same route as route D of black phosphorus. The alloy in the drawing shows the same rhombic crystal structure as black phosphorus at atmospheric pressure. It shows a higher pressure side rhombohedral crystal transition point than black phosphorus. Its shift to the high-pressure side occurs with the increase of arsenic content. The alloy, therefore, begins showing superconductivity at a higher pressure than black phosphorus. It has not shown any higher Tc value than black phosphorus as yet, although its Tc rises with the increase of pressure like that of the other. Arsenic does not appear to contribute to the rise of Tc. The structure of the alloy has not been fully examined in detail. However, it is considered to be similar to that of black phosphorus because the pressure-Tc curves of both are very similar to each other.

5. Conclusion

Phosphorus shows the highest superconductive Tc value among simple elements. Transition metals with d-electrons are widely known to have a high Tc value. That of phosphorus is especially interesting because it concerns no

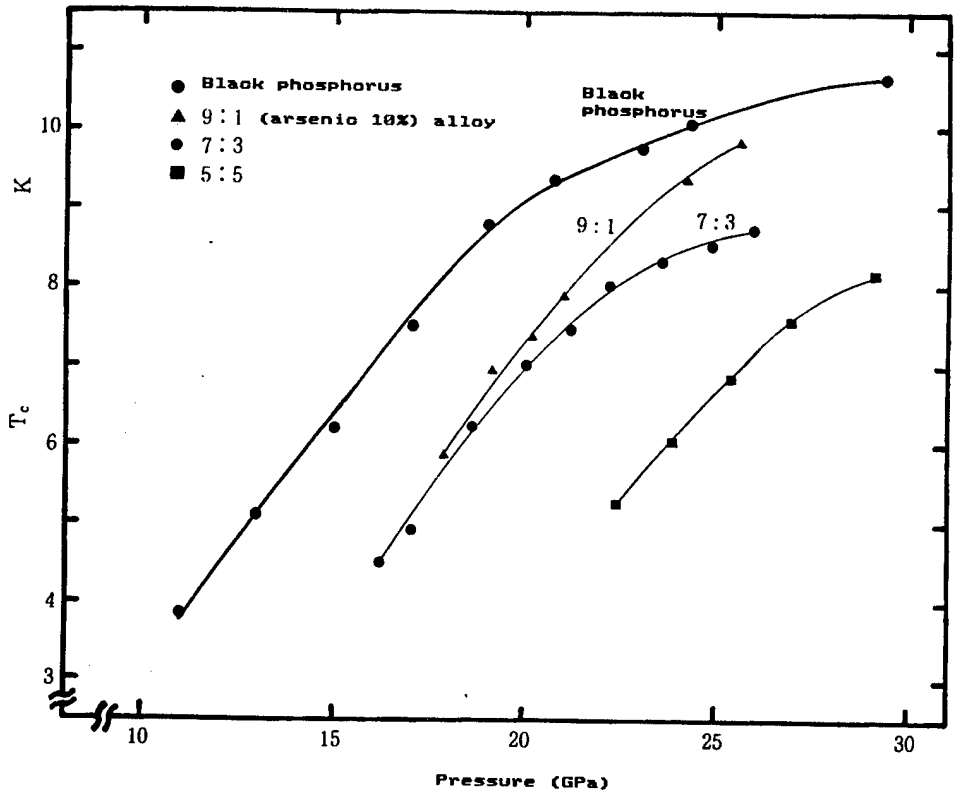

Figure 9. Pressure Dependence of Tc of Black Phosphorus-Arsenic Alloys

d-electrons. The mechanism of its superconductivity is not known in detail. The superconductivity is considered to be substantially influenced by nonstatic water pressure and pressure distribution through phase transition.

The study of phosphorus as a separate element has not been fully carried out since its application has not been apparent. There are no black phosphorus reagents commercially available at present. It is a rare separate element whose study remains backward. It has, however, been learned by the rapidly progressing research on physical properties of its monocrystal grown at high temperature and pressure, that it is an interesting material. Its chemical properties have not been studied as yet. Different ones from those known heretofore may be included among them. Superconductivity is included among its superior properties not found with other elements. Therefore, it is considered that there is a great necessity to further study and review phosphorous element.

FOOTNOTES

1. "Black Phosphorus--Its Physical Properties," MONTHLY PHYSICS, July 1985.

2. I. Shirotani, FUNCTIONAL MATERIAL, Vol 7 No 2, 1987, p 62.

3. P.W. Bridgman, J. AM. CHEM. SOC., Vol 36, 1914, p 1344.

4. J. JAP. CHEM. SOC., 1981, p 1604; I. Shirotani, MOL. CRYST. LIQ. CRYST., Vol 86, 1982, p 1943; MONTHLY PHYSICS, Vol 6 No 7, 1985, p 380.

5. J.C. Jamieson, SCIENCE, Vol 139, 1963, p 1291.

6. D. Schiferl, PHYS. REV., B19, 1979, p 806; K.J. Chang and M.L. Cohen, Ibid., B33, 1986, p 6177.

7. Y. Yamada, Y. Fujii, Y. Akahama, S. Endo, S. Narita, J.D. Axe, and D.B. McWham, Ibid., B30, 1984, p 2410.

8. T. Kikegawa and H. Iwasaki, ACTA CRYST., B39, 1983, p 158; M. Yoshizawa, I. Shirotani, and T. Fujimura, J. PHYS. SOC. JAPAN, Vol 55, 1986, p 1196.

9. PF Symposium, November 1986.

10. J. Wittig and B.T. Mattias, SCIENCE, Vol 160, 1968, p 994; I.V. Berman and N.B. Brandt, SOVIET PHYS. TETP LETT., Vol 7, 1968, p 323.

11. N. Sakai, T. Kajiwara, K. Tsuji, and S. Minomura, REV. SCI. INSTRUM., Vol 53, 1982, p 499; H. Kawamura, O. Shimomura, and K. Tachikawa, Ibid., Vol 56, 1985, p 1903.

12. H. Kawamura, I. Shirotani, and K. Tachikawa, SOLID STATE COMMUN., Vol 49, 1984, p 879, and Vol 54, 1985, p 775.

13. J. Wittig, B. Bireckoven, and T. Weidlich, "Solid State Physics Under Pressure," ed by S. Minomura (KTK Scientific Publisher, Tokyo, 1985), p 217.

14. E.N. Yokovlev, et al., SOLID STATE PHYS., Vol 28 No 4, 1986, p 1188.

20115/9365
CSO: 4306/7559

NAL NEWS UPDATED: FY87 BUSINESS PLAN, DEVELOPMENTS

Tokyo KOGIKEN NYUSU in Japanese May 87 pp 1-14

FY87 Business Plan

[Text] 1. Basic Policy

In accordance with the space development program determined by the Space Activities Commission as well as the findings and recommendations of the aviation and electronics technology councils, in the promotion of fiscal 1987 operations, 1) research will proceed on aviation technology, centering on the establishment of technology considered necessary for the future development of Japanese aircraft; 2) in striving to expand unrestricted space development activity, research and development of space science technology will be promoted, aimed at development of the necessary independent technology base; 3) an effort will be made for appropriate maintenance and operation of facilities as a public agency of large test facilities concerned with aerospace technology in Japan; and 4) the conduction of positive support and cooperation with foreign and domestic research and development agencies and research and development of related industries will form the basis for promotion of international cooperation and the organic collaboration of industry, academia, and government to meet the demands of the age.

1.1 Organization and Authorized Personnel

In fiscal 1987, research will proceed with 450 authorized personnel (of which 337 are research positions and in addition 1 is a coordinator in a nine-month position) in an organization comprised of a management department, eight research departments, three research groups, and the Tsunoda branch office.

In particular, the computing center will be renamed the mathematical analysis department in aggressively striving to promote numerical simulation technology from an overall National Aerospace Laboratory (NAL) point of view as an important basic aerospace technology due to its main tasks of research support using computers and the operation of large computers.

In addition, there will be an attempt to utilize a guest research officer system in order to promote organic coordination with industry and academia.

1.2 Budget

Research and facilities maintenance will be promoted according to the below stated plan in fiscal 1987 with a total budget of 10,352,419,000 yen consisting of 10,266,829,000 yen for Science and Technology Agency Test Research Office related expenses, 36,891 yen (transfer) for Environment Agency national agency pollution prevention test research expenses, and 48,699 yen (expenditure charge) for Ministry of International Trade and Industry energy technology research and development expenses. (Earmarked in addition are science and technology promotion coordination expenses and government and civilian special joint research expenses.)

1.3 Research Program

1.3.1 In fiscal 1987, research will proceed in the following six fields.

1.3.1.1 Research regarding STOL aircraft.

1.3.1.2 Research regarding innovative aerospace transport technology.

1.3.1.3 Research regarding space transport systems.

1.3.1.4 Research regarding space environment utilization and satellite systems.

1.3.1.5 Research regarding numerical simulation technology.

1.3.1.6 Research regarding application of aviation and space technology to other fields.

1.3.2 Among these special research and research with other agency expenditures are:

1.3.2.1 In research regarding STOL aircraft, continued promotion of research and development of fanjet STOL aircraft based on an overall National Aerospace Laboratory system.

1.3.2.2 In research regarding innovative aerospace transport technology, research and development of innovative aerospace transport elementary technology will proceed anew as special research.

1.3.2.3 In research regarding space transport systems, continued promotion from the previous fiscal year will be made of research on liquid oxygen and liquid hydrogen rocket engine elements as special research.

1.3.2.4 In research regarding space environment utilization and satellite systems, continued promotion from the previous fiscal year will be made of research on space environment utilization test technology and research regarding basic satellite technology as special research.

1.3.2.5 In research regarding application of aviation and space technology to other fields, continued promotion from the previous fiscal year will

be made of research on atmosphere pollution and noise pollution prevention with Environment Agency national agency pollution prevention test research expenses, along with being in charge of research and development on a high efficiency gas turbine and research and development on a general stalling engine with Ministry of International Trade and Industry large energy saving technology research and development.

1.4 Other Operation Plans

The following operations will be promoted, based on the special character of the National Aerospace Laboratory, to expand research activities befitting an international era, along with appropriately meeting demands from various quarters, including the industrial world.

1.4.1 Strengthening of industry-academia-government cooperation

Commissioned testing, consigned research, and facility loans from national test research agencies and civilian companies will be accorded, along with conducting joint research as needed in striving to upgrade aviation technology and space science technology. In particular, joint research with the National Space Development Agency will actively be conducted concerning space science technology research to contribute to the establishment of an independent technology base along with making serviceable the Laboratory's leading research.

1.4.2 Promotion of International Research Cooperation

The exchange of research based on international vision as well as joint research cooperation will be promoted to contribute to the promotion of research and development of superior aerospace technology.

1.5 Research Facilities Maintenance Plan

A survey will be conducted in fiscal 1987 on a composite materials structure testing facility, which is an indispensable facility for the research and development of innovative aerospace technology, along with continued promotion from the previous fiscal year of improvement of the transonic wind tunnel and improvement of the hypersonic wind tunnel auxiliary instruments, for the maintenance of a large research facility that is markedly outdated.

2. Research Program

The major research work for each research field in fiscal 1987 is as follows:

2.1 Research Regarding STOL Aircraft

Research and development of a fanjet STOL aircraft (Special research: fiscal 1977-1988)

Research with development of a test aircraft and flight tests as the core will be promoted regarding the fanjet STOL aircraft that will be equipped with both

short-range takeoff and landing and low noise features in anticipation of activity as a future air transport. Various types of new technology such as powered uplift capability technology will be substantiated.

2.1.1 Flight Tests (fiscal 1984-1988)

Flight tests will be conducted with the STOL test aircraft ASUKA. Along with substantiating the effectiveness of various kinds of new technology such as powered uplift capability technology used in the test aircraft and computer flight control technology, as well as the practicality of low noise STOL technology integrating these, topics of technology related to fanjet STOL aircraft operation will be pointed out and clarified.

2.1.1.1 Test Aircraft Operation (fiscal 1985-1988)

Along with conducting flight tests of the test aircraft ASUKA, operation of a companion aircraft will be conducted to guarantee the flight test support personnel to ensure smooth operation.

In fiscal 1987, flight tests will be conducted centering on the confirmation of STOL take off and landing performance for a comprehensive evaluation of the test aircraft ASUKA.

2.1.1.2 Test Aircraft Maintenance (fiscal 1984-1988)

Maintenance and repairs of airframe and engine will be conducted to execute smoothly flight tests of the test aircraft ASUKA.

In fiscal 1987, procurement of replacement parts of the engine aboard the test aircraft, repair and engine overhaul will be conducted along with maintenance, inspection and servicing of the airframe and repair of functional parts accompanying execution of flight tests. Also measures to upgrade flight performance of the test aircraft begun last fiscal year will be completed.

2.1.1.3 Related Support Tests (fiscal 1984-1988)

Safety and effectiveness of the test aircraft ASUKA flight tests will be ensured and various types of ground tests will be conducted either before or parallel with the flight tests in an attempt to upgrade the accuracy of test data analysis.

In fiscal 1987, high speed wind tunnel tests, flight simulation tests, and engine run tests will be conducted.

2.1.2 Technology Research (fiscal 1977-1987)

Essential technology particularly important in the development of a fanjet STOL aircraft will be conducted to contribute to the establishment of new technology important for the fanjet STOL aircraft of the future, along with supporting the development of the test aircraft ASUKA.

In fiscal 1987, research will be conducted on five items: research on

aerodynamic characteristics aimed at confirming permissible flight territory and upgrading the performance of the STOL aircraft through aerodynamic methods, research on flight performance aimed at establishment of landing entry methods appropriate for STOL aircraft, research on engine outfitting aimed at optimizing and making high performance the propulsion system equipment method for the STOL aircraft, research on structure aimed at lightening structure weight, and research on the piloting system aimed at making the flight control system high performance.

2.1.3 Maintenance of Fanjet STOL Aircraft Data Base (fiscal 1986-)

Technical information concerning the fanjet STOL aircraft obtained from development of the test aircraft ASUKA, flight tests, and related tests will be compiled as a data base and provided for development of a serviceable STOL aircraft in the future.

In fiscal 1987, continuing from the previous fiscal year, design standards of STOL aircraft will be studied and along with proceeding in the accumulation of technical data and provision of data base system software, a GAD program for the conceptual design of a serviceable aircraft will be created and aerodynamic calculations of a USB method STOL aircraft using a numerical simulator will commence.

2.1.4 Joint NAL-NASA International Research (fiscal 1986-)

Cooperation will proceed on research concerning a study of the design standards of a USB method STOL aircraft with the U.S. NASA Ames Research Center, which is proceeding with research and development of a USB method STOL aircraft.

In fiscal 1987, continuing from the previous fiscal year, along with conducting exchanges of technical data, a study will proceed concerning the design standards of a USB method STOL aircraft, including the results of high speed wind tunnel tests and the interim results of flight tests.

2.2 Research Concerning Innovative Aerospace Transport Technology

Research and development of essential technology for innovative aerospace transportation (Special research: fiscal 1987-)

Research and development will be conducted on vanguard elementary technology with an innovative aircraft capable of large volume and long range transport with high efficiency and a space shuttle/hypersonic aircraft that meets the needs of super high speed transportation and free expansion of space development activities as the core, striving to establish innovative aerospace transport technology for the 21st Century.

In fiscal 1987, research will proceed in the various fields of aerodynamics technology, structural technology, flight control technology, and propulsion systems technology.

2.2.1 Research on Aerodynamics Technology

Along with conducting research in an effort to reduce the aerodynamic drag of aircraft, research will be conducted to obtain the optimum aerodynamic shape and aerodynamic characteristics for the wide range of flight conditions of a space shuttle.

2.2.1.1 Research on Laminar Flow Control Technology (Special research: fiscal 1987-)

Research will proceed on laminar flow control technology to maintain a laminar flow shape with no disturbance to the air flow on the airframe surfaces of the aircraft and bring about an epochal reduction of aerodynamic drag.

In fiscal 1987, an absorptive surface with porous plates and an absorption regulating device will be trial manufactured, and performance characteristics tests conducted with a large low speed wind tunnel.

2.2.1.2 Research on New Configuration Aerodynamic Technology

A model in which drag diffusion and lift diffusion characteristics are uniform in the wingspread direction will be designed and manufactured for a forward sweep wing, which has good stall performance and for which low drag can be anticipated compared to a back sweep wing, and performance will be confirmed by transonic wind tunnel tests.

2.2.1.3 Research Concerning Tests/Numerical Simulation Regarding the Super High Speed Aerodynamic Characteristics of a Space Shuttle (Special research: fiscal 1987-)

Research will proceed on a basic shape to check aerodynamic heating during hypersonic flights. In fiscal 1987, research will proceed on numerical simulation and basic flight tests with a hypersonic wind tunnel, gun tunnel, and arc heating wind tunnel concerning hypersonic aerodynamic characteristics, which are particularly important in the acceleration climb and and return reentry phase.

2.2.2 Research on New Composite Material Structure Technology

Along with proceeding in research on monolithic structure technology and aerodynamic elasticity tailoring technology for thermoplastic composite materials which make possible large-scale reduction of airframe structural weight and are superior in shock resistance, a drawback of existing composite materials, research will be conducted on heat-resistant heat shield materials for aerodynamic heating during hypersonic flights.

2.2.2.1 Research on Strength Characteristics of Thermoplastic Composite Material Structural Elements (Special research: fiscal 1987-)

A part material specimen and structural element model will be designed and manufactured to grasp the characteristics of thermoplastic resins and static strength tests, fatigue strength tests, and shock tests will be conducted.

2.2.2.2 Research Concerning Aerodynamic Elasticity Tailoring

Research will proceed with the goal of developing a basic algorithm for designing a composite material wing that is superior in wing aerodynamic elasticity characteristics, using the anisotropy of new composite materials.

2.2.2.3 Research on Heat and Strength Characteristics of Super Heat Resistant Heat Shield Materials

Trial manufacture of three dimensional textile strengthened ceramic heat resistant and adiabatic composite materials as well as the conduction of a basic evaluation of their heat conduction rate and high temperature strength.

2.2.2.4 Basic Research on Materials and Structures in a High Temperature Environment

Research will be conducted regarding the basic characteristics of polymide type heat resistant composite materials along with an evaluation of the heat and strength characteristics of materials.

2.2.3 Research on Flight Control Technology

Along with conducting research on intelligent and active control in an effort to upgrade the safety of aircraft and upgrade environment adaptability, research will be conducted regarding control technology to have space shuttles fly in the optimum orbit.

2.2.3.1 Research Regarding Active Control of Aerodynamic Elasticity Systems

Reduction of wind gust weighting and suppression of flutter will be realized by automatic control and the first total aircraft preliminary tests will be conducted in a large low speed wind tunnel, incorporating a measuring control device in the total aircraft model for research on active control technology in striving to upgrade safety and for aircraft high efficiency. Also trial manufacture and research will be conducted on a cable type model support device to make wind tunnel tests with good accuracy possible.

2.2.3.2 Research on an Innovative and Intelligent Navigation System and the Application of Artificial Intelligence to Flight Control Systems of Space Shuttles

Along with reducing the burden of the pilot, research will proceed on intelligence technology to make highly accurate flight control possible, striving to upgrade safety and reliability by the application of artificial intelligence technology to piloting systems. Also, research will be conducted on control through intelligence technology regarding unmanned test aircraft.

2.2.3.3 Research on Innovative Aircraft/Space Shuttle Flight Systems by VSRA (Variable Stability Response Aircraft)

Flight evaluation research will proceed by VSRA for FBW (fly-by-wire: electrical type)/FBL (fly-by-light:optical type) piloting systems to make

possible highly accurate flight control and upgrade safety and reliability in place of current piloting systems which are chiefly hydraulic. Also, acquisition of flight performance data will be made regarding unmanned test aircraft by VSRA along with research on the flight characteristics of space shuttles at low altitude.

2.2.4 Propulsion System Technology

Along with conducting research on the essential technology necessary for the realization of an ultrahigh bypass ratio variable shape engine equipped with the super low fuel consumption, high speed flight characteristics and low noise demanded in high subsonic speed aircraft in the 21st century, research will be conducted on an air induction engine and multiple mode propulsion system which will be necessary for a space shuttle.

2.2.4.1 Research on an Ultrahigh Bypass Ratio Variable Shape Engine (Special research: fiscal 1987-)

A basic aerodynamic model will be trial manufactured and tests conducted regarding a ducted fan, which is the propulsion generating part of the engine, to grasp basic performance. Also, along with commencing creation of a three-dimensional aerodynamic design program for the compressor and turbine of a high performance engine, which has the engine as the core, program validation will be made by tests. Furthermore, research will proceed in an effort to establish technology for variable shape engine control principles, blade tip clearance control and optimized cooling system.

2.2.4.2 Research on Hypersonic Speed Air Induction Engine (Special research: fiscal 1987-)

Trial manufacture and testing of burner will proceed on the scramjet engine, which is an air induction type engine at hypersonic speed, to obtain design data regarding combustion performance.

2.2.4.3 Research on Air Induction Engine for High Speed Aircraft

Along with proceeding with performance calculations and systems study of engine systems such as turbo ramjet engines and air turbo ramjet engines, research will be conducted regarding the materials and structure and performance of various engine elements. Also, a conceptual study will be made of engine elements and engine test facilities.

2.3 Research Concerning Space Transport System

Continuing from the previous year in research regarding space transport systems, besides proceeding with research on liquid oxygen and liquid hydrogen rocket engine elements centering on trial manufacture of the H-II rocket first stage engine LE-7 high pressure liquid oxygen turbo pump, research will proceed on rendezvous and docking technology and reclamation technology as research on rocket applicable technology, along with proceeding in research on the liquid apogee engine for the large stationary engineering test satellite No. VI (ETS-VI). Also, basic, vanguard research necessary for development of

future rockets and rocket applicable technology through independent technology will proceed.

2.3.1 Research on Liquid Oxygen and Liquid Hydrogen Rocket Engine Elements (Special research: fiscal 1984-1988)

Research will proceed centering on trial manufacture of a liquid oxygen turbo pump for the first stage liquid oxygen and liquid hydrogen engine LE-7 of the H-II rocket which will launch a two ton class large stationary satellite in the 1990's.

In fiscal 1987, research will be conducted on upgrading inducer performance and hydrogen brittleness of the high pressure turbine blade for the turbo pump system as elementary research. Along with conducting research, continuing from the previous fiscal year on cooling limit durability of the high pressure burner, materials and manufacturing technology for the combustion system, vanguard research will be conducted on high high-pressure burners aimed at rather high performance.

Also, along with conducting engine system tests incorporating the liquid hydrogen turbo pumps No. 1 and No. 2 trial manufactured by the National Space Development Agency for the prototype engine, as trial manufacture research of a large high pressure liquid oxygen turbo pump, trial manufacture will commence on No.3 aimed at upgrading the performance of the prototype liquid oxygen turbo pump and evaluating critical performance. Also, dynamic characteristic tests will be conducted as research for the actual engine and research will proceed on the pogosuppressor.

2.3.2 Research on 2 Liquid Type High Performance Engine

Development tests will be conducted centering on upgrading high altitude performance of the liquid apogee engine for the two ton class large stationary engineering test satellite No. VI (ETS-VI) scheduled to be launched in fiscal 1987. Also, expanding these results, research will be conducted regarding the propulsion system for orbit changes of future spacecraft.

2.3.3 Research on Future Propulsion System

Along with promoting basic combustion experiments centering on an evaluation by rocket engine of a high performance hydrocarbon as a propellant for candidate propulsion systems of space transports in the mid 1990's and thereafter, investigation and systems design study will be conducted regarding other candidate propulsion systems.

2.3.4 Research on Rendezvous and Docking Technology

Research will proceed through flight simulation tests aimed at optimizing the man-machine system with realization of rendezvous and docking technology by remote control from the ground as the goal.

2.4 Research Concerning Space Environment Use and Satellite Systems

Along with proceeding in research aimed on the establishment of technology that will form the foundation of the space utilization age that is to come, research will be conducted on elementary technology and common test equipment for space stations for effective use of the space environment.

Also, with regard to satellite systems, research will proceed centering on research of the major components common in two ton class large stationary satellites.

In addition, space tests and research on remote control technology will be conducted using the space shuttle.

2.4.1 Research on Space Environment Utilization Test Technology (Special research: fiscal 1986-)

Research will proceed aimed at space station structural elements, common test equipment, and establishment of an energy plant to promote effective use of the space environment, which will become more diversified and advanced in the future.

In fiscal 1987, continuing from the previous fiscal year, trial manufacture of a model for confirmation of the function of a transexpansion control system and research on transexpansion control systems will be conducted for an extension type test bed. There will be trial manufacture of a distiller, tanks types, and a dehumidifier among the major component elements, and evaluation tests of functional characteristics conducted for the water and gas circulator.

Research will proceed on motion simulation from payload release to return for the boomerang system and for the tether payload system, including vibration, for the tether.

Also, along with conducting research on a materials test support expert system applying artificial intelligence technology, as research to promote the utilization of space, research will be conducted on simulation of fluid motion under low gravity. In addition, a conceptual study will begin regarding a solar heat condenser type heat engine electric generator system appropriate for use in space.

2.4.2 Research Concerning Basic Satellite Technology (Special research: fiscal 1980-1990)

Research will proceed on various types of basic technology, common and basic to the composition of a satellite system in order to promote domestic production through independent technology and high performance of satellite technology, contributing to the establishment of an independent technology base.

In fiscal 1987, research will proceed continuing from the previous fiscal year on bearings for use in space, control of a flexible structure satellite, and a xenon ion engine necessary for the two ton class large stationary engineering test satellite No. VI (ETS-VI).

Research will proceed and evaluation of performance conducted concerning the optimum solid lubricating film for promoting domestic manufacture of contact type bearings for research concerning bearings for use in space.

Provision will be made of a structural simulation model similar mechanically to the real one for research concerning control of flexible structure satellites, and clarification of vibration characteristics and control characteristics promoted by tests.

For research on the xenon ion engine, secondary trial manufacture will be conducted in an effort to upgrade the performance of a cusp magnetic field type xenon ion engine, and evaluation tests will commence on durability.

2.4.3 Research on Manned Support Technology

Basic research will proceed to create the optimum environment according to human physiological metabolism and physical circulation as research on the circulatory system to maintain ecology within a closed system in preparation for future manned space activity. Also, investigative research will proceed on space suits, portable life support equipment, and MMU (manned maneuvering units) as research concerning ship outside activity technology.

2.5 Research Concerning Numerical Simulation Technology

Research will proceed on numerical simulation technology as basic technology required for research and development of innovative aerospace technology such as space shuttles and innovative aircraft airframes as well as propulsion systems. In particular, the promotion of research anticipates effective operation of the numerical simulator (NS) system introduced in the previous fiscal year.

Visible Boundary Layer Transition Points Through Flight Tests

Tokyo KOGIKEN NYUSU in Japanese May 87 pp 7,8

[Article by Takeru Onuki, New Aircraft Research Group]

[Text] The problem of the transition from a laminar flow boundary layer to a turbulent flow boundary layer is a basic problem of fluids such as stability of the laminar flow boundary layer and the mechanism of the shift to the transition. It is also an important research topic in the applications area from the relationship to aircraft friction drag. Stability of a two dimensional laminar flow boundary layer can be estimated by solving the Orr-Sommerfield equation considering minute disturbances analytically, but judgement of the transition point position must depend upon the rules of experience. Also, due to recent advances in large computers, numerical solutions of the Navier-Stokes equation have been made, but the transition point position seems to be half an experience consideration. Consequently, the acquisition of test data on the transition point position has been basically necessary, but precautions are necessary to control adequately air

current characteristics during tests since an inherent air current turbulence exists, though slight, in the wind tunnel. Also, it is extremely difficult to match the basic parameter Reynolds number in transition to actual aircraft and eliminate influence on the transition by air current characteristics to conduct tests. Finally, a method for the most reliable flight tests with actual aircraft was considered. This time we attempted to make the transition point visible with a remodeled Fuji FA-200 (Figure 1) owned by the National Aerospace Laboratory with the objective of establishing a method to confirm the boundary layer transition point through actual flight tests in order to acquire test data concerning boundary layer transition.

A sublimation method was employed, which has a record in flight tests as a method for making the boundary layer transition point visible. For the sublimation method, a thin film was made with a drug that has sublimation properties on the surface of physical objects. It is a method which confirms the boundary layer transition point by the speed of that sublimation. In other words, there is greater shear stress on the wall surface in a turbulent boundary layer than in a laminar flow boundary layer, sublimation accelerates and the film disappears rather quickly. Generally, except for cases of adhered roughness, distance from the beginning to the end of the transition is necessary in a natural transition. The end point of the transition can be observed by the sublimation method. In other words, at the point where there has been sufficient turbulence in the boundary layer it is then called the transition point. In this test, acenaphthene was used as the sublimation agent but since the color of the film is white, a part of the wing surface was painted black beforehand and visibility planned within that area. In the test, the state of sublimation was recorded by a camera and video camera. Speed, altitude, and angle of attack also were measured and included in a data recorder.

Figure 2 shows an example of the visible results. Based on flight conditions of an altitude of about 300 meters (1000 feet), speed of about 45 meters/second (100 mph), and temperature of 12 degrees Centigrade, the photo was taken after about 150 minutes of steady level flight. (Movement of the center of gravity position at this time was 0.2 percent MAC.) A mark was made every 10 percent c from the front edge to 50 percent c at two cross section locations in the wingspread direction. The part that can be seen as white is laminar flow. What is seen as the ground color (black) is considered the turbulent flow area. The turbulent flow wedges seen on the front edge and near the front edge were generated by the stall warning device installed on the front edge, and bolts for slat installation as well as heads of rivets and adherence of bugs. It is discerned that the area maintaining laminar flow is to a position about 27 percent c. This is about 1.4 times 10 to the 6th if corrected by the transition Reynolds number by the distance from the front edge.

Tests are continuing at present and in the future, an analysis of data as well as analysis and comparison with boundary layer stability are scheduled. This test was done with the cooperation of the Flight Test Department.

Numerical Simulation of Flight Body Circumference Flow

Tokyo KOGIKEN NYUSU in Japanese May 87 pp 8-10

[Computer Research Office, Computer Center]

[Text] Large scale numerical calculations, which up to now have been totally impossible to calculate, have become possible through the introduction of a numerical simulator. A calculation which up to about half a year ago would have taken a month or so to obtain the results now can be done in less than an hour. The quality of research in this field depends greatly on the performance of the computer used. Thanks are again extended to those people who exerted effort regarding introduction of the numerical simulator.

In the numerical simulator, a calculation is possible using about 1.5 million grid points for a three dimensional flow. Numerical simulation of the flow for an entire aircraft model has slowly entered the stage of practicality. The creation of a calculation grid to resolve the flow spots around a complex shaped physical body has become an important problem. There have been many proposals about methods to form the calculation grid that have respective merits and drawbacks and there is no definitive grid formation method. We sought a calculation grid by the method of solving a three dimensional hyperbolic type differential equation. If the physical body surface coordinates are assigned by a hyperbolic type grid formation method, the coordinates of the outside are automatically determined by designating the volume forming the base and orthography of the coordinate lines and a excellent grid mesh can be formed comparatively easily for a convex body. We made the following improvement to form a non-intersecting grid for a intermixed concavo-convex complex physical body shape, and surmounted the difficulties in a hyperbolic grid formation.

1. The volume of the grid is determined by the geometric volume of curved surfaces (second base measure).

2. The orthography is eased by using a simple elastic body model.

An example of a calculated grid obtained by applying this improved method to the complete NASA shuttle (shape date: Jane's Yearbook) is indicated in Figure 3. Regardless of the considerably uneven physical body surface, there was success in covering the shuttle exterior by a single grid mesh.

If the grid is made, the flow calculation can be done comparatively easily if there is a basic analysis code. An example solving a three dimensional Euler equation is shown in Figure 4. The TVD scheme reported in the March issue of NAL News is used as the variance scheme and is calculated filling in a separate grid in the cylindrically shaped physical body slipstream area. The number of grid points is about 400,000. The figure shows a pressure distribution on the shuttle surface for 0.6 Mach. A solution to the Navier-Stokes equations currently is being sought to increase the number of grid points and Mach number, and minutely correct the grid sought by the above mentioned method in the wall vicinity. However, severe turbulence of the physical body slipstream cannot be calculated because of the limit on the number of grid points. Even with a large capacity computer and fast computer speed, still only about 200 grid points can be taken in one direction.

Consequently, an even higher performance computer is necessary to solve accurately turbulent flow phenomena around a large, complicated shape physical body. There is not doubt that the role of the numerical simulator currently is becoming very important for development of a shuttle, which has been placed on the agenda even in Japan.

Research on Internal Fluid Mechanism Between Turbine Blades

Tokyo KOGIKEN NYUSU in Japanese May 87 pp 10,11

[Takamasa Yamamoto, Motor Department]

[Text] Up to now many turbo engines have been designed and manufactured by the method of determining the most efficient blade shape and blade arrangement based on test data such as cascade loss. Such design methods based on overhaul cascade data is very useful from the standpoint of practicality, but marked progress in upgrading performance cannot be expected with just this method. Detailed test information between blades is necessary. Also, the high speed and capacity seen in super computers recently has been remarkable and there is no doubt that the time is not far off when cascade loss data itself will be sought by solving completely fluid equations. In verifying the results calculated by a numerical simulator and improving the program, it is necessary to grasp detailed physical phenomena through tests. In other words, it is necessary to clarify in detail the internal fluid and cascade loss generation mechanism by making a searching inquiry directly into the flow between blades, not just a test analysis of before and after cascade flow as done up to now. By doing this, the various demands in high efficiency of recent years can be answered along with being able to offer rather universal design data. Also there is the possibility that new concepts in design will be generated.

In this research, a low speed cascade wind tunnel was manufactured with the objective of a detailed investigation of flow between blades in an axial flow turbine. A clarification was made of the complicated three dimensional flow phenomena and its mechanism, the comprehension of which has been inadequate up to now. For the test cascade, a linear cascade and toroidal cascade were manufactured, which have been widely manufactured based on air cooled turbine blades used in the high pressure turbine stage of actual engines. First, the flow between blades simplified with no centrifugal force in the linear cascade was measured based on various conditions. Afterwards, the flow in a nearby place in the actual engine with considerable centrifugal force in a toroidal cascade was measured. In order to make these measurements in detail and with high accuracy, the measurement system was made fully automatic. On the other hand, the expanded measurement data was analyzed making free use of visual drawings to enable simple understanding. Also, by devising post processing of the measurement data, minute data that previously had been difficult to grasp also was extracted. This cascade wind tunnel means that in many cases the flow between blades can be clarified in a short time with a very detailed mesh and it can be called a kind of test simulator as opposed to the above mentioned numerical simulator. Introduced below is a portion of the results and the current status of research is indicated.

Figure 5 is an example of a measurement cross section and a measurement mesh to capture quantitatively the flow between various kinds of blades. It is a detailed mesh that would be employed in a numerical simulation. Figure 6 is an example of a measurement that shows the loss generation mechanism from the blade tip clearance, which occupies a large percentage in cascade loss. It shows the flow on the blade tip wall surface in a static linear cascade (the surface projected vector and its streamline) and the flow of the cascade downstream cross section (secondary flow vector and uniform loss line). As shown in the flow on the blade tip wall surface, the major portion of the wall surface flow at the cascade entrance is transferred to the blade negative pressure surface side and the state of combination and interference with the blade tip clearance in the vicinity of the negative pressure surface is discerned. On the other hand, the loss generation status from the secondary flow between the blades can be understood from the flow at the downstream cross section. In the future, perfection of a test wind tunnel and measurement technology which enables easy simulation of the flow between high speed/rotary blades is important.

Development of Transonic Speed Cascade Design Method Using Euler Code and Inverse Solution

Tokyo KOGIKEN NYUSU in Japanese May 87 pp 12-14

[Naoki Yokose, Aerodynamics No. 2 Department]

[Text] The Aerodynamics No. 2 Department has proceeded over the past ten odd years in making computed aerodynamics useful for aerospace technology. In particular, the results of application to transonic aerodynamic design, development of analysis code, and development of the YXX (next generation commercial transport) have been as reported in this NAL News. Recently, these results have been applied to needs from various related fields inside and outside of NAL. The aim is to establish Japanese aerospace technology using computed aerodynamics by striving to extend it to these fields where development of technology in applied computed aerodynamics has by no means been adequate. At present, with NS (numerical simulators) in full-scale operation, improvements in analysis and design codes as aerodynamic tools fit to be practical are becoming more rapid. In research and development on computation methods, it can be said that the era already has ended in creating schemes for a simple stake that is unconscious of future applications.

Recently, research on transonic blade design technology for an ATP (innovative shaped turboprop) and gas turbine cascade is proceeding strongly in various nations of Europe and the United States. Consequently, not only is there a great advantage in using computed aerodynamics technology which we have developed and fostered in transonic blade design and analysis, but it is simple. Actually, a NSCAS code, improving and expanding the high Reynolds number transonic Navier-Stokes analysis code NSFOIL, was created with the cooperation of the Motor Department and an analysis of the transonic buffet of compressor blades has been realized.

However, in a cascade blade design, NS code is still not economical. On the other hand, a method using EULER code is desired since there are times when a potential code is by no means adequate because there are cases where strong shock waves appear. In design of the main blades, the logical design method WINDES, which realizes a designated pressure distribution as desired, has been made serviceable by combination with various transonic blade analysis codes, FLO-22, FLO-27, WIBCO, IFPWING+BLAY, and NSFOIL. We have estimated that the WINDES theory can be applied to cascades and attempted a design combining it with a transonic cascade analysis code created by a quick adjustment to the transonic obtuse physical object EULER analysis code BBFVM. This was reported to the Gas Turbine Society in November 1985. Afterward, upon completing the structure of a rigid design theory for cascades (code CASDES, 4th Computed Aerodynamics Symposium, Takanashi), a grid mesh creation code CSMESH capable of easily handling actual ATP blades, compressors, and turbine blades, and EULER analysis code CSFVM was developed. Development of a full-scale cascade design method was conducted and as good results were obtained, it was reported.

A design example is show in Figure 7 with a stagger angle of 45 degrees, a Mach number of 0.775 inflow in a compressor cascade with a 1.0 pitch, an ınitial inflow angle of 55 degrees, and outlet pressure ratio of 1.309. No. (a) is the initial pressure distribution (triangles) and target (solid line). No. (b) indicates the blade shape obtained as the result of design and a comparison of its pressure distribution (triangles) and target. The Mach number directly before the shock wave was reduced from 1.32 to 1.13 and the close flow when there is no shock wave is discerned. In Figure 8, the pressure distribution in the initial and designed flow areas is shown. By these results, it is clear that design suitable for actual use is possible, regardless of using the old MacCormack FVM analysis method. In the future, design of ATP and compressor cascades using this method are scheduled.

Figure 1. Remodeled FUJI FA200 (unit = meter)

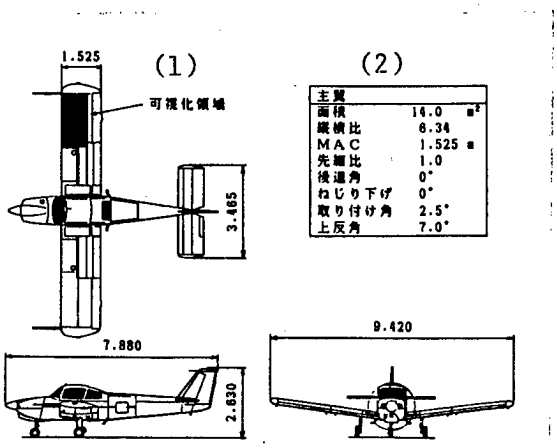

図1 FUJI FA 200改機(単位 m)

Key:

1. Visible Area

2. Main Wing Data Chart

Area	14.0 meters square
Lengthwise/ crosswise ratio	6.34
MAC	1.525 meters
Tapering ratio	1.0
Backsweep angle	0 degrees
Torque drop	0 degrees
Attached angle	2.5 degrees
Upward curve angle	7.0 degrees

Figure 5. Various Types of Measurement Cross Sections and Measurement Mesh

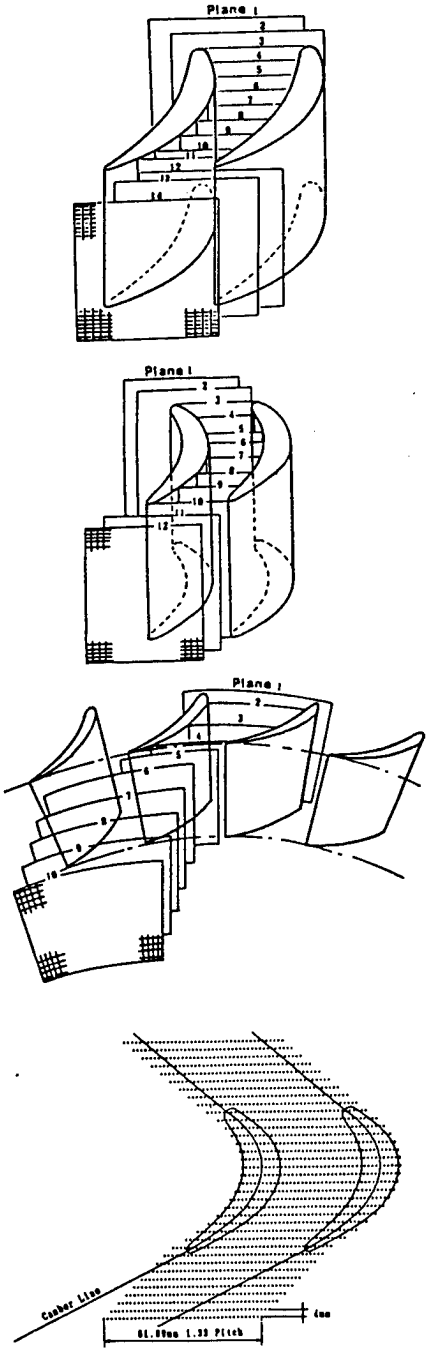

図1 各種計測断面と計測メッシュ

Figure 6. Example of Measurement of Flow Between Turbine Blades With Blade Tip Clearance

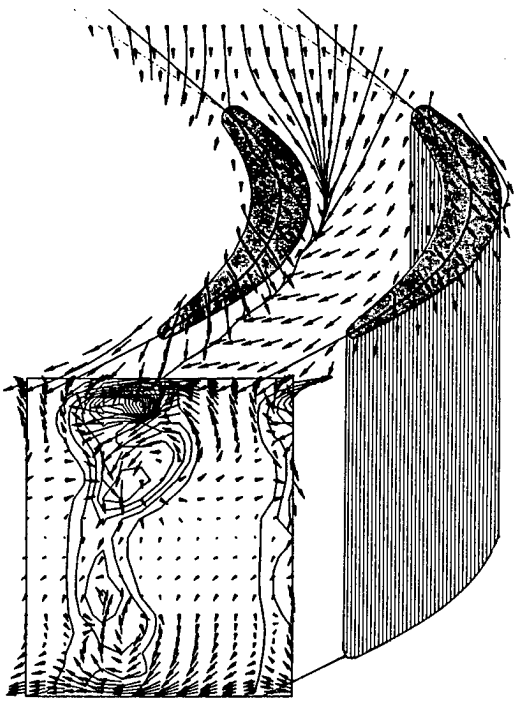

図2 翼端すきまを有するタービン翼間の流れの計測例

Figure 7. Cascade Shape and Pressure Distribution

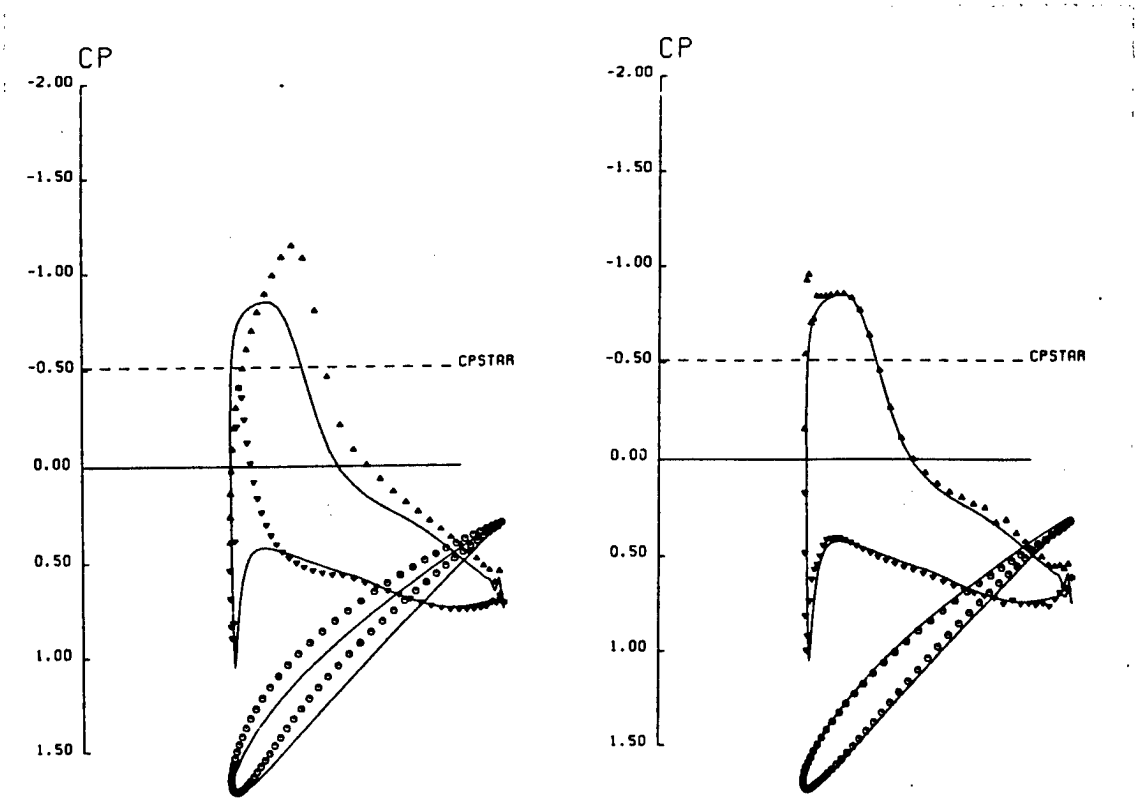

(a) 初期(△, ▽)及びターゲット圧力分布(実線)

(b) 設計翼列形状(○)とその圧力分布(△, ▽)

図1 翼列形状とその圧力分布

Key:

(a) Initial (triangles) and target pressure distribution (solid line).

(b) Designed cascade shape (circles) and pressure distribution (triangles).

Figure 8. Flow Area Pressure Distribution

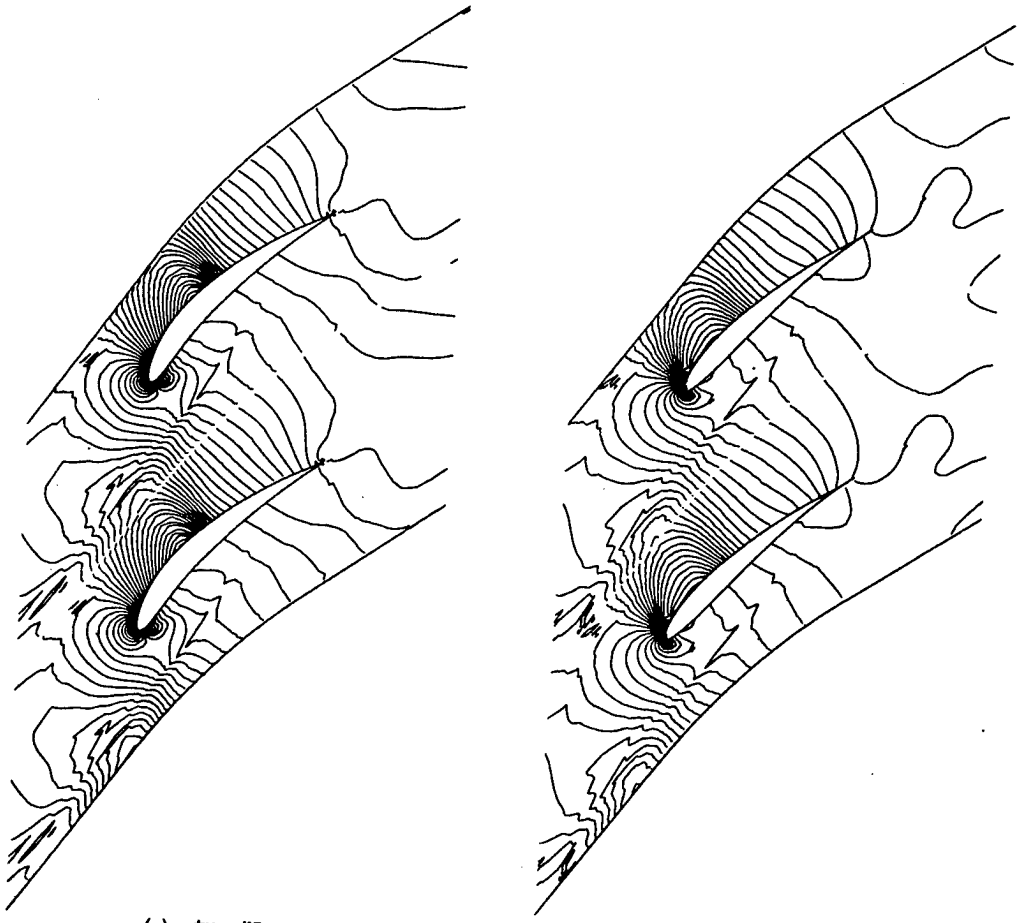

(a) 初 期　　(b) 設計結果

図 2　流れ場の圧力分布

Key:

(a) Initial

(b) Design results

12256

CSO: 4306/2058

HIGH POLYMER SENSOR MATERIALS DISCUSSED

Polymers for Material Sensors

Tokyo SENSOR GIJUTSU in Japanese Dec 86 pp 50-53

[Article by Sachio Hirose, Central Laboratory, Mitsubishi Petrochemical Co. Ltd.]

[Excerpts] Material sensors are mostly for measuring chemical materials. There are four types: the ion-selective electrode, the humidity sensor, the biosensor, and the gas sensor.

Sensors, in general, are conversion elements. That is, they are elements that convert physical and chemical quantities, for example, chemical substances are converted into signals of electricity or light which are amenable to signal processing.

Sensors are built into certain devices such that the element functions efficiently, and a system utilizing the device is set up in order to make the device available for practical use. In developing such devices and systems, polymer raw materials are often found to play a significant role in, for example, the elimination of contaminants and an improvement in device durability. This article discusses principally this conversion element.

Polymer raw materials, along with inorganic and organic materials have been widely investigated and used as the raw materials for material sensors. Polymer raw materials exhibit superior characteristics of their own such as: 1) amenability to molding and processing into films, fibers, and other forms; 2) a wide range of electrical properties from insulation to high conductivity; 3) permeability to gases and liquids, etc.; 4) mechanical strength.

Besides the above advantages, it is easy to use polymer raw materials to form composite materials by mixing them with other types of raw materials. Biosensor elements, in which a biological material, such as an enzyme, is mixed with or immobilized into a different type of material, represents a good example of a new conversion element of a sensor.

This article also deals with the characteristics of sensor materials, examples of the practical application of the materials, and the prospects and future problems of the four types of sensor materials.

Ion-Selection Electrode

Ion selective electrodes are used to measure various types of ions, and are of four types: glass-film, solid-film, liquid-film, and gas-sensing. The liquid-film and gas-sensing type of electrodes, typically use the polymer raw materials, polyvinyl chloride (PVC) and fluorine resin (Teflon), respectively. Besides these, epoxy resin finds application in the supporting material of the solid film type of electrodes.

Polymer Raw Material for the Liquid-Film Type of Electrodes

The film of the liquid-film type of electrodes involves a so-called "liquid film" which is made up of an organic solvent into which an activated substance is dissolved. Recently, however, a polymer film made up of polymer raw materials and an activated substance is often used as a type of liquid film. Polymer film is favored because it dispenses with the filling up and replacement of the liquid film solution and hence makes handling of the electrode simpler. The PVC, which is highly amenable to film formation, is widely used as a raw material for polymer film. The films of polyvinyl acetate, silicone rubber, etc., on the other hand, permit only poor dispersion in the film of the activated substance. The properties of PVC as a raw material for liquid film are:

1. PVC is soluble in diverse organic solvents and, in particular, in the polar solvent tetrahydrofurane (THF).

2. PVC is easily turned into a film of satisfactory strength using a casting method.

3. In general, PVC mixed intimately with activated substances and, when turned into film, permits satisfactory dispersion of the substance therein.

4. The thickness of the PVC film thus obtained is easy to control and the permeability of ions for the liquid film, fine.

The characteristics of the polymer-film type of electrode involving PVC is identical to those of the conventional liquid film type and many ions including Ca^{+2}, Ba^{+2}, Na^{+}, K^{+}, ClO_4^{-}, SCN^{-}, naphthalene sulfonic acid ions, and phthalic acid ions are detectable. The problems involved in using polymer raw materials for the liquid-film type of electrodes concerns improvement of the uniformity of dispersion of an activated substance of high concentration, and the better mobility of the substance in the film.

Polymer Raw Materials for Gas Sensing Electrodes

Figure 1 shows the structure of an electrode of the gas sensing type. The electrode incorporates an ion electrode, such as a glass electrode, on which the sensing surface is coated with a water-repellent porous film. When the

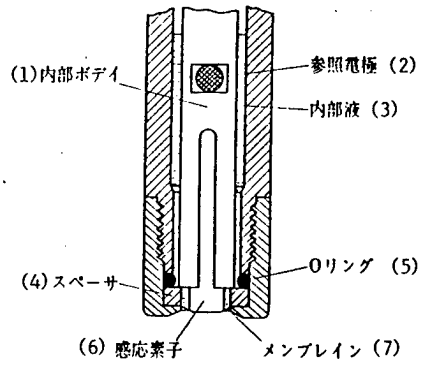

Figure 1. Structure of Gas Sensing Electrodes

Key:
1. Internal body
2. Reference electrode
3. Internal solution
4. Spacer
5. O ring
6. Sensing element
7. Membrane

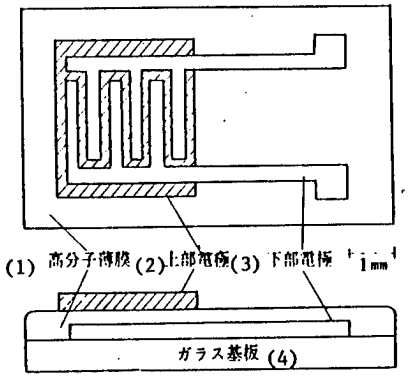

Figure 2. Structure of Humidity Sensor

Key:
1. Polymer film
2. Top electrode
3. Bottom electrode
4. Glass substrate

electrode is immersed in a solution of the specimen, the gas in the solution passes through the porous film and dissolves in a solution in the electrode, leading to a change of, say, the pH of the solution, thus revealing the concentration. Hence the electrode is a kind of gas sensor.

The characteristics of the porous film applied to this sensor are:

1) The diameters of the pores are less than 1 micron with a narrow distribution of pore diameters; the pores permit a high degree of permeation.

2) The porous film is less than 100 microns thick. It is of proper film strength and functions as a sealing material for the solution contained in the electrode.

3) The porous film is water repellent such that the solution inside the electrode is kept completely separate from the specimen.

To give an example, the gas sensing electrode for ammonia uses a porous Teflon film which has pore diameters of around 1.5 microns, a film thickness of 100 microns, and a porosity, a measure of permeability for gases, of around 60 percent. Thus, porous Teflon film finds widespread application in gas-sensing electrodes, as an excellent water-repellent material. The electrode, nevertheless, has difficulties in response time, which is dictated by such factors as the thickness of the porous film, pore diameter, pore-diameter distribution, and porosity. The manufacture of porous Teflon film, meanwhile, is adjusted by using methods of sintering Teflon powder, which provides a rough film in comparison with those produced by the phase-separation phenomenon of Teflon and producing pores with an electronic beam. It is hoped that a high-grade polymer raw material for gas-sensing electrodes will be developed through the application of water-repellent Teflon on the surface of a porous film of, for example, cellulose, which has high permeability for gases with a porosity of over 80 percent and a fine pore-diameter of a uniform size of less than 0.5 micron.

2. Humidity Sensor

Humidity sensors are devised to detect the various phenomena associated with the water vapor components of air, for example, relative humidity, cloudiness, and dewing.

Figure 2 shows the structure of a humidity sensor. The polymer material is fabricated into a device such that it blocks short circuit between the top and bottom electrodes; at the same time, the material is made into as thin a film as possible in order to shorten the response time; a film thickness of less than 1 micron is usually desirable. The principles involved in humidity sensors and the characteristics of humidity-sensitive polymer raw materials are largely divided into four groups: 1) Sensors based on the changes of electrical resistance of the polymer electrolyte film and in which ions over the surface of the film are disassociated by virtue of the water absorbed, (according to the formula $R\text{-}SO_3H+H_2O \rightleftarrows R\text{-}SO_3+H_3O^+$,) thereby allowing the passage of ionic current; resins of the sulfonic-acid group are most frequently used. 2) Sensors based on the changes of the electrical resistance

of polymer films swelling due to water absorption and film's polymer has an electroconductive powder, such as carbon or a metal, intimately mixed in order to make a humidity sensitive polymer film. The polymer films, which swell due to the absorption of water, increase the distance between individual particles of the electro-conductive powder and thereby increase the electrical resistance. Resin of the acrylic acid group is under investigation for relevant purposes. 3) Sensors based on the changes of the capacitance of a polymer film, in which a polymer film, with a large dielectric constant, has the apparant dielectric constant which grows due to the absorption of water in such a way that the change in the capacitance of the polymer film is proportional to the humidity to be measured. A wide range of materials, including the cellulose group, the polyamid group (nylon), polyvinyl acetate, and polyethylene oxide, are being studied. 4) Sensors based on a change in the resonance frequency of a vibrator coated with a hydrophylic polymer raw material. Polyamide resins are frequently used.

The characteristics of humidity sensors using a polymer may be summarized as follows: First, precision is high and the reproducability of a measured value is excellent. When a humidity sensor using cellulose was placed in standard humidity cells of relative humidity (RH) 33.6 percent and 75.5 percent, which conceivably are used with high frequencies, the results of the measurement were in agreement with an error factor of less than $\pm$ 1.5 percent, thereby displaying the high reproducability and reliability shown in Figure 3. Second, measurement is performed in a simple and convenient step. Third, the sensor is easy to manufacture. The sensor, nevertheless, has some shortcomings in that, because of the use of polymer raw materials, it is available under neither the atmosphere or an organic solvent, nor at a temperature of above 80 degrees C, where ceramics are favored over polymers.

Besides the above, research on composite materials, where the above polymer is coupled with, for example, an electroconductive material or a salt, is necessary in order to improve the response of the sensor.

Henceforth, the range of application of the humidity sensor is expected to widen in areas such as medicine, where an improved sensor response is of utmost importance; in meteorological observation where the stable functioning of the sensor is needed; and in room air-conditioning and humidity control in hothouses in which on-line, real-time processing finds application.

3. Biosensor

It is important that material sensors recognize specific chemical compounds, a function which is exemplified by the ion-selection elecrodes described above. It is also necessary to detect one compound from among many similar compounds in a more precise manner, for example, to detect glucose among many types of sugars. For this purpose, biosensors, have been devised to detect specific compounds intended for use with highly selective biological agents such as enzymes.

Biological materials used in biosensors are themselves unstable. Once the material is immobilized in some polymer, the activity of the expensive material is made more durable and the material, hence, can be used repeatedly.

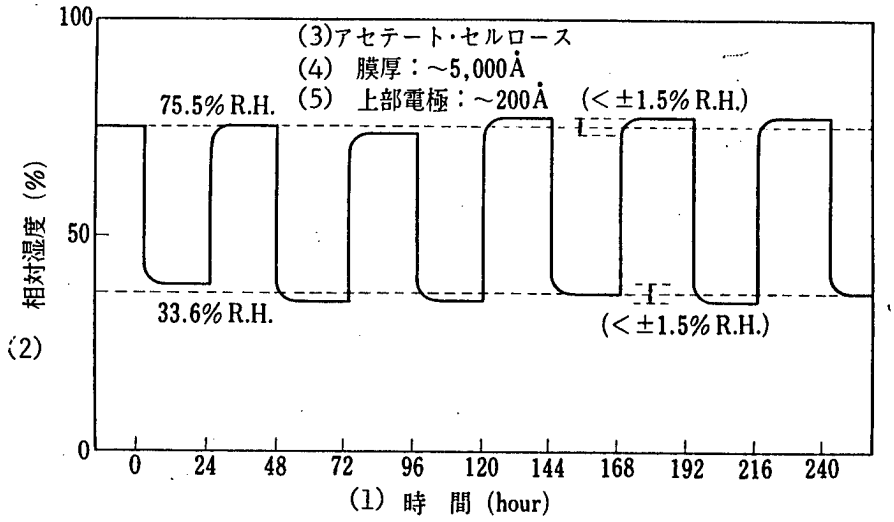

Figure 3. Reproducibility and Stability of the Humidity Sensors of the Cellulose Group

Key:

1. Time
2. Relative humidity
3. Cellulose acetate
4. Membrane thickness
5. Top electrode

Table 1. Polymer Material for Biosensors

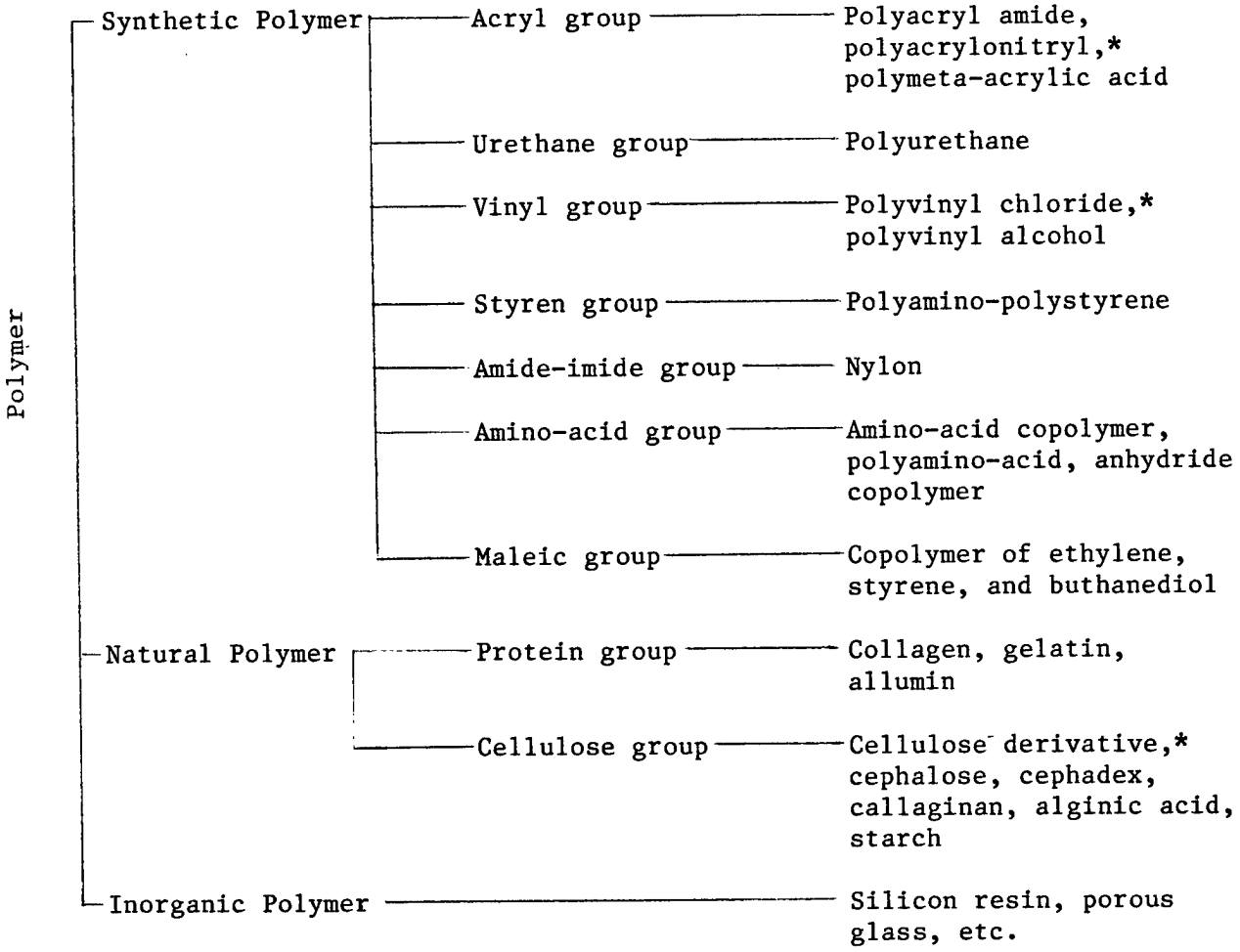

*Examples of practical application

To date, a wide range of polymer materials have been studied for use for this purpose as shown in Table 1, and among those finding practical applications are cellulose, polyacrylonitril, and hydrated polyvinyl chloride.

The characteristics common to this type of polymer materials are as follows:

1. The polymer has affinity for water suitable for use with biological materials.

2. The polymer is easy to fabricate and process into films and other forms as the mode of measurement requires.

3. The polymer is made porous in order to permit high permeability to relevant substrates and products.

The biosensors currently put to practical use are limited to those for clinical tests, those for glucose in fermentation tanks, those for biological oxygen demand (BOD) in monitoring water quality and a few others. The features of these sensors, which reflect relevant requirements that are not very exacting, are the following: 1) They have only single functions; 2) they are neither reduced in weight nor compact in size; they have neither high precision nor a low threshold level in measurement. Nevertheless, if biosensors are to become widely available commercially, the following criteria must be met: 1) the sensor must have multiple functions through device integration; 2) the sensitivity of the sensor must be improved to allow measurement to the order of magnitude of picomols for the concentration of biological materials; 3) the sensor must be compact and lighter so implantation in the body is feasible; or it must be a microsensor capable of measuring individual cells.

The above requirements, in effect, make it necessary for the electrochemical device involved to be converted from electrodes to semiconductors and then to microtransducers and diverse technologies for the fine processing of polymer materials to be developed along with it.

Polymer materials used in various material sensors have been reviewed generally above. Gas sensors, meanwhile, largely use ceramics and semiconductors as the raw materials of the elementary conversion device. The gas sensing type of electrode, which detects gases by electrochemical means, uses an ion-selection electrode and is classified in the electrode category and discussed as such in this article. Rain sensors and touch sensors, which may be considered as kinds of material sensors in a wider sense of the term, and in which piezoelectric polymer materials currently being developed are playing a vital role, are omitted in this article.

The author hopes, as mentioned above, that the characteristics of various polymer materials agree with individual requirements for sensors, leading to continued development of new sensors.

Polymer Materials for Pressure Sensors

Tokyo SENSOR GIJITSU in Japanese Dec 86 pp 54-57

[Article by Hiroji Ohigashi, professor, and Kiyoto Koyama, assistant, Polymer Material Technology Section, Department of Technology, Yamagata University]

[Text] Pressure sensors fall largely into three categories: one is based on a change of electrical resistance and is represented by a strain gauge, one is based on a change of capacitance, as seen in a differential pressure sensor, and one, on the piezoelectric property as seen in hydrophones. Polymer materials have recently begun to be put to use for pressure sensors mostly for the third group, i.e., as piezoelectric sensors. Piezoelectric material not only serves as a sensor, converting pressure into electrical signals, but also, conversely, as a transducer, generating pressure or sound waves from electrical input. This article deals with polymer raw materials for both of these applications.

Until very recently, polymer materials were used in the sensor area as conductor materials, semiconductor materials, and materials protecting the sensor, where they served merely as an auxiliary material, supporting sensor functions. Their superior properties, such as, electrical insulation and resistance to shock were indeed exploited. Since the discovery of the piezoelectric property of polyvinylidene fluoride (PVDF), however, research on polymer piezoelectric material has advanced rapidly as has the performance of the material. The result has been a great push towards the commercialization of the material as a piezoelectric sensor.

The piezoelectric power factor of, for example, PVDF, has advanced around 10 times in the last 10 years. This is attributable to progress in the structural design of polymer materials.

Polymer Materials for Pressure Sensors

When the permanent dipoles of a polymer film are oriented in a particular direction, the film becomes permanently polarized and, furthermore, exhibits piezoelectricity, that is, the extent of polarization of the film varies with the pressure applied to it. PVDF, meanwhile, is a polymer in chain form in which repeating $+CH_2-CF_2+$ units extend linearly. Because of the high dipole moment involved in CF_2, a permanent dipole occurs in the direction normal to the long linear molecule.

Such a polymer chain, nevertheless, does not produce piezoelectricity if the forces of individual dipole moments counterbalance each other in the crystals formed. In fact, in PVDF which is newly processed into film from its melt, the crystals lack permanent polarization because the moments of their dipoles counteract each other as in Figure 1(a). When the PVDF film prepared from its melt is subjected to extension, however, the structure of the relevant crystals undergoes changes such that the permanent dipoles of the molecule orient themselves in the crystal as in Figure 1(b). Hence, the crystals

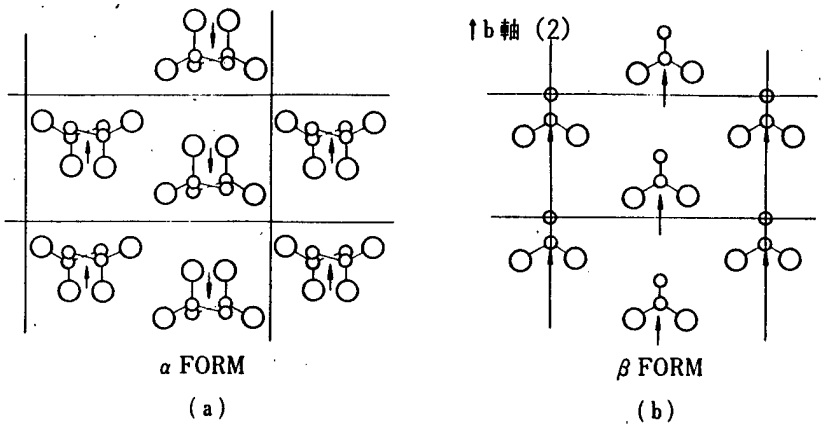

(1) 分子鎖の方向からみたＰＶＤＦの結晶構造
(矢印は双極子モーメントの方向，大円はフッ素原子，
小円は炭素原子を表す．水素原子は省略してある)．

Figure 1. Crystalline Structure of PVDF Analyzed in Terms of the Orientation of the Molecular Chain

Key:

1. The arrow indicates the direction of the dipole moment; the large circles represent fluorine atoms and the small ones, carbon atoms; hydrogen atoms are not represented.
2. b axis

Table 1. Physical Values of Raw Materials for Piezoelectric Sensors

	PVDF	P(VDF-TrFE)	P(VDCN/VAc)	PZT	Quartz
Density ρ (10^3kg/m^3)	1.78	1.88	1.20	7.50	2.65
Dielectric constant ε	6.2	6.0	4.9	635	4.5
Modulus of elasticity C_{33} (10^9N/m)	9.1	11.3	7.5	159	86
Sound velocity V (km/s)	2.26	2.40	2.60	4.63	5.74
Acoustic impedance Z (10^6 kg/m^{2}s)	4.0	4.5	3.1	34.8	15.2
Piezoelectric power factor (constant) d_{31} (pC/N)	33	12.5	6.0	160	2
g_{31} (10^{-3} Vm/N)	260	170	170	10	50
d_{33} (pC/N)	18	20	19	100	2.3
g_{33} (10^{-3} Vm/N)	330	370	438	17	50
Electromechanical coupling constant k_t	0.2	0.3	0.25	0.51	0.10

themselves are permanently polarized. In this case, nevertheless, the direction of polarization of individual fine crystals in the film is not uniform and the film itself is not polarized.

Applying high voltage to this film, a procedure called poling, in turn, allows regular orientation of these fine crystals with respect to their polarization and hence, produces a piezoelectric film. The permanent dipoles in the film become parallel to the electric field applied in this procedure. The PVDF film subjected to extension is highly dielectric and the electric field to be applied to the film needs to be over 0.5 MV/m at room temperature.

Piezoelectric PVDF films have two shortcomings. One is low crystallinity. PVDF is made up of crystalline and non-crystalline parts with the former accounting for no more than 50 percent. Hence, improvement of its piezoelectricity is limited.

Another shortcoming is that PVDF films have to be subjected to extension in order to become piezoelectric. This produces problems in connection with the stability of the size of the films and changes, with time, of their piezoelectric power. This also leads to difficulties in fabricating very thin sensors, or sensors of special shapes or high sensitivity. To cope with these difficulties, however, polymers with piezoelectricity have been developed, such as, a copolymer of vinylidene fluoride and trifluoroethylene, P(VDF-TriFE), vinylidene fluoride and tetrafluoroethylene, P(VDF-TeFE), and an alternating copolymer of cyanovinylidene and vinyl acetate, P(VDCN-VAc). Though polymer piezoelectric materials, compared with inorganic ones, have so far not been sufficiently reliable in terms of their durability, the materials above are now affording materials sufficiently practical in terms of sensitivity and reliability.

Practical Performance as Sensor Materials

The practical applications of piezoelectric films include those for low frequency waves up to several hundred kHz and those for radiofrequency waves of several hundred kHz or over; each use different directions of piezoelectric factors of film. The application for low-frequency waves uses transverse effects(d_{31} and g_{31}) where a change in the volume of the film largely produces piezoelectricity. Application to those for radio frequencies, in turn, use longitudinal effects (thickness effects)(d_{33} and g_{33}) wherein the change in direction of the dipoles themselves, in addition to the change in the volume of the film, causes piezoelectricity. The physical parameters of polymers involving piezoelectricity are presented in Table 1.

Piezoelectric factors d_{31} and d_{33} represent strands in length and in thickness, respectively, of a piezoelectric film when a unit voltage is applied to the film with a surface free of any stress. The values of these constants for polymer materials are limited compared with those for organic materials such as PZT. The sensitivity of the pressure sensor, nevertheless, is dictated by the voltages(g_{31} and g_{33}) generate in the film by a unit of stress applied to it. Polymer materials make excellent sensor materials when compared to inorganic materials in terms of these piezoelectric factors.

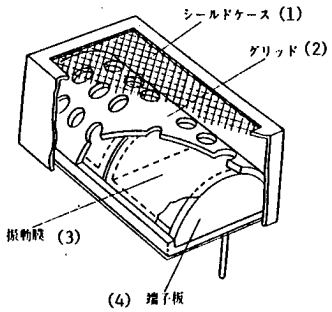

Figure 2. Structure of Supersonic Wave Wide Band Microphone (Matsushita Denki Sangyo [Matsushita Electric Industrial Co. Ltd.]

Key:
1. Shield case
2. Grid
3. Vibration membrane
4. Terminal board

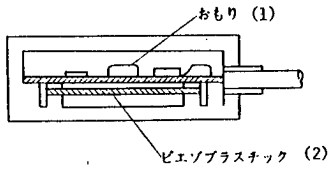

Figure 3. Structure of Acceleration Sensors (Mitsui Yuka or Mitsui Sekiyu Kagaku Kogyo [Mitsui Petrochemical Industries, Ltd.])

Key:
1. Weight
2. Piezoplastic

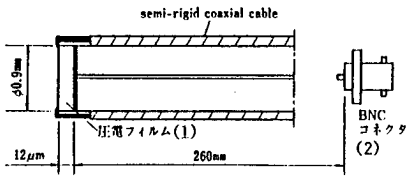

Figure 4. Structure of a Miniature Hydrophone

Key:
1. Piezoelectric film
2. Connector

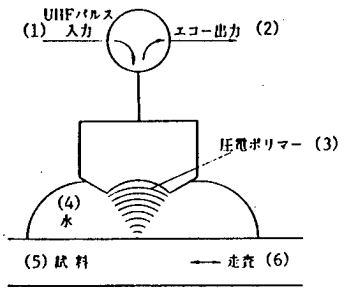

Figure 5. Supersonic Wave Microscope of the Reflection Type

Key:
1. UHF pulse input
2. Echo output
3. Piezoelectric polymer
4. Water
5. Specimen
6. Scan

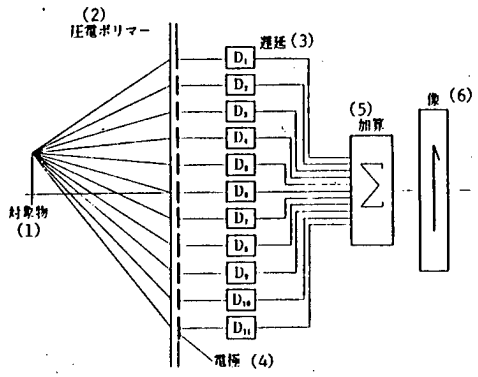

Figure 6. Imaging With an Array Sensor

Key:
1. Object
2. Piezoelectric polymer
3. Delay
4. Electrode
5. Computation or addition
6. Image

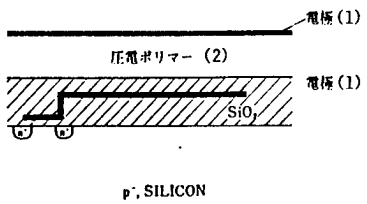

Figure 7. Structure of POSEFT (Schwartz, Plummer, 1979)

Key:
1. Electrode
2. Piezoelectric polymer

Where application of the sensor for radiofrequency waves is concerned, polymer materials are of low Q value and make sensor materials with large bandwidths. The acoustic impedance of polymer materials is far less than in inorganic materials, and also in comparison with water. Providing its structural conditions are properly adjusted, the sensor can exhibit sufficient sensitivity in the range of wave frequency covering around two digits in non-resonance application as well as resonance-mode application when used as a supersonic wave sensor in water. As for the temperature characteristics of the sensor, it is available up to a temperature as high as 160 degrees C and its sensitivity at a temperature as low as -180 degrees C is little different from that at room temperature. Another notable feature is the potential capability of deterioration the piezoelectric functions of polymer material which is larger by about two digits than the same for ceramic high-grade dielectrics. To put it another way, polymers make a sensor material highly resistant to the application of voltages. In addition to the advantage of being affected neither by high-humidity nor by hydrostatic pressure, polymer materials, an aggregate of enormously long chains of molecules, are characteristically soft and flexible and, hence, can resist shock and withstand large deformation. Since they are highly amenable to processing, they are readily affordable for sensors not only of large area but also of compact size. They thus make a valuable sensor material with properties not available in ceramic piezoelectric materials.

Practical Examples and Prospects for Sensors

A practical application of piezoelectric polymer materials in sensors of low frequency wave is a microphone of large bandwidths. An example of the application of the transverse effect in the supersonic region is shown in Figure 2. Furthermore, an acceleration sensor for low frequency wave, as shown in Figure 3, has been put on the market and a differential-pressure sensor, based on similar principles is expected to be marketed sooner or later. Among other examples of a sensor for low-frequency waves is the generation of electrical energy from sea waves, quantitative measurement of eddies in a current, sensing of pressure by robot feet, and a quantitative estimation of the movement and shape of the tongue in the mouth.

One application of the sensor of radio frequency waves is transducers for medical and NDT purposes. These utilize the characteristics of the incorporated polymer and have been put on the market. These range from an annular transducer with a diameter as large as 70 millimeters to a miniature hydrophone with a diameter less then 1 millimeter, shown in Figure 4. Coating of electric wires with piezoelectric polymers has afforded extremely long hydrophones. AE (acoustic emission) sensors making use of the wide band characteristics of the polymer have also been trial manufactured. Based on the characteristics of polymers, that they can be turned into film or into any shape of transducers with ease. Research on the development of transducers for supersonic wave microscopes has been underway in the author's laboratory (see Figure 5). Also on the basis of the polymer's characteristic that the mechanical losses are large in addition to those mentioned above, a transducer of the array type has also found practical applications and has afforded lucid supersonic wave pictures. Furthermore, array transducers using omnidirectional elements and lacking the grating globe have been trial-

manufactured. By coupling the transducer with a digital processing system, an intelligence function of the sensor, such as a supersonic-wave holograph, is being developed (Figure 6). The merit of polymer materials in these transducers is that the material affords reduced accoustic impedance. Their adaptability to water and life, as compared with PZT and others is excellent.

Another possible application for sensors of these piezoelectric polymer materials is for surface accoustic waves. Though the amount of research is yet limited, application to various types of sensors as well as pressure sensors seems possible.

One factor which has to be noted in the application of polymer materials in sensors is their low dielectric contants. This is an advantage rather than a disadvantage for radio frequency waves of over 100 MHz, but produces large impedance, a major disadvantage of low-frequency waves.

To deal with this difficulty, means for lamination of polymer films and piezoelectric oxide semiconductor, POSFET, have been devised (see Figure 7). Coupling of semiconductor and IC technologies with polymer piezoelectric polymer materials, as seen in this example, must play a significant role in the coming years.

Conclusion

Seventeen years have passed since the discovery of the piezoelectric function of polymers. The application of this function, though having advanced rapidly these years, may be considered to have just gotten on track in view of the enormous potential applications for polymers in this area and much is expected of future developments.

Polymer Material for Heat Sensors

Tokyo SENSOR GIJITSU in Japanese Dec 86 pp 58-61

[Article by Ikuo Sato, Industrial Chemistry Technology Section, Technology Department, Ikutoku Institute of Technology]

[Text] Few substances, if any, are inert enough to show no changes in their physical property upon external thermal stimulation. In polymer materials, the input signal of thermal changes produces output signals in the form of electrical polarization and resistance. Infrared sensors and thermistors based on this property, as is well known, have been finding practical applications. Changes in the physical property, resulting from thermal changes, represent a phenomenon observed in raw materials in general, not limited to polymer. Therefore, thermal sensors are the most universally used and the most diverse. Polymer materials which permit quantity production are, in turn, readily available and their processability is excellent. They are therefore, being tested as sensors not only in electric blankets and other appliances but also as sensors for medical purposes and, in particular, in the treatment of cancer.

This article deals with changes in the physical properties of polymer materials resulting from temperature changes and also with their application in material sensors.

Polymers as an Elementary Device for Conversion of Thermal Energy

In thermal sensor materials, it is necessary that thermal changes, such as temperature changes, be converted directly into changes of electrical signal (See Figure 1). In polymer materials, the electric charges on the surface divert or polarize in response to various stimuli.

Whereas electrical polarization due to mechanical stimulation is referred to as the piezoelectric effect, electrical polarization due to temperature change is called the pyroelectric effect. Upon exposure to infrared rays, a highly dielectric polymer material's temperature rises and the ratio of the change of polarization to that of temperature is given by

$$p = \partial P/\partial T = (1/A)(\partial Q/\partial T) \qquad (1)$$

where stands for the ratio, A for the area exposed to infrared rays, P for polarization, and Q for the electric charge produced.

On the other hand, when different metals, or different semiconductors, or one metal and one semiconductor are coupled such that they make contact with one another, forming a closed circuit, and subsequently, a difference in temperature is caused at the contact point, an electromotive force is produced. This phenomenon is referred to as the Seebeck effect.

This effect has been noted in, among other things, the pyrolytic product of polyacrylonitry. In sensors measuring such thermal electromotive forces, it is necessary that the ratio of the change of the electromotive force to that of the temperature different at the contact point of the two substances and, hence, the value of the Seebeck effect, be as large as possible.

An example of thermal energy being converted reciprocally into electric energy is the change in resistance. The resistance R is given by the following formula:

$$R = R_o \cdot \exp\left[\frac{B}{1/T - 1/T_o}\right] \cdots\cdots \qquad (2)$$

where B is the thermistor constant $\triangle$ E2k with ΔE denoting activation energy and k the Boltzmann constant. B is a measure of the sensitivity in measuring temperature for thermal sensors.

Besides the sensors above, which directly yield electrical output, sensors based on mechanical changes, on phase changes (fusion, decomposition, etc.) and on thermochronic changes have been devised and have found practical applications in fuses and fire alarms.

Pyroelectric Type of Sensors

The pyroelectricity index is a measure of the assessment of the pyroelectricity of a material and is given by

$$\eta = p/(C_v \cdot \varepsilon) \quad \cdots\cdots\cdots\cdots \qquad (3)$$

where C_v is the specific heat at constant volume and ε, the specific dielectric constant. The crucial point in designing an infrared sensor of high sensitivity from formulas 1 and 3 above is to make the area for accepting the relevant ray as large as possible, and to pick up a material with as low a dielectric constant and heat capacity as possible. Polymer raw materials are easy to process into film and into a material of high density, and provide high sensitivity, high efficiency for energy conversion, and, also have rapid response. Another feature is the diminished sharpness of mechanical resonance and resistance to vibration noise. Polyvinylidene fluoride has so far been studied the most comprehensively and put to practical use. The material is of the order of magnitude of 10^{-10} assuming C_v at 2.4[J/cm^2 K] and ε at approximately 13, a performance which compares with those of lead titanate and other inorganic pyroelectric materials (Table 1).

The material, as a sensor operable at ambient temperatures and capable of detecting infrared rays emanating from humans, has been finding applications in automated vending machines (customer indicators) and sensors for safeguarding buildings (intruder alarms).

Figure 1. Thermal Response of Polymer Materials in Sensors

Thermal stimulation (thermal energy) ⟶ Polymer materials

	Change of physical property	Raw material
Electrical signals	→ Surface charge (pyroelectric effect)	→ Polyvinylidene fluoride
	→ Thermoelectric force (Seebeck effect)	→ Polyacrylonitril pyrodecomposition products
	→ Resistance	→ Graphite-parafine-polyethylene-polyvinyl chloride (composite material)

Table 1. Properties of Pyroelectric Materials[2]

Material	Curie Point Tc (°C)	Pyroelectric Constant p_2 ($C/cm^2 \cdot K$)	Specific Dielectric Constant ε	Specific Heat at Constant Volume Cv_2 ($J/cm^2 \cdot K$)	Thermal Conductivity K ($W/cm \cdot K$)	Thermal Diffusion Coefficient α (cm^2/S)	Pyroelectricity (Performance) Index η
PVDF*	120	0.24×10^{-3}	13	2.4	1.3×10^{-3}	0.53×10^{-3}	8.5×10^{-11}
TGS**	49	3.5×10^{-3}	42	2.5	6.4×10^{-3}	2.6×10^{-3}	3.3×10^{-11}
$PbTiO^3$	470	6.0×10^{-3}	200	3.2	3.2×10^{-3}	9.9×10^{-3}	9.4×10^{-11}

* Polyvinylidene fluoride
** Triglycine sulfate
PVDF is one type of fluorine resin with a crystallinity (factor) of 30 to 50 percent and exhibits superior resistance to weathering, to heat, to medical agents, to abrasion, etc. With the main chain involving $\{CH_2-CF_2\}$ units, a dipole moment made up of CF_2 of 1.6 debye and CH_2 of 0.5 debye is produced for every monomer unit, resulting in dielectric constant as much as 9 to 13.[6]

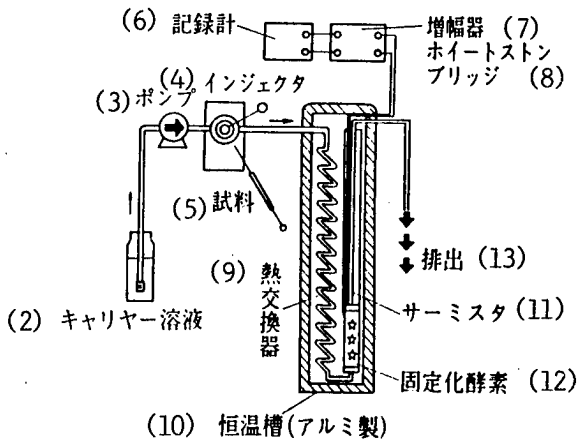

(1) (生体触媒反応に伴う微少な温度変化をサーミスタを用い，ホイートストンブリッジを介して物質量を計測するセンサシステムで，恒温槽以外は通常のフローインジェクション分析 (FIA) システムをそのまま適用できる．恒温槽は高性能の温度制御を実現し得る(30℃ ±0.001℃) もので，1 m℃ を 1 %の精度で計測できる．本システムは別に酵素サーミスタと呼ばれる[*]．

Figure 2. Measuring System of a Material Sensor of the Heat Detecting Type

Key:

1. The sensor system represents one measuring physical quantities [indirectly] by measuring fine temperature changes accompanying biological catalytic changes with a thermistor connected to a Wheatstone bridge; the ordinary flow-injection-analysis (FIA) system is wholly applicable except for the thermostat, which permits control of temperature of high precision (30 degrees C ± 0.0001 degrees C) and measurement of temperature of 1 m[ili] degrees C with an error of less than 1 percent. This system is alternatively called an enzyme thermistor.
2. Carrier solution
3. Pump
4. Injector
5. Specimen
6. Recorder
7. Amplifier
8. Wheatstone Bridge
9. Heat exchanger
10. Thermostat of aluminum
11. Thermistor
12. Immobilized enzyme
13. Discharge

Thermistor Type of Sensors

Composite materials made of a thermoplastic polymer and an electroconductive carrier are used for elementary devices that detect heat on the principle of changes of resistance due to changes of temperature. (Among the plastic thermistors are: plastic polyvinyl chloride plus an ionic additive or electroconductive substance; polyamide plus a surfactent; PVC plus polyurethane plus TCNQ complex; polyamide plus copper halide.

Plastic and ceramic thermistors have been compared in composition, electrical property, mechanical property and productivity, etc. The plastic thermistor is favored over the other in the following:

1) The variance among individual lots is limited.

2) The temperature coefficient of resistance stands at 7.0 ~ 9.0 percent per degree C, i.e., the sensitivity is around double that of the other.

3) Errors due to the heat generated in the sensor itself are fewer.

4) The polymer may be molded into any shape desired or it can be tailor made.

5) The cost per unit of the material is lower.

These features are made the most of in their application in electrical appliances such as electrical blankets.

Thermoelectric-Force Type of Sensors

Temperature measurement of high sensitivity in a wide range with the thermoelectric type of sensors requires that the Seebeck coefficient be large enough and its dependence on temperature be as low as possible.

The value of the thermoelectric force is dictated by the difference between relevant substances, of the Fermi level and the temperature. So far, semiconductors of conjugated polymers have been synthesized for this purpose. Some of their Seebeck coefficients, as shown below, are large compared with those of the Si-Pt series and the Fe-Pt series which, are at 500μV/deg. and 14.5~18.9μV/deg, respectively.

polyacrylonitril, 40 108 V/deg.
polymer xanthene dyestuff, ~ 900μV/deg.
(polyacene) (ginone) radical polymer, -19~350μV/deg.
polyacetylene, 600~1,000 μV/deg.
polyvinyl carbazole (34~77 wt percent I_2 doped) 250μ V/deg.
(polythiazil) $(SN)_x$, $(SNBr_{0.4})_x$, -10~30μV/deg.
(poly-p-phenylene,) 4~125μV/deg.

These materials have yet to be commercialized, possibly because they involve some difficulties in durability, reproduceability, linearity, and, also in power.

Sensors for Medical Purposes

Temperature sensors for medical purposes aim at measuring temperatures either at the surface or deep inside of the body. Thermistors and infrared detectors are the sensors generally used.

Recent years, meanwhile, have seen hyperthermia spotlighted as a means treatment for cancer and several related reports are made at every annual meeting of the ME [Medical Engineering] Society.

If this type of treatment is to be safe and effective, an accurate measurement of the temperature of the cancer lesion is indispensable and has been accomplished by an intervention measurement wherein a sensor probe is sent into the body. The sensors so far used involve thermistor, thermocouple, etc. Hence, they produce errors in measurement if they are affected by a strong electromagnetic field. Barth, et al., successfully reduced the error to within 0.2 degrees C over a temperature range from 37 to 45 degrees C. They developed a very small, flexible temperature-sensor 0.4 mm thick, 1 mm wide, and 3.5 20 cm long, which incorporates an electroconductive polymer polyimide of high resistance as the lead wire and a silicon diode as the detector of temperature and which is coupled with a microcomputer for relevant measurement. In this sensor, one may see a fine example of the coupling of flexibility, which is one feature of polymers, with the fine processing technology of silicon technology.

Applications to Material Sensors

Most of the chemical reactions that occur are accompanied by expending or acquiring heat, that is, a change in enthalpy. It is, therefore, possible to determine the quantity of a substance participating in a reaction by measuring the caloric changes involved in the reaction.

Enzymes, meanwhile, which are known as biological catalysts capable of selectively detecting some particular substances under mild conditions, make a general-purpose biosensor when coupled with a thermistor, etc. as a transducer-temperature-detecting element.

The biological catalysts, in turn, are generally very unstable and easily lose their characteristic properties. This is referred to as the loss of activity, and hence they must be rendered stable by immobilizing them to a support, e.g., polymers and porous glasses. This is referred to as elementalization. These immobilized elements are then packed into a microscopic column and set into a cartridge holder mounted on the thermistor.

The cartridge holder is then connected to a system for continuous measurement, as shown in Figure 2, such that it functions as a material sensor. When a solution of a specimen is introduced into the sensor, the solution, along with a carrier solution, runs to the thermostat and reaches the column where the

particular component of the solution alone reacts with the immobilized element. The thermal changes involved are measured as changes in temperature with a Wheatstone bridge. Provided the relationship between the change in the concentration of a substance and the change of the relevant temperature has been made known beforehand, the concentration of the substance is easy to determine.

In principle, a general-purpose material sensor (bio-analyser) capable of measuring any substance may be designed if the proper enzymes, the so-called natural polymer materials of high function, can be selected. This type of biosensor, which is also referred to as an enzyme thermistor, has reached the commercial stage of development as a material sensor of the omnipotent type and has been finding diverse applications in diverse measurements in the areas of medicine, food processing, fermentation, and environment.

Conclusion

The author has reviewed generally above the thermal sensor based on the characteristics of the polymer itself. Polymer, as a material for thermal energy transducers, exhibits diverse sensor functions. Almost all products commercialized, nevertheless, are in composite form and a hybridization of a polymer with a material of another type at the molecular level is expected to develop with the accompanying enhancement of functions.

Unique application of a polymer material like the one seen in medical temperature sensors may be brought about by making the best of the characteristics of the polymer, including: 1) softness; 2) workability; 3) film forming; and 4) mass production.

20,128/9599
CSO: 4306/7511

NEW CABLE FOR OFFSHORE MOORING INTRODUCED

Tokyo FUNE NO KAGAKU in Japanese Feb 87 pp 57-62

[Article by Kazuhiro Masuda, member of Surface Treatment Research Center, Shin-Nippon Steel Corp., and Hideo Okamura, member of Ocean Bridge-Building Investigation Foundation]

[Text] 1. Introduction

Backed by the acquisition of minerals, oil, and marine resources together with the effective utilization of the sea area space, the ocean development industry has become particularly important in recent years. For example, large offshore structures, either fixed to the sea bottom or floated, such as sea airports and large ocean bridges, are under construction or are being planned.

A number of different devices--including steel pipe tazzas, chains, wire ropes, and fiber ropes, employed separately or in combination--are used to moor offshore structures. When they are to be used in deep sea areas where great durability is required, it is necessary that the mooring materials be lightweight, feature high fatigue strength, and be corrosion resistant.

The New-Parallel Wire Cable (New-PWC) to be introduced here is a wire cable whose development has been promoted as a long-period mooring member for the tension leg platform (TLP), which is considered to place more severe using conditions on its mooring members than the more typical jacket type offshore structure.

The traditional parallel wire cable has many positive features as a suspension member for long suspension bridges. The New-PWC differs from the PWC in that it has been layed in the same pitch and has been subjected to a double anticorrosion treatment for withstanding deep sea use.

Development of the TLP has changed from the forged steel pipes employed in the CONOCO-Hutton project to cheaper welded steel pipes and ropes. The water depth is from 1,500 feet to 4,000 feet, and one of the

characteristics of this environment is high seawater pressure (up to 120 kg/cm^2).

Since the volume of oil consumption has presently decreased worldwide, the development of new oil fields is on the decline. However, it is believed that the development of deep sea mining areas will continue to be pushed forward.

Figure 1 [omitted] is a concept drawing of a TLP applying the New-PWC.

2. Characteristics Demanded of Long-Period Mooring Members for Offshore Structures

The following can be viewed as the basic technical characteristics demanded of long-period mooring members in deep sea areas:

1. They should maintain their durability throughout the designed life of the structure (fatigue resistance).

2. They should maintain their strength under the severe natural conditions of the sea (pressure resistance, corrosion resistance).

3. They should be designed and manufactured to include the structures for connecting parts both to the floating body and to the anchor.

4. They should be easy to work with.

5. It should be possible to check the structures during use.

6. They should be replacable.

7. Repair of the anticorrosion layer should be possible.

8. Safety inspection must be confirmed by indoor and actual sea demonstration tests.

3. Development of New-PWC for Offshore Use and Its Characteristics

When measured against the requirements set out in condition 2 above, the chains and cables that have been used up to now have both strengths and weaknesses. However, it cannot be said that they necessarily have satisfactory characteristics.

The newly developed New-PWC for offshore use is a type of cable, and it has the following characteristics when used for long-period deep-sea mooring.

(1) High static tensile strength and elasticity modulus

The wire that becomes the strength member is a high-tension piano wire with a tensile strength of 160 kg/mm^2. Its quality standard is shown in Table 1.

The New-PWC wire has been layed in the same pitch as shown in Figure 2 by using galvanized (more than 330 g/m^2) wires of 5 mmø, and the wires are structured so that they mutually make a line contact. In this, they differ from general cables by having no points where the wires mutually cross, and it has a high tensile strength equal to that of the PWC.

The comparison between this cable arrangement and conventional cables is shown in Figure 3 by the relation between the unit weight (kg/m) and fracture strength (t_f). The high strength and yet lightweight feature that is one of the characteristics of this cable is apparent from this diagram. The same elasticity modulus (about 20,000 kg/mm^2) as the PWC has been guaranteed.

(2) High fatigue strength

Since the wires do not cross, the cable body has a high fatigue strength. However, the cable and processing method greatly affects overall fatigue strength.

In addition to the widely used copper-zinc alloy casting method, a socket using epoxy resin on the mouth part, which possesses greater fatigue strength (Figure 4), has been developed as the end processing method[1].

The results of the test of this high fatigue socket are shown in Figure 5.

The test results showed that the socket was not fractured, and it was confirmed that the socket strength had the same strength as the conventional PWC.

(3) Double anticorrosion specification with high reliability

While steel is always subject to corrosion in seawater, the degree of corrosion differs according to the depth. Corrosion is least around a depth of 2,000 feet, where the amount of oxygen dissolved in the water is low[2]. In addition to the effect of the dissolved oxygen, the steel is also greatly affected by the water temperature, conductance, and flow velocity. The static and fatigue strengths of the steel decline when it is subject to corrosion. Therefore, it is necessary to take sufficient anticorrosion measures to protect cables.

To meet this need, the double anticorrosion specification developed for the New-PWC has combined high-density polyethylene extrusion with lead

Table 1. Quality Standard of Galvanized Steel Wire

Testing Items	Quality Standard (Based on JSCC)	
	Wire Diameter 5 mm	Wire Diameter 7 mm
Dimensions		
Wire diameter	5.00 ± 0.06 mm	7.00 ± 0.08 mm
Diameter deviation difference	Less than 0.06 mm	Less than 0.08 mm
Mechanical properties		
Tensile strength	More than 160 kgf/mm^2 and less than 180 kgf/mm^2	More than 160 kgf/mm^2 and less than 180 kgf/mm^2
0.7 percent resistance	More than 118 kgf/mm^2	More than 118 kgf/mm^2
Elongation	More than 4.0 percent	More than 4.0 percent
No. of twisting times	More than 14 times	More than 14 times
Winding	3d x 8 times	3d x 8 times
Galvanizing		
Adhesion amount	More than 300 g/m^2	More than 300 g/m^2
Increase of wire diameter	Less than the average of 0.13 mm	Less than the average of 0.13 mm
Plating adhesion	5d x 2 times	5d x 2 times
Appearance	Free from harmful flaws and defects	Free from harmful flaws and defects
Linearity		
Free coil diameter	More than 4.0 m	More than 4.0 m
Free ring lift	More than 15 cm	More than 15 cm

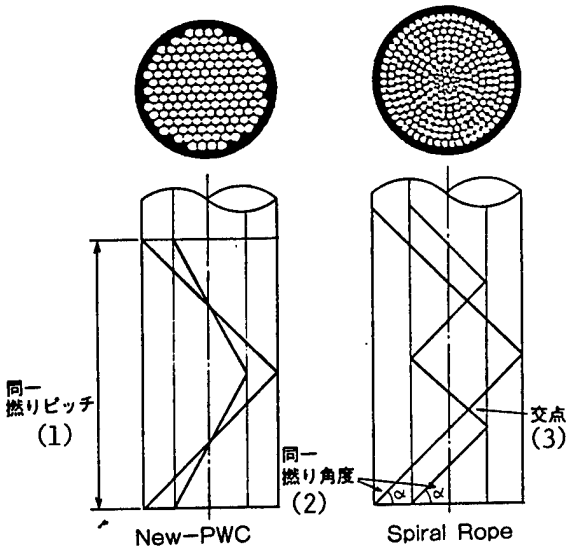

Figure 2. Lay Structure of Ropes

Key:

1. Same lay pitch
2. Intersecting point
3. Same lay angle

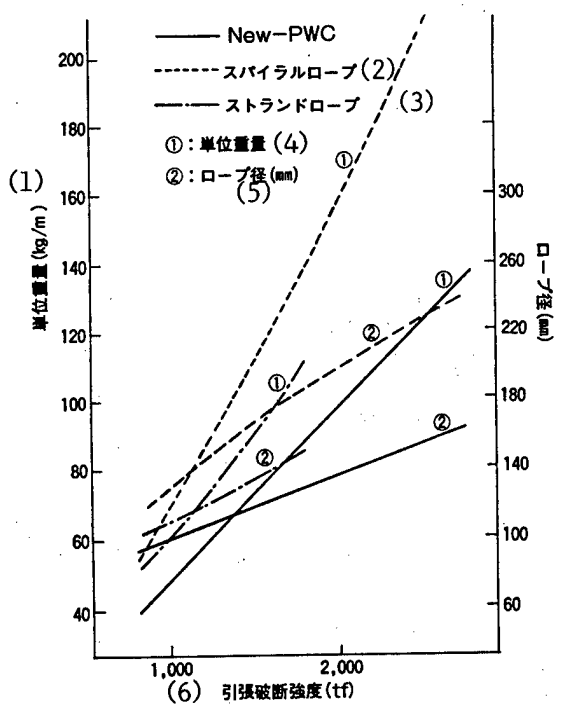

Figure 3. Unit Weight, Unit Diameter, and Tensile Rupture Strength of Various Ropes

Key:

1. Unit weight (kg/m)
2. Spiral rope
3. Strand rope
4. ① : Unit weight
5. ② : Rope diameter (mm)
6. Tensile rupture strength (t_f)

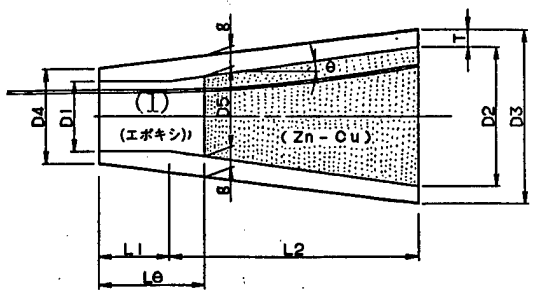

Figure 4. High Fatigue Resistance Socket (NS Socket)

Key:

1. Epoxy

Lay Structure	Dimension Diameter x No. of Wires	Lay Angle	Degree of Stress			No of Repetitions for Initial Disconnection (*)
			Max.	Min.	R	
PWC Structure	7 mm x 127	-	64	44	20	5.04×10^{-6} *
	7 mm x 127	-	64	39	25	0.8×10^{-6}
	7 mm x 127	-	64	39	25	0.67×10^{-6}
	7 mm x 127	-	64	29	35	0.18×10^{-6}
New-PWC Structure	7 mm x 127	3	64	44	20	2.07×10^{-6}
	5 mm x 127	2	60	40	20	2.0×10^{-6}
	5 mm x 127	2	64	44	20	5.0×10^{-6}
	5 mm x 127	2	64	39	25	2.0×10^{-6}

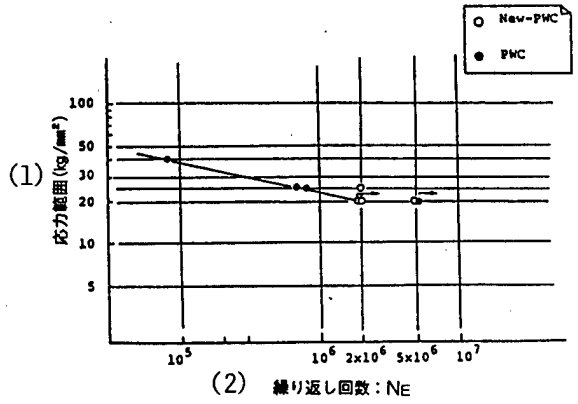

Figure 5. Fatigue Test Results of Parallel Wire Cable

Key:

1. Stress range (kg/mm^2)
2. Repetition times: N_E

laminate tape, and has aimed at a high seawater intercepting capacity in high pressure seawater (100 kg/cm^2).

The polyethylene coating is connected to the end socket by insertion. The maintenance of adhesion strength in the connecting part becomes extremely important and this controls the life of the cable.

A protective metal tube was used on the upper surface of the socket, as shown in Figure 6, and an end socket of double anticorrosion structure, which has molded the entire socket with polyethylene of the same property as that for the cable coating layer, has been developed.

The New-PWC and the end socket part have been experimentally shown to have absolutely no problem of seawater permeation, even at a high pressure of 100 kg/cm^2.

An example of the New-PWC that has been trial designed as a ladder material for the TLP is shown in Figure 7. The purpose of each layer of the double anticorrosion coating and their estimated effects are as follows:

1. Polyethylene outer layer--Resistance against the external force is the main objective. The thickness of the layer is determined by assessing the degree of restraint and anticorrosion necessary for the cable.

2. Lead tape--By inserting a lead tape adhered to a rein that forces a metal layer between the two polyethylene coating layers, the interception property against seawater permeation has been sharply improved compared with polyethylene used by itself.

Moreover, using this metal layer makes it possible to detect seawater when it starts to penetrate the outer layer of polyethylene as the metal acts as a seawater permeation sensor.

3. Inner layer polyethylene--Using a double layer structure for the polyethylene coating layer prevents propagation of cracks or damage to the external polyethylene layer produced by external stress.

It is designed so that the inner layer of polyethylene alone is sufficiently thick to prevent corrosion. From studies made on the pressing force against the drum surface both during execution and basic experiments, it was learned that a thickness of more than 4 mm is necessary.

4. Repair of polyethylene coating layer--It has the advantage that the external polyethylene layer can be easily repaired at the damage site. The repair method differs according to the extent of the damage. When the damage is great, repair can be completed in about 5 to 10 minutes by combining the same quality polyethylene with the chip by flame

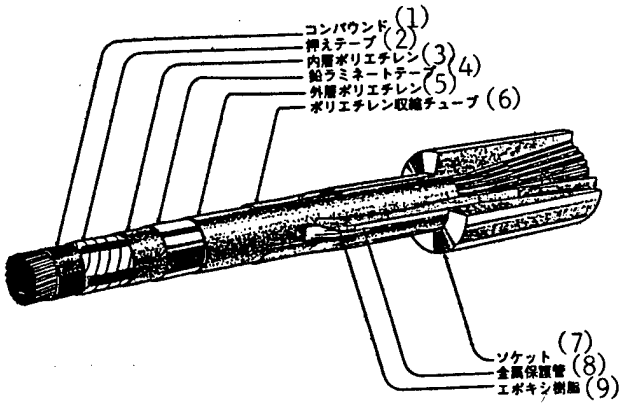

Figure 6. Concept Drawing of New-PWC

Key:

1. Compound
2. Check tape
3. Inner layer polyethylene
4. Lead laminate tape
5. Outer layer polyethylene
6. Polyethylene shrinkage tape
7. Socket
8. Metal protective tape
9. Epoxy resin

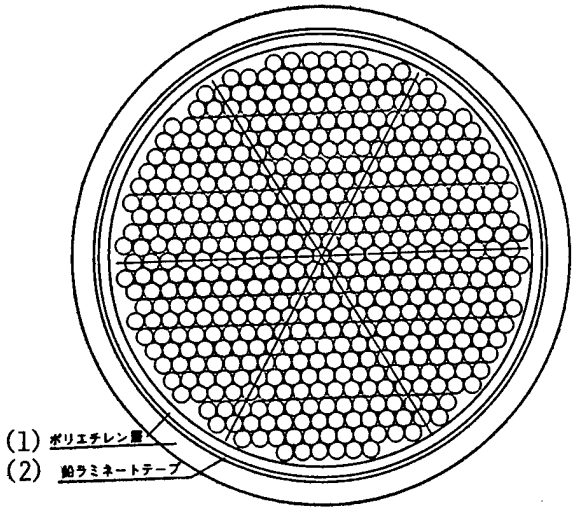

Figure 7. Cross-Section of 499 New-PWC

Key:

1. Polyethylene layer
2. Lead laminate tape

treatment. When the damage is small, it is possible to use the same method using the chip only.

The basic characteristics of the double anticorrosion system materials are shown in Table 2.

(4) Work execution ease

Up to now, the method used to perform anticorrosion treatment after site installation was generally the same as that used for cables used on land. This had great drawbacks in terms of transportation, weather, and workability.

The New-PWC is an anticorrosion cable that has done away with all anticorrosion treatments on site, and has the additional great advantage of being easy to coil on a reel.

The condition of the New-PWC coiled to a reel is shown in Photo 1 [omitted] and coiling is governed by the equation $D/d \geqq 20$, where D represents the reel diameter and d represents the cable diameter.

When the cable is pulled from the reel, the cable will be pressed against the reel surface by the weight of the extended cable, which causes great deformations. However, it has been shown in such cases that the cable will regain more than 95 percent of its former circular shape within 24 hours of being released from the compressive stress.

4. Demonstration Test

(1) Evaluation on practical use capacity--extended ocean exposure test

A deep-sea simulator device (seawater pressure chamber) was used to evaluate the effectiveness of the anticorrosion coating layer and to check the New-PWC's safety and reliability through various winding and development tests.

As a result, it has been confirmed that it has superior characteristics not found in conventional steel cables.

Therefore, Kochi Prefecture, which wanted to investigate the New-PWCs practical use capacity, used the New-PWC as the mooring cable for its floating fish bank in the Kochi offing (Tosa Kuroshio Current No 1 Farm) which it was promoting by commissioning the work to the National Coastal Fishery Promotion and Development Association. Tests on the cable were carried out over a period of 2 years[3].

The Tosa Kuroshio Current No 1 Farm is a floating fish bank that has been established for experimental purposes at a spot 40 km in the Kochi offing where the sea depth is 550 m.

Table 2. Basic Characteristics of Double Anticorrosion System Materials

Type of Member	Checking Items	Standard and Others
Galvanized Wire	Galvanizing amount	More than 300 g/m^2
	Increasing amount of wire diameter	Less than the average of 0.13 mm
	Plating adhesion	Should be free of defects such as cracks, etc., when coiled 8 times on a 10 d drum
Compound	Polyisobutylene	Fill up in end processing part
High Density Polyethylene	Specific gravity	0.95 g/cm^3 (JIS K 6760)
	Yield strength	232 kg/cm^2 (JIS K 7113)
	Rupture strength	324 kg/cm^2 (JIS K 7113)
	Elongation	700 percent (JIS K 7113)
	Initial modulus of elasticity	9,200 kg/cm^2 (JIS K 7113)
	Hardness (shore hardness)	64 (ASTM D 2240)
	Softening temperature	125°C (JIS K 6760)
	Melting point	130°C (DSC)
	Brittle temperature	-75°C (JIS K 6760)
	Stress cracking	More than 1,500 hours (ASTM D 1693)
	Thickness	Inner layer more than 4 mm, outer layer from 4 to 11 mm
Lead Laminate Tape	Structure	Reinforced lead tape provided with adhesion layer on both sides

The main body of this floating fish bank is a circular buoy made of steel with a diameter of 6 m, a height of 7.8 m, a weight of 12 tons, and a buoyancy of 43.5 tons.

The mooring cable, whose full length is 830 m, is a compound cable consisting of a 48 mmø chain (Class 3, Class 4) and a 60 mmø New-PWC. The New-PWC is used in an intermediate part running from 15 to 500 m underwater.

The New-PWC is made of galvanized wires with a diameter of 5 mm and a tensile strength of 160 kg/mm^2. These are formed into a large pitch stranded wire of 55 wires and then bundled. For the anticorrosion layer, a lead laminate tape was wrapped on an extrusion layer of polyethylene 4 mm thick, and an external layer of polyethylene coating also 4 mm thick was applied on top of that. An NS socket excelling in fatigue resistance was attached on both ends, and a double anticorrosion coating (shown in Figure 6) was provided between the New-PWC and the sockets. The design conditions were as follows:

Water depth	550 m
Wave height	10 m (1/3 significant wave)
Wave period	14 seconds
Tidal current	5 knots
Wind speed	60 m/second
Use (test) period	2 years

The Tosa Kuroshio Current No 1 Farm is shown in Photo 2 [omitted] and the concept drawing and the general view of the main body and mooring cable are shown in Figures 8 and 9, respectively.

The practical use test of the New-PWC was conducted under the extremely severe conditions described above in the actual sea area and it was recovered on land after the test.

Following that test, no cracks or damage were observed on the polyethylene coating layer surface of the New-PWC. Seawater permeation from the end sockets was nil, and it has been demonstrated to be a superior ocean mooring member, even under severe actual conditions.

5. Conclusion

It is believed that technical developments aimed at the development of industrial and marine resources in deep ocean areas will advance more rapidly in the future.

We entertain the hope that various experiments will also be made on the New-PWC described in this text to enhance its safety and reliability, and that the New-PWC will emerge in the future as one of many new functional compound materials.

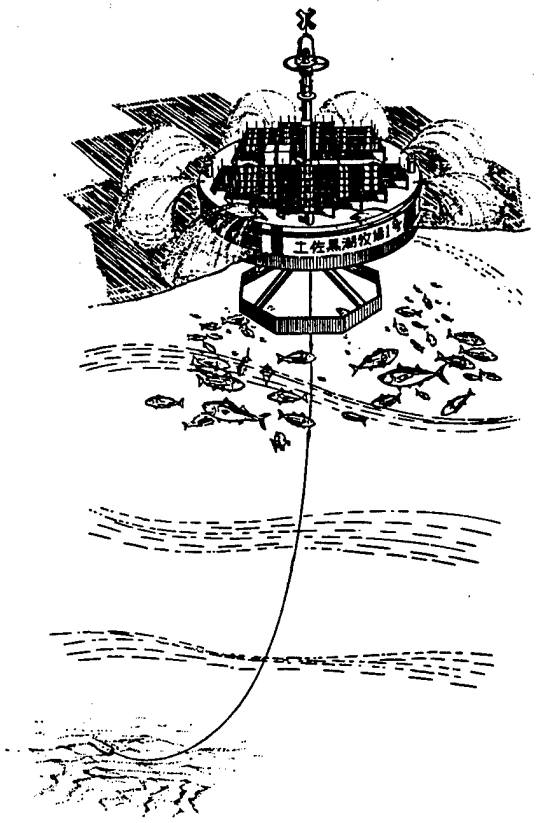

Figure 8. Concept Drawing of Tosa Kuroshio Current No 1 Farm

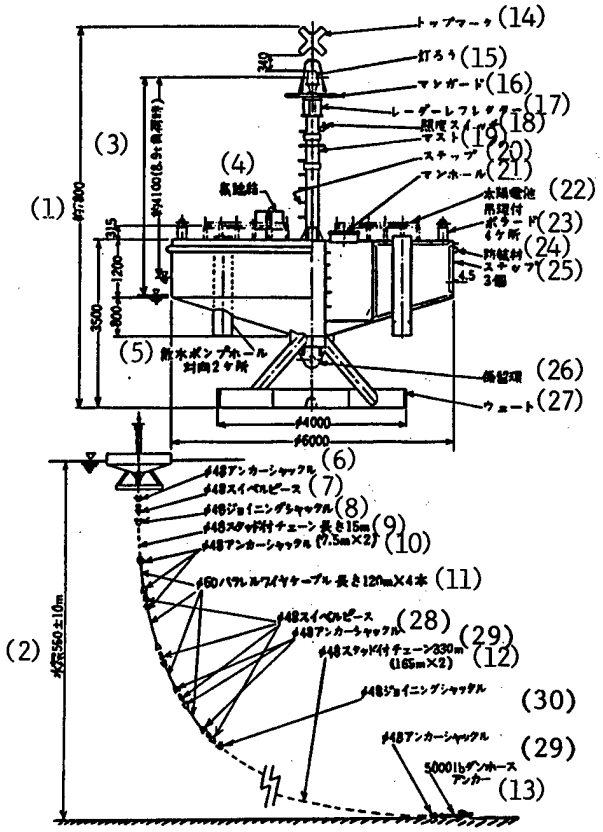

Figure 9. General View of Tosa Kuroshio Current No 1 Farm and Mooring Cable

Key:

1. About 7,800
2. Water depth 550 ± 10 m
3. About 4,100 (at 8.9 t load)
4. Wire collecting box
5. Water spraying pump holes (facing holes in two places)
6. ϕ48 anchor shackle
7. ϕ48 swivel piece
8. ϕ48 joining shackle
9. ϕ48 chain length with stud 15 m
10. ϕ48 anchor shackles (7.5 m x 2)
11. ϕ60 parallel wire cable with a length 120 m x 4 each
12. ϕ48 chain with stud 330 m (165 m x 2)
13. 5,000 lb anchor
14. Top mark
15. Toro (hanging lantern)
16. Mesg guard
17. Radar reflector
18. Illumination switch
19. Mast
20. Step
21. Manhole
22. Solar cell with ring
23. Bollard in four places
24. Fender
25. Step in three places
26. Anchoring ring
27. Weight
28. ϕ Servo piece
29. ϕ Anchor shackle
30. ϕ Joining shackle

BIBLIOGRAPHY

1. Kunihiko Yokayama, et al., "Iron and Steel," 65, S1066, 1979.

2. F. M. Reinhart, "Technical Note," U.S. Naval Civil Engineering Laboratory, N-900, 1967.

3. Kuniaki Hirosawa and Hideo Okamura, "Steel Design," 263, 1980.

20,158/9599
CSO: 4306/7563

- END -